Drop-Weight Test for Determination of Nil-Ductility Transition Temperature

User's Experience with ASTM Method E 208

Holt/Puzak *editors*

ASTM STP 919

DROP-WEIGHT TEST FOR DETERMINATION OF NIL-DUCTILITY TRANSITION TEMPERATURE: USER'S EXPERIENCE WITH ASTM METHOD E 208

A symposium
sponsored by
ASTM Committee E-28
on Mechanical Testing
Williamsburg, VA, 28–29 Nov. 1984

ASTM SPECIAL TECHNICAL PUBLICATION 919
John M. Holt, consultant, and
P. P. Puzak, consultant, editors

ASTM Publication Code Number (PCN)
04-919000-23

1916 Race Street, Philadelphia, PA 19103

Library of Congress Cataloging-in-Publication Data

Drop-weight test for determination of nil-ductility transition temperature: user's experience with ASTM method E 208.

(ASTM special technical publication; 919)
"ASTM publication code number (PCN) 04-919000-23."
Includes bibliographies and indexes.
1. Steel—Testing—Congresses. 2. Metals—Impact testing—Congresses. I. Holt, John M. II. Puzak, P. P. (Peter P.). III. ASTM Committee E-28 on Mechanical Testing. IV. Title. V. Series.
TA465.D76 1986 671.5'20423 86-25913
ISBN 0-8031-0487-1

Library of Congress Catalog Card Number: 86-25913

Printed in Fairfield, PA
December 1986

Foreword

This publication, *Drop-Weight Test for Determination of Nil-Ductility Transition Temperature: User's Experience with ASTM Method E 208*, contains papers presented at the symposium on NDT Drop-Weight Test (E 208 Standard), which was held 28–29 Nov. 1984 in Williamsburg, Virginia. The symposium was sponsored by ASTM Committee E-28 on Mechanical Testing. John M. Holt, consultant, served as editor of this publication, along with P. P. Puzak, consultant, who was chairman of the symposium.

Related ASTM Publications

Fracture Mechanics: Seventeenth Volume, STP 905 (1986), 04-905000-30

Fracture Mechanics: Sixteenth Symposium, STP 868 (1985), 04-868000-30

Through-Thickness Tension Testing of Steel, STP 794 (1983), 04-794000-02

A Note of Appreciation to Reviewers

The quality of the papers that appear in this publication reflects not only the obvious efforts of the authors but also the unheralded, though essential, work of the reviewers. On behalf of ASTM we acknowledge with appreciation their dedication to high professional standards and their sacrifice of time and effort.

ASTM Committee on Publications

ASTM Editorial Staff

Helen P. Mahy
Janet R. Schroeder
Kathleen A. Greene
William T. Benzing

Contents

Overview

In November 1984, ASTM Committee E-28 on Mechanical Testing held an international symposium to discuss users' experience with the ASTM Method for Conducting Drop-Weight Test to Determine Nil-Ductility Transition Temperature of Ferritic Steels (E 208). The objectives of the symposium were to determine (1) unusual material behavior; (2) advantages of the test, including correlations of the results with service experience and other tests; (3) shortcomings of the method; and (4) unique testing equipment or experimental techniques. Of the twelve papers presented at the symposium, nine have been published in this Special Technical Publication. These nine papers cover the symposium objectives well; it is interesting to note that most of the authors found shortcomings in ASTM Method E 208-81 (the then current version of ASTM Method E 208) and made recommendations to overcome these shortcomings. The task group of ASTM Committee E-28 charged with oversight for the drop-weight (DW) test was aware of several of these deficiencies and had initiated appropriate action—for example, the crack-starter weld bead was changed to a single stringer bead without weave to minimize the heat input and thereby reduce the possibility of tempering the base metal at the notch. There were other deficiencies, however, of which the task group was not aware, and these are currently being studied.

The opening paper, by *Ando et al,* presents the results of a study of welding parameters—welding current, preheating, shape of the bead, and other parameters—which shows that the welding current is the most influential parameter. In this study, the authors tested a sufficient number of specimens to make probability statements about the occurrence of nil-ductility transition (NDT) at specific temperatures.

The second paper, by *Satoh et al,* also shows the importance of the welding current and points out how heat sinks can influence the NDT temperature by changing the cooling rate of the heat-affected zone (HAZ), thereby producing a tough or not-so-tough microstructure. The authors indicate that good correlation between the NDT and Charpy impact transition temperatures can be obtained. (The editors caution that the correlations are probably based on the use of the Japanese Industrial Standard Charpy striker geometry and not on the ASTM test geometry; thus, the absolute values of the constants may be slightly affected.)

The next three papers, by *Onodera et al, Lundin et al,* and *Koshizuka et*

al, discuss the effect that the crack-starter weld bead has on the NDT temperature. They, too, demonstrate that the then standard two-pass technique of laying down the bead can temper the HAZ, which, in some materials, can significantly increase the toughness (lower the NDT temperature). (Because of these and other similar studies, ASTM Method E-208 was revised in 1984, prior to this symposium, to require that only the one-pass method be used when laying down the crack-starter bead.)

Koshizuka et al, in the fifth paper, also go on to estimate the NDT temperatures from K_{Id} values obtained from instrumented precracked Charpy specimens; they obtained good agreement.

The sixth paper, by *Hartbower,* points out the difficulties in interpreting the results when there is a through-thickness toughness gradient in the material and the DW test specimen is taken from the surface, as specified by ASTM Method E 208-69(1975). This gradient also manifests itself in the visual determination of whether the top-surface crack extends to the specimen edges and thus whether or not the specimen is "broken." The author suggests heat tinting the specimen after the test and then breaking it open to examine the extent of the original fracture.

Low and Early present the results of DW tests using specimens with curved surfaces, which had been removed from plates that were curved in two orthogonal directions. Their results indicate that the effect of the curvature is greater when the crack-starter weld is on the tension surface than when it is on the compression surface; however, they caution that the shift in NDT temperature may be masked by the inaccuracy associated with the E 208 test method.

Because many material specifications couple DW transition temperatures with Charpy V-notch transition temperatures to obtain a "reference temperature," data contained in a data bank were investigated by the authors of the eighth paper, *Oldfield and Server,* using computer techniques to determine reference temperatures for several steels. Predictions by the model of the NDT temperature and reference NDT temperature from dynamic fracture toughness data are in excellent agreement with measured values. They also show the dependency of the upper-shelf Charpy energy values in setting the reference temperature.

The final paper discusses the DW test from a fracture mechanics point of view. The author, *Sumpter,* postulates that shear lip development may be the common factor, which explains the empirically observed correlation between K_{Id} and the DW nil-ductility transition temperature.

The end of this volume contains an appendix, in which ASTM Method E 208 is reprinted in full. The version printed, E 208-85, was approved in 1985 and is the most recent version of this standard.

The editors of this publication would like to thank the authors and presenters at the symposium for their papers and the continuing discussion. A thank-

you is also extended to those who reviewed the manuscripts, and to the editors at ASTM, especially Helen Mahy, who saw to it that this Special Technical Publication was published.

John M. Holt

Consultant, Pittsburgh, PA 15235; editor.

P. P. Puzak

Consultant, Carlsbad, CA 92008; symposium chairman and editor.

Yoshio Ando,[1] *Nobukazu Ogura,*[2] *Hiroshi Susukida,*[3] *Masanobu Satoh,*[3] *Yasuhiko Tanaka,*[4] *and Ejo Ando*[5]

Effect of the Brittle-Bead Welding Conditions on the Nil-Ductility Transition Temperature

REFERENCE: Ando, Y., Ogura, N., Susukida, H., Satoh, M., Tanaka, Y., and Ando E., **"Effect of the Brittle-Bead Welding Conditions on the Nil-Ductility Transition Temperature,"** *Drop-Weight Test for Determination of Nil-Ductility Transition Temperature: User's Experience with ASTM Method E 208, ASTM STP 919*, J. M. Holt and P. P. Puzak, Eds., American Society for Testing and Materials, Philadelphia, 1986, pp. 1-15.

ABSTRACT: The drop-weight test plays an important role in determining the reference nil-ductility transition temperature (RT_{NDT}), which indicates the fracture toughness characteristics of ferritic steels in the design of nuclear power plant components. In recent years, however, it has been shown by various papers that the nil-ductility transition temperature (NDTT) obtained by this test depends on such parameters as the welding conditions of the crack-starter bead, notch location, and other factors.

In this paper, the authors have investigated the scattering of NDTT and discuss the necessity of revising Japan Electric Association Code 4202, The Method of Drop-Weight Testing of Ferritic Steels, under the auspices of the Japan Electric Association; this standard refers to the practical welding conditions employed by many research organizations in Japan.

From the results of this study on the effects of such parameters as the welding current, preheating, interpass temperature, shape of bead, welding speed, and notch location on NDTT, the authors conclude that the most influential factor to be determined for prevention of wide scattering of NDTT is the welding current. Based upon these results, standard JEAC 4202 was revised on 20 March 1984.

KEY WORDS: nil-ductility transition temperature, drop-weight test, scattering, crack-

[1]Professor emeritus, University of Tokyo, Tokyo 113, Japan.

[2]Professor, Yokohama National University, Yokohama 240, Japan.

[3]Advisor and assistant chief research engineer, respectively, Material and Strength Research Laboratory, Takasago Technical Institute, Mitsubishi Heavy Industries, Ltd., Takasago 676, Japan.

[4]Research engineer, Research Laboratory, The Japan Steel Works, Ltd., Hokkaido 051, Japan.

[5]Manager, Nuclear Power Division, Ishikawajima-Harima Heavy Industries, Ltd., Yokohama 235, Japan.

starter bead, welding current, notch location, preheating, ferritic steel, nuclear power plant components, ASTM standard E 208

The drop-weight test has played an important role in determining the reference nil-ductility transition temperature (RT_{NDT}), which represents the fracture toughness of ferritic steels in the design of nuclear power plant components. In recent years, however, several papers have been presented stating that the nil-ductility transition temperature (NDTT) depends on such parameters as the welding conditons of the crack-starter bead, notch location, and other factors [*1-5*].

As clearly shown in these papers, the phenomenon of NDTT scattering has been considered to relate closely to the toughness of the heat-affected zone formed by crack-starter bead welding. Since the drop-weight test is to be conducted at intervals of 5°C using several test specimens, it may be difficult to eliminate the scattering entirely. However, in view of its influence on the reliability of the design of nuclear power plant components, a difference in NDTT of more than 25°C, as shown in Table 1 [*1,3*], should be avoided. Although the question leaves room for discussion, it would be desirable to limit the difference in NDTT to within 10°C.

TABLE 1—*Effect of the welding conditions of the crack-starter bead on NDTT (from Refs* 1 *and* 3*).*

Material Tested : A508 Cl.3

Crack-Starter Bead \ Test Temp. °C				-45	-40	-35	-30	-25	-20	-15	NDTT °C
A	Standard (2 pass)	160A	FOX-D	●	○ ○		○				-45
B	Standard (2 pass)	180A	FOX-D	●		● ○	○ ○				-35
C	Standard (2 pass)	200A	FOX-D				● ○	● ○	○ ○		-25
D	Standard (2 pass)	160A	Murex-H	●	●	○ ○					-40
E	Standard (2 pass)	180A	Murex-H				●	○ ○			-30
F	1 Pass	180A	FOX-D				●	●	●	○ ○	-20
G	1 Pass	200A	FDX-D				●	●	●	○ ○	-20
H	Fatigue Crack Notch	-	-			●		●	●	○ ○	-20

Electrode··· FOX-D:FDX DUR 350,Murex-H:Murex Hardex N, ● : Break ○ : No Break

According to the papers referred to [*1-5*], the parameters that are supposed to be influential in determining the phenomenon of scattering show a wide range of changes: that is, some of the data differ widely from those of the welding conditions actually adopted.

In this paper, the authors have investigated the phenomenon of scattering of NDTT by referring to the welding conditons employed in practice by many research organizations and have discussed the problem of whether or not it would be necessary to revise the provisions of the Method of Drop-Weight Testing of Ferritic Steels, Japan Electric Association Code (JEAC) 4202, which was enacted in 1970 and refers to the ASTM Method for Conducting Drop-Weight Test to Determine Nil-Ductility Transition Temperature of Ferritic Steels (E 208-69).

Effect of Parameters on NDTT

Welding Current

Table 1 [*1,3*] and Table 2 [*2*] show the effect of welding conditons of the crack-starter bead on NDTT. These tables show that NDTT varies over a range of 25°C, depending on the value of the welding current. As the result of tests for ASTM A508 Class 2 and 3 steels, the lower NDTTs are given when the welding current is lower, and the difference in NDTTs between specimens welded at 160 A and those at 200 A reaches 25°C. However, if the result is rearranged by limiting the welding current within the range of 180 to 210 A, which is recommended by the provisions of Standard JEAC 4202, the maximum difference in NDTT is less than 10°C, as shown in Table 3.

Tables 4 and 5 [*6*] show NDTTs obtained when the bead was welded at between 180 and 210 A for ASTM A508 Class 3; A533 Grade B, Class 1; A533 Grade A, Class 1; and A516 Grade 70 steels. In this test, the test specimens were prepared from the different thickness locations of the steels and the weld metals, and Murex Hardex N and NRL-S electrodes, recommended in ASTM Method E 208-81, were used as the electrodes. According to the result, the maximum difference in NDTT remains within 10°C.

Figure 1 [*7*] shows the results of tests carried out for 80 test specimens cut out from an A508 Class 3 steel at the same thickness location of the steel. The test specimens were divided into two lots of 40 specimens each and the crack-starter beads were welded at 180 A for one lot and at 200 A for the other. Two specimens, one from each lot, were tested at the same temperature at intervals of 5°C, and the results are shown in Fig. 1 divided into "break" and "no break" categories. Specimens welded at 180 A showed a "no break" trend. Figure 2 [*7*] shows the results of calculations of the probability with which each temperature becomes the NDTT under the test conditions used. For the specimens welded at 200 A, NDTTs lie in the range of −40 to −30°C with a scattering of 10°C; for the specimens welded at 180 A, NDTTs lie in the range

TABLE 2—*Effect of the welding conditions of the crack-starter bead on NDTT (from Ref 2).*

Material Tested : A508 Cl.2

	Welding Sequence	Amperage A	Test Temperature °C											NDTT °C
			-50	-45	-40	-35	-30	-25	-20	-15	-10	-5	0	
A	2 pass	150/160	●	●	○○		○							-45
B	2 pass	170/180	●	●	○○		○							-45
C	2 pass	190/200			●	●	●	○○						-30
D	1 pass	150/160					●				●	●	○○	-5
E	1 pass	170/180					●				●	○○	○	-10
F	1 pass	190/200					●				●	○○	○	-10

Electrode : FOX DUR 350 ● :Break ○ :No Break

TABLE 3—*Effect of the welding conditions of the crack-starter bead on NDTT (from Ref 7).*

Material Tested : A508 Cl.3

Amperage(A)	Polarity	Electrode	Test Temperature °C				NDTT °C
			-35	-30	-25	-20	
180A	AC	Fox Dur 350	● ○	○ ○			-35
200A	AC	Fox Dur 350		● ○	● ○	○ ○	-25
180A	AC	Murex Hardex N		●	○ ○		-30

●: Break ○: No Break

TABLE 4—*Results of the drop-weight test (from Ref 6).*

Material Tested: A508 Cl. 3, A533 Gr. B Cl. 1, A533 Gr. A Cl. 1, A516 Gr. 70 Base Metals

Steel	Welding Condition		Test Temperature, °C											NDTT °C
			-65	-60	-55	-50	-45	-40	-35	-30	-25	-20	-15	
A508 Cl. 3 Base Metal (1/4t)	NRL-S	210A									●	7 Ⓓ4 ●	5 Ⓓ6 5 Ⓓ6	-20
		190A									●	6 Ⓓ8 ◐10	7 Ⓓ8 6 Ⓓ9	-25
		190A									◐7	◐6	0 Ⓓ1 7 Ⓓ3	-20
	Murex Hardex N	190A						●		●	0.3 Ⓓ0.3 1 Ⓓ1			-30
		180A				●		●	12 ◐	◐10	1 Ⓓ1 0 Ⓓ0			-30
A508 Cl. 3 Base Metal (Surface)	NRL-S	210A						●	◐11	7 Ⓓ5 4 Ⓓ4				-35
		190A				●	8 Ⓓ7 ●	8 Ⓓ7.5 5 Ⓓ8		5 Ⓓ5.5				-45
		190A					●	1.5 Ⓓ6 ●	8 Ⓓ5 7 Ⓓ5	6 Ⓓ6				-40
	Murex Hardex N	190A					●	4 Ⓓ5 1 Ⓓ0.5						-45
A533 B Cl. 1 Base Metal (1/4t)	NRL-S	210A							●	5.5 Ⓓ7 8 Ⓓ8				-35
		190A						●	◐ 10	8 Ⓓ7.5 11 Ⓓ7.5				-35
		190A							●	8 Ⓓ5 2 Ⓓ1				-35
A533 A Cl. 1 Base Metal (1/4t)	NRL-S	210A									●	5 Ⓓ2 ●	3 Ⓓ6 3 Ⓓ7	-20
		190A								◐16	10 Ⓓ9 ●	1 Ⓓ1 5 Ⓓ6		-25
		190A								◐13	5.5 Ⓓ1 ●	1 Ⓓ1 1 Ⓓ1		-25
A516 Gr. 70 Base Metal (1/4t)	NRL-S	210A						●	12 Ⓓ12 12 Ⓓ12					-40
		190A							●	10 Ⓓ10 10 Ⓓ13	1 Ⓓ1			-35
		190A						●	11 Ⓓ13 11 Ⓓ8					-40

● :Break(Both sides) ◐ :Break(One side) Ⓓ:No Break(Numerals indicate crack extension)

of −45 to −30°C with a scattering of 15°C. As the probability with which NDTT becomes −45°C is 0.03, it may be expected that the scattering of NDTTs at 180 A will remain within 10°C.

While the scattering of NDTTs is expected to remain within 10°C if the welding current lies within the range of 180 to 210 A, which is recommended

TABLE 5—*Results of the drop-weight test for welded joints (from Ref 6).*

Material Tested : A533 Gr. B Cl.1 Weld Metals

Welded Joint	Welding Condition		Test Temperature, °C											NDTT °C
			-80	-75	-70	-65	-60	-55	-50	-45	-40	-35	-30	
A533 B Cl.1 SAW Weld Metal	NRL-S	210A			●	●	ⓓ13 ⓓ16 ⓓ13 ⓓ14							-65
		190A				◐15	ⓓ15 ⓓ13 ⓓ15 ⓓ16							-65
		190A			●	◐	ⓓ7 ⓓ8 ⓓ14 ⓓ13							-65
A533 B Cl.1 SMAW Weld Metal	NRL-S	210A									●	◐15	ⓓ9 ⓓ14 ⓓ5 ⓓ3	-35
		190A								◐6	ⓓ5 ⓓ6 ⓓ12 ⓓ15			-45
		190A									◐11	ⓓ12 ⓓ15 ⓓ13 ⓓ14		-40

● :Break(Both sides) ◐ :Break(One side) ⓓ : No break(Numerals indicate crack extension)

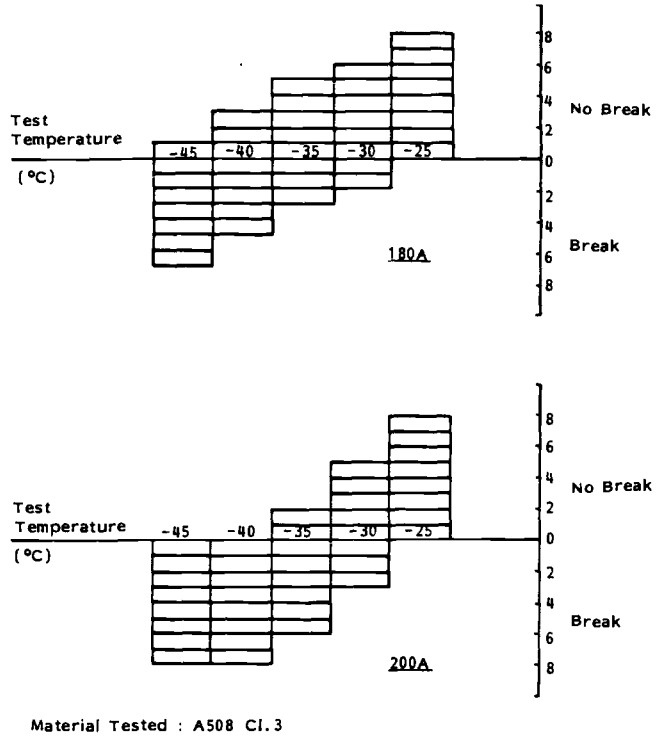

FIG. 1—*Results of the drop-weight test [7]. The vertical axes indicate the number of specimens.*

by Standard JEAC 4202, the possibility of occurrence of an extraordinary NDTT value still exists if an extreme value of the welding current is used. Therefore, if the provisions of Standard JEAC 4202 are to be revised, the value of the welding current should be clearly stated. The range of 180 to 200 A is considered appropriate as the value of the welding current.

Notch Location

While the notch location has been raised as one of the factors that affect NDTT, it is difficult to standardize or unify it sufficiently, because a slight difference in the welder's skill in the treatment of the crater would cause a subtle difference in the shape of the weld bead. However, it has been possible to get nearly the same notch location if normal welding—namely, the welding method in accordance with the provisions of Standard JEAC 4202—is employed.

Figures 3 [*7*] and 4 [*8*] show distributions of the distance between the crater edge of the weld bead of the second pass and the center of the notch measured

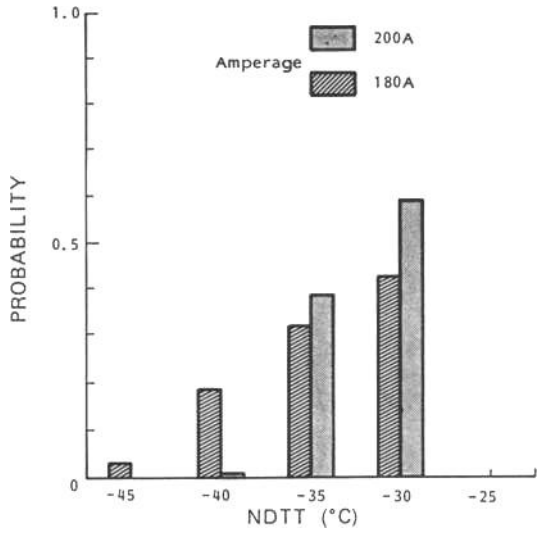

Probability on No Break at each temperature

Amperage	-45°C	-40°C	-35°C	-30°C	-25°C
180A	$\frac{1}{8}$	$\frac{3}{8}$	$\frac{5}{8}$	$\frac{6}{8}$	1
200A	0	0	$\frac{2}{8}$	$\frac{5}{8}$	1

Example of Calculation

Probability at NDTT=-40°C(180A)

(a) -30°C --- 2 Specimens No Break

$$\frac{6}{8} \times \frac{6}{8} = \frac{36}{64}$$

(b) -35°C --- 2 Specimens No Break

$$\frac{5}{8} \times \frac{5}{8} = \frac{25}{64}$$

(c) -40°C --- 1 Specimen or 2 Specimens Break

$$\frac{3}{8} \times \frac{5}{8} \times 2 + \frac{5}{8} \times \frac{5}{8} = \frac{55}{64}$$

$\therefore$ (a) and (b) and (c)

$$\frac{36}{64} \times \frac{25}{64} \times \frac{55}{64} = \frac{49500}{262144} = 0.19$$

FIG. 2—*Probability of NDTT determined by two lots of 40 specimens at each temperature [7]*

on test specimens, with weld beads in accordance with the provisions of Standard JEAC 4202, used in two research organizations. Although there is a wide difference in the number of specimens—230 versus 14—the average values for both examples—9.15 and 9.45 mm—nearly coincide, and their standard deviations give similar values of 0.96 and 0.75 mm, respectively. It is also known

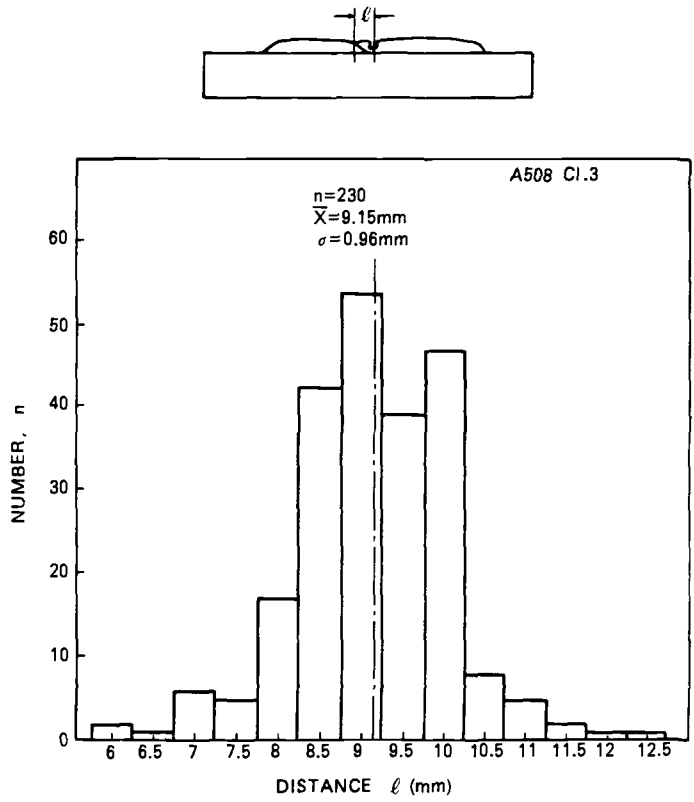

FIG. 3—*Distance from the crater edge of the second bead to the notch center for A508 Class 3 steel [7].*

from Fig. 5 [*4*] that for scattering on the order of 9.0 to 9.5 mm, no significant difference in NDTT occurs. However, if the length of overlap is extremely small, the possibility of occurrence of an extraordinary NDTT exists.

Preheating and Interpass Temperature

In Table 6 [*8*], NDTTs for A533 Grade B, Class 1 steels of two heats welded at 190 A with preheating at 150°C and without preheating are presented. From the table it is apparent that the preheating does not have any significant influence on NDTT. However, applying preheating gives an unnecessary heating history to the test specimen, and a high interpass temperature has an effect on the second-pass welding similar to that of preheating.

According to the data in Table 6, no significant difference is observed from

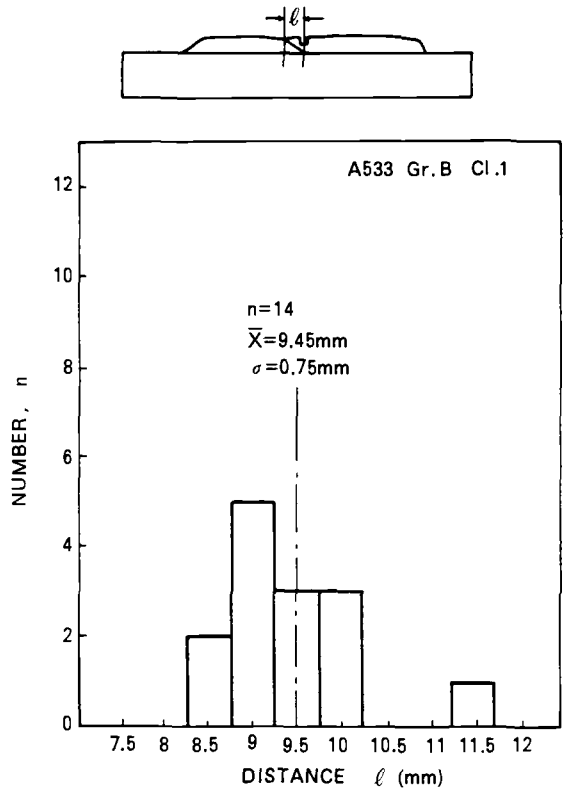

FIG. 4—*Distance from the crater edge of the second bead to the notch center for A533 Grade B, Class 1 steel [8].*

preheating. However, in view of the principles that giving an unnecessary heating history to the test specimen should be avoided and that the brittle bead should be welded, preheating is not needed, and the interpass temperature should preferably be kept at the room temperature as well.

Shape of Bead

There has been no paper stating that the shape of the bead affects NDTT. Some provision about the shape is necessary, if only because the crack does not always initiate from the notch if the height of the bead is unusually low. If the welding is performed within the range recommended by Standard JEAC 4202, the height of bead necessary to make a crack initiate at the proper position can be obtained.

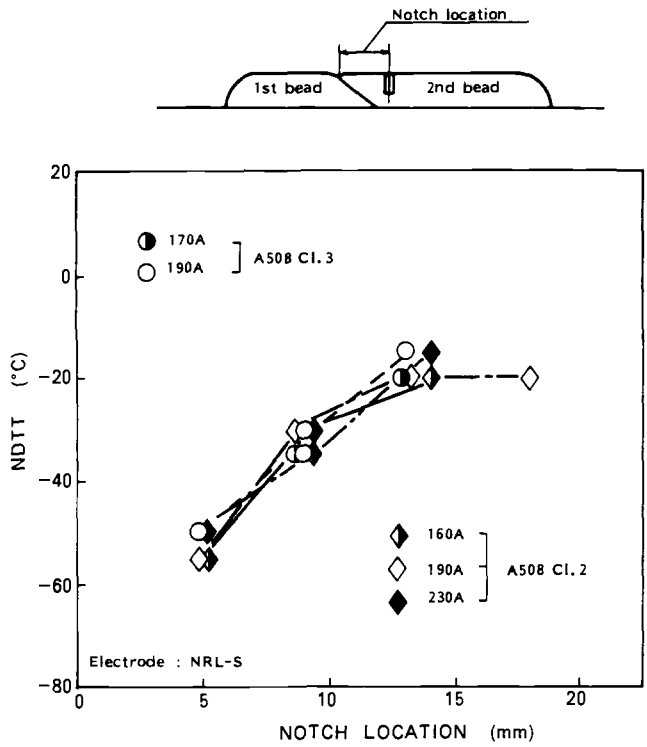

FIG. 5—*Effect of notch location on NDTT [4].*

Welding Speed

There has been no paper stating that welding speed affects NDTT. It has been made clear from the experiences of the research organizations concerned, that in order to satisfy fully the conditions recommended by Standard JEAC 4202 for the shape of the bead, the welding speed should be within a maximum of 170 mm/min.

Summary

From the investigations described, one may conclude that in reviewing the provisions of Standard JEAC 4202 for preventing scattering of NDTT, the most influential factor is the welding current. By clearly stating mandatory values of welding current as a provision of Standard JEAC 4202, the problem of scattering of NDTT is considered to be solved. The recommended values, 180 to 200 A, are considered to be adequate from the results of this study and are consistent with a recommendation of ASTM Method E 208-81. Other conditions, such as notch location, drying of electrodes, preheating, continu-

TABLE 6—*Effect of preheating on NDTT (from Ref 8).*

Test No.	Amperage	Preheating	Polarity	NDTT °C											
				A533 Gr. B Cl.1 (Heat A)						A533 Gr. B Cl.1 (Heat B)					
				-50	-45	-40	-35	-30		-50	-45	-40	-35	-30	
1	190A	YES	DC-RP			O	O					O	O		
2	190A	NO	DC-RP		O							O	O		
3	190A	YES	AC									O	O		
4	165A	YES	DC-RP			O	O					O		O	

ous welding, dimensions of the bead, and welding speed, should preferably be included in the interpretation section of Standard JEAC 4202.

Based upon the recommendations just made, Standard JEAC 4202 was revised on 20 March 1984. The principal items revised are the following:

Welding Current and Welding Speed

Content of Revision—The welding current was specified to be between 180 and 200 A in the provision section and was stated in the interpretation section as well. The welding speed was stated to be a maximum of 170 mm/min in the interpretation section.

Reasons—The welding current range was narrowed to reduce scattering, and to conform with ASTM Method E 208-81, thus, giving the standard an international nature. The welding speed follows the conventional practice. (The minimum speed of 150 mm/min stated earlier in the interpretation was difficult to maintain.)

Notch Location

Content of Revision—Remarks were inserted in the interpretation that the notch location should not come closer to the crater edge of the weld bead than about 5 to 6 mm. However, a notice was added that measurement of the distance was not particularly required, since the notch location is placed at a distance of about 9 to 10 mm, if the welding is done normally.

Reasons—Since an abnormal NDTT would be produced if the notch location were placed at a distance closer than 5 to 6 mm from the crater edge of the weld bead, weld beads with extremly small overlap are forbidden.

Drying of the Electrode, Preheating, and Continuous Welding

Content of Revision—The conditions for drying of the electrode, preheating, and continuous welding were stated in the interpretation as follows:

1. *Drying of the Electrode*—This is done at above 150°C and for longer than 1 h.
2. *Preheating*—There is no preheating.
3. *Continuous Welding*—After the welding of the first pass is finished and cooled in air, the welding of the second pass is applied. Rapid cooling after welding is forbidden.

Reasons—The welding conditions that have generally been practiced and that research organizations have considerable experience with are indicated. Extraordinary methods of welding are forbidden. Preheating is not employed because the purpose of the crack-starter weld is embrittlement. At the time of continuous welding if rapid cooling by way of an air blast or others means

after welding is adopted to save time, the characteristics of the heat-affected zone or the NDTT may be influenced.

Dimensions of the Weld Bead

Content of Revision—The provisions for the dimensions of the weld bead were left as they were.

Reasons—According to past experience, a sufficient height of bead is invariably achieved if the welding curent and the length and width of bead required maintained.

Acknowledgments

This study was conducted by the Working Group on the Method of Drop-Weight Testing of Ferritic Steels, under the sponsorship of Subcommitee 2-PF (H. Susukida, chairman) of the Atomic Energy Committee of the Japan Electric Association. The authors wish to express their hearty thanks to other members of the Working Group for their advice.

References

[1] Onodera, S., Tsukada, H., Suzuki, K., Iwadate, T., and Tanaka, Y., "A Study on Pellini Test: Reproducibility and Welding Procedure," *Proceedings*, Sixth Staatliche Material Pruefungs Anstalt, University of Stuttgart, Stuttgart, West Germany, October 1980.

[2] Tsukada, H., Suzuki, K., Iwadate, T., and Tanaka, Y., "A Study on Drop Weight Test Using A508 Cl.2 Steel," JSW Report R MS 81-60, The Japan Steel Works, Tokyo, Japan, December 1981.

[3] Tsukada, H., Suzuki, K., Satoh, I., Iwadate, T., Tanaka, Y., and Kurihara, I., *Journal of the Iron and Steel Institute of Japan*, Vol. 66 No. 5, 1980.

[4] Takano, M., Kushida, S., and Abe, N., *Journal of the Iron and Steel Institute of Japan*, Vol. 67 No. 5, 1981.

[5] Koshizuka, N., Enami, T., Tanaka, M., Hiro, N., Yoshimura, S., Kusuhara, H., Fukuda, H., and Shinohara, T., *Journal of the Iron and Steel Institute of Japan*, Vol. 66, No. 5, 1980.

[6] Mitsubishi Heavy Industries, Ltd., data presented at a meeting of Subcommittee 2-PF of the Atomic Energy Committee, Japan Electric Society, Tokyo, Japan, 1982.

[7] Japan Steel Works, Ltd., data presented at a meeting of Subcommittee 2-PF of the Atomic Energy Committee, Japan Electric Society, Tokyo, Japan, 1982.

[8] Ishikawajima-Harima Heavy Industries Co., Ltd., data presented at a meeting of Subcommittee 2-PF of the Atomic Energy Committee, Japan Electric Society, Tokyo, Japan, 1982.

Masanobu Satoh,[1] *Tatsuo Funada,*[1] *and Minoru Tomimatsu*[1]

Evaluation of Valid Nil-Ductility Transition Temperatures for Nuclear Vessel Steels

REFERENCE: Satoh, M., Funada, T., and Tomimatsu, M., **"Evaluation of Valid Nil-Ductility Transition Temperatures for Nuclear Vessel Steels,"** *Drop-Weight Test for Determination of Nil-Ductility Transition Temperature: User's Experience with ASTM Method E 208, ASTM STP 919*, J. M. Holt and P. P. Puzak, Eds., American Society for Testing and Materials, Philadelphia, 1986, pp. 16-33.

ABSTRACT: The causes of data scatter in nil-ductility transition (NDT) temperature were investigated to establish appropriate conditions for crack-starter bead welding. Drop-weight tests were carried out for nuclear vessel steels by changing the welding conditions to examine the effects of welding amperage and shapes of heat sinks on NDT temperature. The results show that preparation of the crack-starter bead by low welding amperage should not be allowed, because it makes the measured NDT temperature nonconservative, and that it is important to use a heat sink which increases the cooling rate of the specimen.

In addition, the authors propose methods for estimating the NDT temperature of nuclear vessel steels by using Charpy transition temperatures.

KEY WORDS: nil-ductility transition temperature, welding amperage, heat sink, fracture mechanics, drop-weight test, nuclear vessel steel, crack-starter bead, Charpy transition temperature, ASTM standard E 208

In the American Society of Mechanical Engineers (ASME) Boiler and Pressure Vessel Code, Sections III and XI, the reference nil-ductility temperature (RT_{NDT}) of component materials is essential in fracture mechanics analysis of the integrity of components. Although both the drop-weight test and the Charpy impact test are required to determine RT_{NDT}, in most cases, RT_{NDT} is dominated by the nil-ductility transition (NDT) temperature (NDTT) obtained by the drop-weight test. However, it is becoming recognized [*1,2,3*] that NDTT depends on the drop-weight testing conditions, some of which may yield a nonconservative evaluation for nuclear vessel steels.

[1]Assistant chief research engineers and senior research engineer, respectively, Mitsubishi Heavy Industries, Ltd., Takasago Technical Institute, Takasago 676, Japan.

Therefore, the causes of data scatter in NDTT were investigated to find an appropriate drop-weight testing method with a smaller amount of scatter in NDTT. Furthermore, correlations between NDTT and other toughness parameters were examined and methods for estimating NDTT are proposed.

Effects of Crack-Starter Bead Welding Conditions on NDT Temperature

The data scatter in NDTT may be caused by the scatter in the toughness of the test material itself, crack-starter bead welding conditions, specimen geometry, impact energy, impact velocity, and so on. Setting aside the scatter in the toughness of the material, the crack-starter bead welding conditions for drop-weight test specimens may be a primary factor. Figure 1 shows the toughness of an A508 Class 3 steel after a thermal cycle simulating the temperature history of a drop-weight test specimen during crack-starter bead

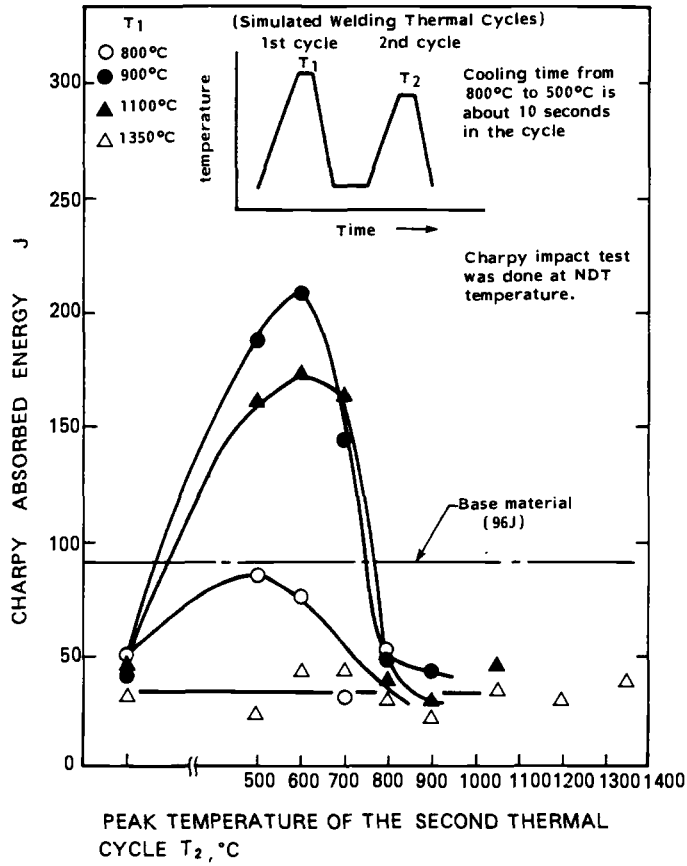

FIG. 1—*Effects of thermal cycles on the toughness of A508 Class 3 steel.*

welding, in accordance with the ASTM Method for Conducting Drop-Weight Test to Determine Nil-Ductility Transition Temperature of Ferritic Steels (E 208-81). The toughness of the steel tends to decrease or increase depending on the temperature history of the first and second thermal cycles. In particular, it is noteworthy that, when the steel is reheated in the temperature range of 500 to 700°C in the second cycle, after being rapidly cooled from 900 to 1100°C in the first cycle, toughness is greatly improved because of the tempering effect. However, for the other steels, the improvement in the toughness is not as great. The results of these thermal cycle tests suggest that toughness depends on the microstructure that forms in the heat-affected zone (HAZ) during crack-starter bead welding.

A schematic diagram of the fracture behavior of a drop-weight test specimen whose HAZ contains the complicated toughness distribution produced by the conditions described is shown in Fig. 2, based on the concept of fracture mechanics. When assuming a semielliptical crack, K_{IA}, which designates the stress intensity factor at maximum crack depth, has the trend shown in the Fig. 2*a*. A crack initiated in a brittle crack-starter bead may penetrate the thickness of the specimen when the toughness of the HAZ is low; however, when the toughness of the HAZ is improved, the crack would be arrested in it. On the other hand, the stress intensity factor K_{IB} at the surface tends to increase as the crack propagates towards the edge of the specimen, as shown in Fig. 2*b*. Whether the crack penetrates the width of the specimen or is arrested depends on the toughness and location ℓ of the improved HAZ.

Koshizuka et al [*4*] report that the toughness level and width vary with the location of the notch. As the depth of a crack increases, K_{IB} increases and the crack tends to propagate to the edge of the tension surface. Since the "break" or "no break" results described in ASTM Method E 208-81 are determined by crack penetration to the edge of the tension surface, NDTT depends strongly on the toughness level and the location of the HAZ on the surface.

Figure 3 shows a typical fracture surface of a drop-weight test specimen. A crack initiated at the crack-starter bead was arrested in the improved HAZ for the case shown in Fig. 3 (*top*). In another case, the crack nearly penetrated the thickness but was arrested in the HAZ on the edge of the tension surface, and it was judged a "no break" result (Fig. 3 (*bottom*)). These fracture mechanics results suggest that NDTT may be affected by the HAZ formed during crack-starter bead welding.

This paper describes the drop-weight test results for nuclear vessel steels with various crack-starter bead welding conditions and proposes appropriate conditions for crack-starter bead welding.

Materials Used

The following six steels were used as testing materials:

1. A508 Class 3 steel (thickness, 300 mm)

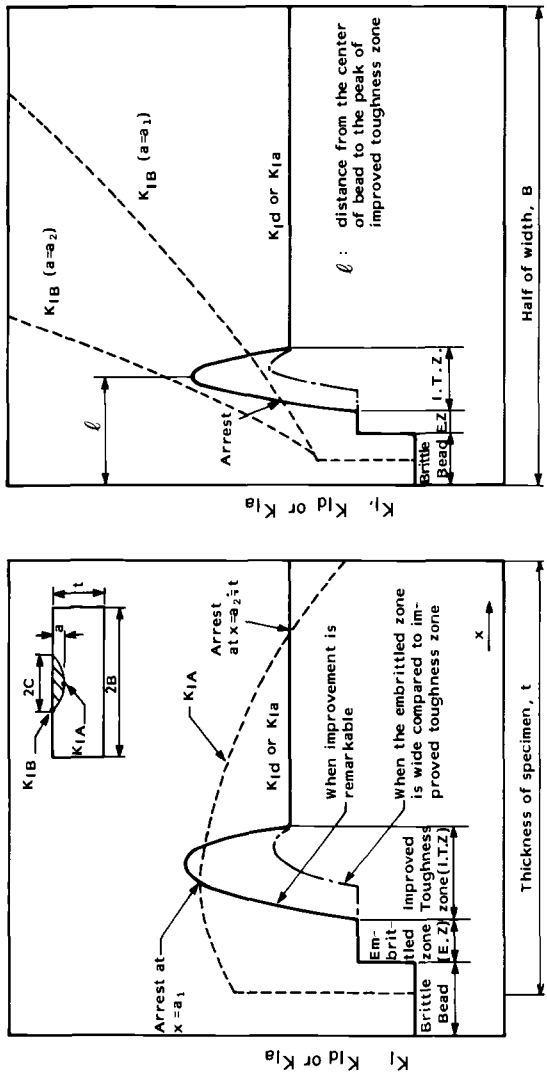

FIG. 2—*Schematic diagrams of fracture behavior of a drop-weight test specimen in accordance with fracture mechanics analysis.*

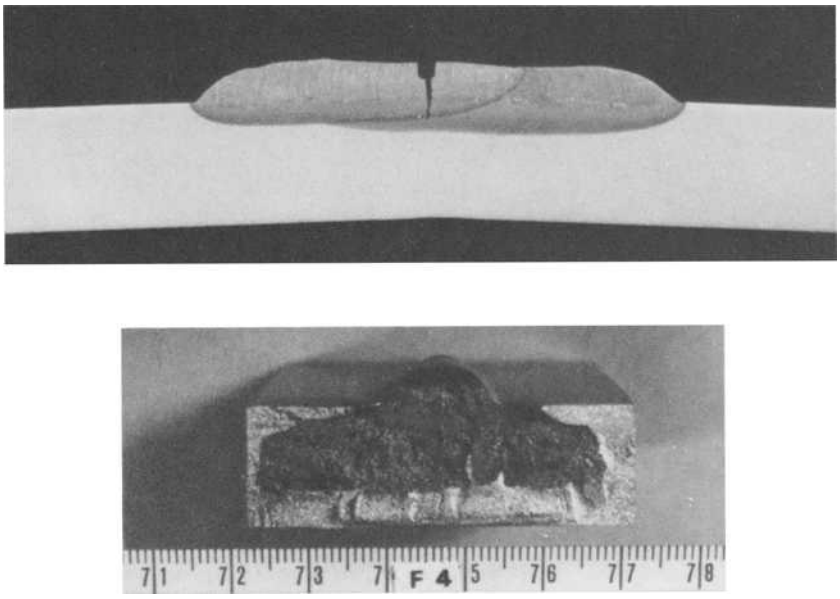

FIG. 3—*Examples of fracture surfaces of drop-weight test specimens—cross sections of A508 Class 3 steels at NDTT + 5°C.*

2. A533 Grade B, Class 1 steel (thickness, 210 mm)
3. A533 Grade A, Class 1 steel (thickness, 115 mm)
4. A516 Grade 70 steel (thickness, 45 mm)
5. A533 Grade A, Class 1 steel (thickness, 115 mm)
6. A516 Grade 70 steel (thickness, 100 mm)

The chemical compositions and tensile properties of these materials are shown in Table 1. Steels 1 through 4 were used to investigate the effect of the welding amperage on NDTT, whereas Steels 5 and 6 were used to examine the effect of the shapes of heat sinks.

Test Procedure

Effect of Welding Amperage

Type P-3 specimens, specified by ASTM Method E 208-81 were used. Crack-starter beads for the specimens were prepared with a wide variety of welding amperages. The welding conditions of the crack-starter beads are summarized as follows:

welding amperage:	160, 180, 190, and 210 A
arc voltage:	24 to 26 V
speed of travel:	14 to 15 cm/min

TABLE 1—*Chemical compositions and tensile properties of the steels used.*

Material	Thickness, mm	Chemical Composition, weight %									Tensile Properties[a]		
		C	Si	Mn	P	S	Cu	Ni	Cr	Mo	$\sigma_{0.2}$, MPa	σ_B, MPa	δ, %
A508 Cl.3	300	0.18	0.28	1.39	0.005	0.003	0.03	0.78	0.09	0.50	420	570	30
A533 Gr. B, Cl. 1	210	0.20	0.27	1.47	0.007	0.003	0.12	0.60	0.12	0.47	490	640	28
A533 Gr. A, Cl. 1	115	0.19	0.27	1.39	0.005	0.005	0.03	0.30	0.09	0.50	490	640	28
A516 Gr. 70	45	0.19	0.29	1.15	0.018	0.002	0.12	0.38	0.16	ND[b]	350	550	28
A533 Gr. A, Cl. 1	115	0.19	0.27	1.46	0.003	0.001	0.01	0.35	0.08	0.51	460	600	28
A516 Gr. 70	100	0.18	0.25	1.15	0.010	0.002	0.11	0.35	0.16	ND	310	502	34

[a]Key to symbols.
$\sigma_{0.2}$ = 0.2% yield strength.
σ_B = ultimate tensile strength.
δ = elongation.
[b]ND = not determined.

Murex Hardex-N and NRL-S electrodes were used after the specimens had been dried at 350°C for 1 h. The crack-starter bead was welded using a heat sink (hereinafter referred to as Heat Sink A) that touched the back surface of specimen tightly. Preheating and postheating of the specimen were not adopted.

The tests were carried out in accordance with ASTM Method E 208-81, and the NDTTs were determined.

Effect of the Shapes of Heat Sinks

To investigate the effect of the specimen cooling rate on NDTT, crack-starter beads were prepared using two different types of heat sinks. One was the previously mentioned Heat Sink A, and the other was Heat Sink B, which does not touch the back surface of the specimen. The cooling rate of the specimen using Heat Sink A was faster than that for the specimen using Heat Sink B. The welding amperage was 190 A and the other conditions were those given previously.

Results and Discussion

Table 2 shows NDTTs obtained for the specimens in which the crack-starter beads were prepared using various welding amperages. The ΔT_{NDT}, which is the difference between the NDTT T_{NDT} for each welding amperage, and the maximum NDTT $T_{NDT}(\max)$, that is

$$\Delta T_{NDT} = T_{NDT} - T_{NDT}(\max) \tag{1}$$

is shown against the welding amperage in Fig. 4. These results suggest that the NDTT tends to become lower with decreasing welding amperage. The scatter in NDTT varies, depending on the testing materials. Although little scatter is observed in the A533 Grade B, Class 1 steel and the A516 Grade 70 steel, a maximum NDTT difference of 35°C is observed in the A508 Class 3 steel.

The data scatter in the NDTT, ΔT_{NDT} for each material, can be correlated with the results of the thermal cycle tests, shown previously in Fig. 1. The greatest data scatter in NDTT was observed for the A508 Class 3 steel, which has a wide improved-toughness zone with a high toughness level, whereas less data scatter is observed for the A516 Grade 70 steel, which has a narrower improved-toughness zone.

The effect of welding amperage on NDTT was then investigated, based on fracture-mechanics considerations, for such steels as A508 Class 3 steel, for which the toughness of the HAZ can be improved. As shown in Fig. 2, the

TABLE 2—*Results of drop-weight tests—effect of welding amperage.*

Material	Electrode	Amperage, A	Test Temperature, °C										NDTT °C
			-60	-55	-50	-45	-40	-35	-30	-25	-20	-15	
A508 Cl. 3 (1/4t)	NRL-S	210								●	●○	○○	-20
		190							●	●○	○○		-25
	Murex Hardex N	190					●		●	○○			-30
		180					●	●	●	○○			-30
		160	●	●	○○		○						-55
A508 Cl. 3 (Surface)	NRL-S	210					●	●	○○				-35
		190			●	●○	○○		○				-45
	Murex Hardex N	190				●	○○						-45
		180	●	●	○○	○							-55
		160	●	●	○○	○							-55
A533 B Cl. 1 (1/4t)	NRL-S	210						●	○○				-35
		190					●	●	○○				-35
		160			●	●	●	○○					-40
A533 A Cl. 1 (1/4t)	NRL-S	210								●	●○	○○	-20
		190							●	●○	○○		-25
		160						●	●	○○			-30
A516Gr. 70 (1/4t)	NRL-S	210					●	○○					-40
		190						●	○○	○			-35
		160				●	●	○○					-40

●Break ○No Break

judgement of a "break" or "no break" result for a drop-weight test specimen is done according to the penetration or arrest of a crack initiated from the bead of the specimen. The lowest temperature at which the crack is arrested in the improved HAZ is assumed to be an apparent NDTT and can be calculated from the equation which follows. Assuming that the flaw size is identified as the boundary separating the embrittled and improved zones of the HAZ, K_I was calculated using the Newman and Raju equation [5], as follows.

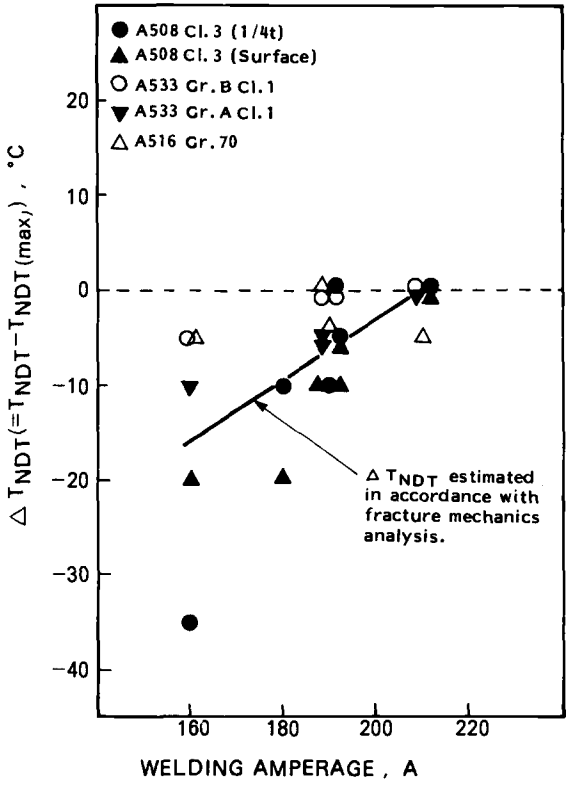

FIG. 4—*Relationship between* T_{NDT} *and the welding amperage.*

$$K_I = M\left(\frac{a}{t}, \frac{a}{c}\right)\sigma_b\sqrt{\frac{\pi a}{Q}} \tag{2}$$

where

a = flaw depth,
c = half of the surface flaw length,
M = correction factor for K_I,
Q = flaw shape parameter, and
σ_b = bending stress (600 MPa).

In addition, the specimen is assumed to be subjected to bending stress corresponding to the dynamic yield strength of the material.

Meanwhile, the crack-arrest fracture toughness K_{Ia} was assumed to be represented by the reference stress intensity factor described in the ASME Boiler and Pressure Vessel Code, Section III, that is

$$K_{Ia} = 29.4 + 1.34 \exp\{0.0261(T - RT_I) + 2.32\} \quad (MPa\sqrt{m}) \quad (3)$$

where

T = temperature, °C, and
RT_I = reference nil-ductility temperature of the improved HAZ, °C.

Since $K_I = K_{Ia}$, the relative temperature $(T - RT_I)$ at which the propagating crack is just arrested was obtained and is shown in Table 3. It can be seen in the table that the relative temperature for a welding amperage of 160 A is about 15°C lower than that for a welding amperage of 210 A and that the measured NDTTs for A508 Class 3 steel and A533 Grade A, Class 1 steel show a similar tendency. From this it is clear that the effect of welding amperage on NDTT depends strongly on the size of the embrittled zone, in other words, on the size and location of the improved HAZ.

The results of the experiment and the discussion of it show that a smaller welding amperage may make the measured NDTT nonconservative. Therefore, the preparation of crack-starter beads by low amperage should not be allowed.

Table 4 shows the NDTTs obtained by using different types of heat sinks, and the authors suggest that the NDTT of the specimen prepared using Heat Sink B is about 5°C lower than that for the specimen prepared using Heat Sink A.

From the viewpoint of thermal conductivity, Heat Sink A has the effect of increasing the thickness of the specimen during crack-starter bead welding

TABLE 3—*Data scatter in NDT temperature estimated in accordance with fracture mechanics analysis.*

Amperage, A	Assumed Crack Size, mm		Stress Intensity Factor K_I, MPa $\sqrt{m}$		Relative Temperature $T - RT_I$, °C	
	Depth, a	Surface Length, $2C$	Point A	Point B	Point A	Point B
160	2	12	39.8	28.6	−10.8	. . .
190	3	15	43.4	36.9	0.8	−23.2
210	4	18	45.0	44.1	4.9	2.6

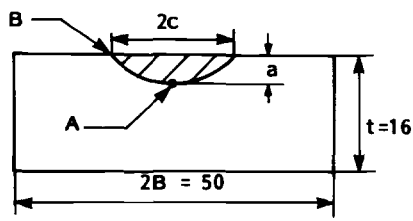

TABLE 4—*Results of drop-weight tests—effect of heat sink.*

Material	Electrode	Amperage, A	Heat Sink [a]	Test temperature, °C						NDTT °C
				-40	-35	-30	-25	-20	-15	
A533 Cl. A	Murex-Hardex N	190	A					●	○ ○	-20
			B				● ●	○ ○		-25
A516Gr.70	NRL-S	190	A			●	● ○	○ ○		-25
			B	●	●	● ○	○ ○			-30

a. Heat Sink

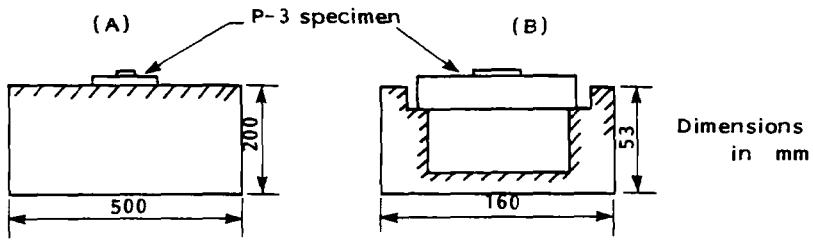

and makes its cooling rate faster than Heat Sink B does. Figure 5*a* shows the relationship between the thickness of the specimen and the time required for the specimen to cool from 800 to 500°C at the center of the bead. The cooling time was calculated by using Rosenthal's temperature distribution equation [*6*]. The measured values are also shown in the figure. It was confirmed experimentally that the Heat Sink A shortens the cooling time by about one half and has the apparent effect of increasing the thickness of the specimen when compared with Heat Sink B. Figure 5*b* shows the relationship between the cooling time and the hardness of the crack-starter bead. The hardness of the bead tends to increase as the cooling time becomes shorter [*3,4*], in other words, as the cooling rate becomes faster. Figure 5*c* shows the relationship between the hardness of the crack-starter bead and ΔT_{NDT}, and the authors suggest that, although the relationship changes from one material to other, stable NDTT are obtainable when the hardness of the bead exceeds a certain level. According to the continuous cooling transformation (CCT) curves for various steels, the effect of the cooling rate mentioned earlier may stem from the fact that the weld metal and HAZ formed in the first pass are well hardened by the satisfactory quenching effect when the cooling rate becomes faster and from the fact that the tempering effect in the second pass is minor and makes improvement of the toughness difficult.

In short, the adoption of a heat sink which tightly touches the back surface of a specimen enables the thickness of the specimen to be apparently increased during crack-starter bead preparation, thereby making the cooling rate faster. As a result, a maximum bead hardness is obtainable and a stable NDTT can be measured. In the case of P-3 specimens in particular, a heat sink of this kind should be used.

Relationship of T_{NDT} to Charpy Impact Characteristics and Fracture Toughness

The preceding sections revealed that NDTT is greatly affected by the welding conditions of the crack-starter bead and that the drop-weight test specimen should be carefully prepared in order to measure NDTT. However, in cases in which the specimen is not appropriately prepared or NDTT has not been previously measured, the NDTT must be estimated as accurately as possible by some means.

The material that follows describes such a method for estimating NDTT after examining the correlation between NDTT and the parameters obtained by the Charpy impact test or fracture toughness test.

Correlation Between T_{NDT} *and Charpy Impact Characteristics*

To investigate the relationship between the NDTT and Charpy impact characteristics, data on about 50 base metals obtained by the authors and

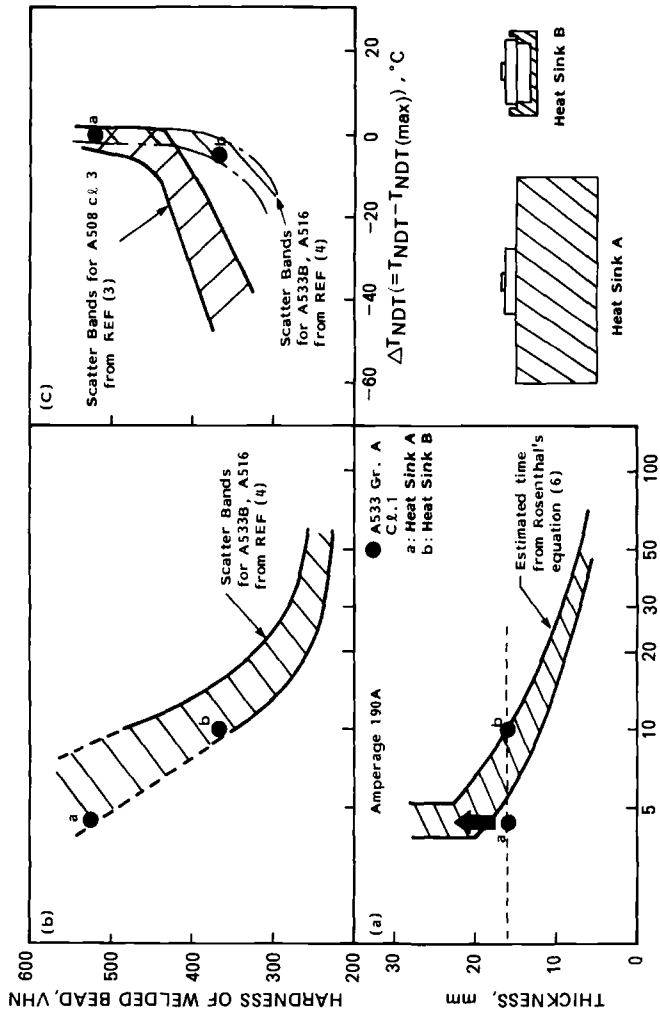

FIG. 5—*Relationships among* T_{NDT}, *the hardness of the welded bead, and the cooling time. This shows the effects of heat sinks on NDT temperature.*

from the Japan Welding Engineering Society [7] were used. As the parameters describing Charpy impact characteristics, three kinds of transition temperatures were employed:

(*a*) the fracture appearance transition temperature vTrs,

(*b*) the temperature at which the absorbed energy reaches 50 ft · lb vTr_{50}, and

(*c*) the temperature at which the lateral expansion reaches 35 mils vTr_{35mils}.

The correlations were obtained by the least squares method as shown here:

$$T_{NDT} = 0.78vTrs - 22.8 \qquad r = 0.93 \tag{4}$$

$$T_{NDT} = 0.70vTr_{50} - 20.4 \qquad r = 0.80 \tag{5}$$

$$T_{NDT} = 0.48vTr_{35mils} - 16.2 \qquad r = 0.86 \tag{6}$$

where T_{NDT} is the NDTT and r represents the coefficient of correlation. Equation 4 gives the best correlation for T_{NDT}. Figure 6 shows the relationship between T_{NDT} and vTrs. Gross [8] and Wilson [9] have proposed the following correlations for base metals.

$$\text{(Gross's equation)} \quad T_{NDT} = 0.89vTrs - 37.5 \tag{7}$$

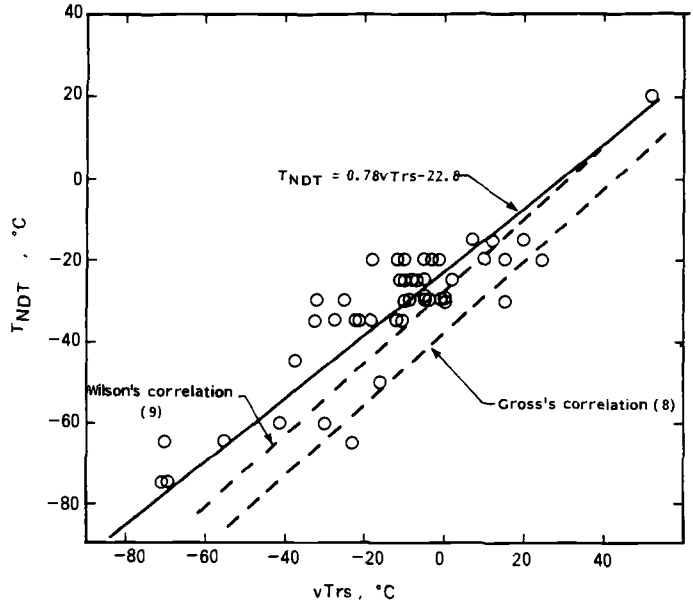

FIG. 6—*Relationship between* T_{NDT} *and vTrs.*

$$\text{(Wilson's equation)} \quad T_{NDT} = 0.89\text{vTrs} - 27.5 \tag{8}$$

The two equations are plotted in Fig. 6 as the dotted lines. For the data examined in this study, both Gross's and Wilson's equations tend to give T_{NDT} on the nonconservative or low-temperature side.

The correlations described indicate that T_{NDT} can be estimated accurately in Eq 4 by using vTrs, which correlates best with T_{NDT}. When T_{NDT} should be estimated conservatively because of the existence of data scatter, the highest T_{NDT} among those obtained from Eqs 4 through 6 can be employed, that is

$$T_{NDT}(\text{estimated}) = \max \{T_{NDT}(\text{vTrs}), T_{NDT}(\text{vTr}_{50}), T_{NDT}(\text{vTr}_{35\text{mils}})\} \tag{9}$$

where $T_{NDT}(\text{vTrs})$, $T_{NDT}(\text{vTr}_{50})$, and $T_{NDT}(\text{vTr}_{35\text{mils}})$ are the estimated values of T_{NDT} obtained by the substitution of vTrs, vTr_{50}, and $\text{vTr}_{35\text{mils}}$ into Eqs 4, 5, and 6, respectively. In Fig. 7, the measured T_{NDT}s are compared with the T_{NDT}s from both Eq 4 and Eq 9. The T_{NDT} estimated by using vTrs alone agrees with the measured T_{NDT} within $\pm 10°C$ (Fig. 7, *left*), whereas in the case of the conservative estimation by Eq 9, there are few data that show the estimated T_{NDT} as being lower than the measured one by 10°C (Fig. 7, *right*).

Relationship Between T_{NDT} *and* K_{Id}

A "break" or "no break" result for a drop-weight test specimen is determined by the assumed flaw size, applied stress, and crack-arrest fracture toughness K_{Ia}. In the embrittled bead or embrittled portion of the HAZ, a crack can readily propagate. If the embrittled zone is looked upon as the assumed flaw size and the specimen is subjected to the dynamic yield strength level σ_{yd} of the material tested, the condition under which a crack is arrested can be given by the following equation.

$$K_{Ia} = K_I = f \cdot \sigma_{yd}\sqrt{\pi a} \tag{10}$$

where a is the depth of the crack, and f is the crack shape factor. If a and f are nearly constant for drop-weight test specimens prepared under appropriate conditions and K_{Ia} is nearly equal to the dynamic fracture toughness K_{Id}, the following equations can be given at NDTT.

$$\frac{K_{Id}}{\sigma_{yd}} \approx \frac{K_{Ia}}{\sigma_{yd}} = f\sqrt{\pi a} = C \tag{11}$$

where C is a constant, and values of 2.5 to 4.0 $\sqrt{\text{mm}}$ have been reported. (Irwin et al [*10*] proposed the value of $\sqrt{3.9}$ mm, Pellini [*11*] proposed 2.5 to 3.0 $\sqrt{\text{mm}}$, and Rolfe and Barsom [*12*] proposed $\sqrt{3.0}$ mm.) Figure 8 shows the relationship of K_{Id} and σ_{yd} for base metals of nuclear vessel steels. In cases

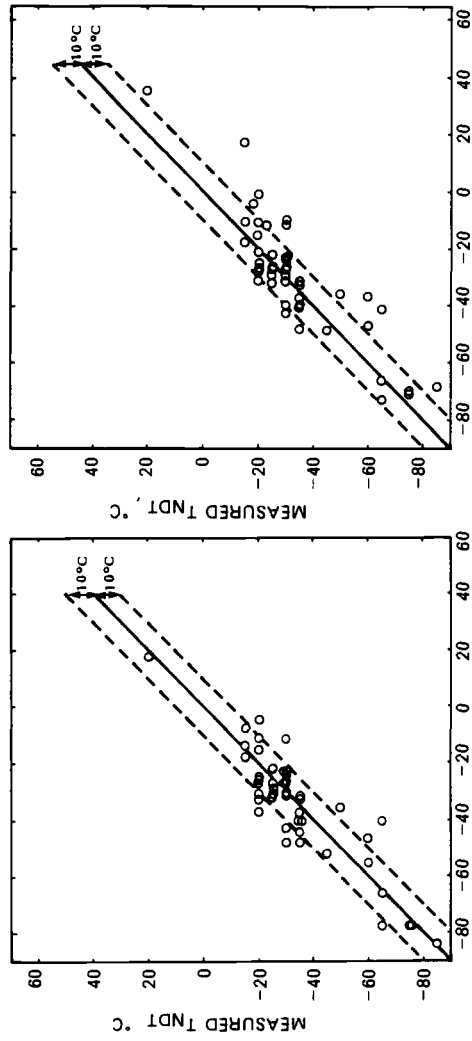

FIG. 7—*Comparison of* T_{NDT} *measured with* T_{NDT} *estimated: (left)* T_{NDT} *estimated by using vTrs: (right)* T_{NDT} *estimated by using three kinds of Charpy impact characteristics (vTrs,* vTr_{50}, vTr_{35mil}*).*

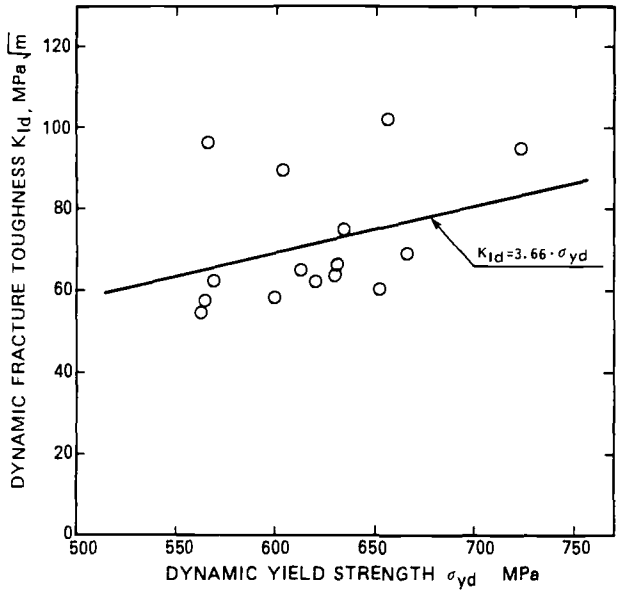

FIG. 8—*Relationship between the dynamic fracture toughness* K_{Id} *and dynamic yield strength* σ_{yd}.

in which σ_{yd} at NDTT had not been measured yet, it was estimated in accordance with the procedure described in Annex 7 of the ASTM Test for Plane-Strain Fracture Toughness of Metallic Materials (E 399-83). As a result, a value of about $\sqrt{3.7}$ mm was obtained for C, and it is within the range of values proposed by various researchers. However, as shown in Fig. 8, the value of K_{Id} tends to scatter to some extent, and it is therefore difficult to estimate NDTT from the value of K_{Id} alone.

Conclusions

The NDT temperatures of typical nuclear vessel steels were measured with a series of drop-weight test specimens prepared with different crack-starter bead welding conditions in order to investigate causes of scatter in NDTT. An investigation was also conducted on the relationships between the crack-starter bead welding conditions and the NDTT scatter from the fracture mechanics point of view, together with the correlations among the NDTT, Charpy impact transition temperatures, and K_{Id} data. The results obtained are the following:

1. The NDT temperature varies with the crack-starter bead welding amperage and is closely related to embrittlement characteristics of the steels. For materials such as A508 Class 3 steel, in which the improved toughness portion

in the HAZ can be relatively wide, the NDT temperature cannot be evaluated conservatively when the welding amperage is small. Therefore, the application of the crack-starter bead by low amperage should not be allowed.

2. Crack-starter bead welding with a heat sink that increases the cooling rate will produce the maximum bead hardness and thus make the NDT temperature stable. For thin Type P-3 specimens in particular, it is important to use such a heat sink.

3. Good correlation was observed between the NDT temperature and Charpy impact transition temperatures (vTrs, vTr_{50}, vTr_{35mils}); methods of estimating NDTT from these transition temperatures are proposed.

References

[1] Onodera, S., Tsukada, H., Suzuki, K., Iwadate, T., and Tanaka, Y., "A Study on Drop-Weight-Tests: Reproducibility and Welding Procedure," *Proceedings*, Sixth Staatliche Material Pruefungs Anstalt (MPA), University of Stuttgart, Stuttgart, West Germany, October 1980.

[2] Tsukada, H., Suzuki, K., Iwadate, T., and Tanaka, Y., "A Study on Drop Weight Test Using A508 CL.2 Steel," JSW Report R MS 81-60, The Japan Steel Works, Hokkaido, Japan, December 1981.

[3] Takano, N., Kushida, S., and Abe, O. in *Proceedings*, 100th Meeting of The Iron and Steel Institute of Japan, Tokyo, Japan, 1980, p. S437.

[4] Koshizuka, N., Enami, T., Tanaka, Y., Hiro, N., Yoshimura, S., Kusuhara, H., Fukuda, H., and Shinohara, T. in *Proceedings*, 99th Meeting of The Iron and Steel Institute of Japan, Tokyo, Japan, 1980, p. S434.

[5] Newman, J. C. and Raju, I. S., NASA Technical Paper 1578, National Aeronautics and Space Administration, Washington, DC, 1978.

[6] Rosenthal, D., *Welding Journal*, Vol. 20, 1941, p. 220S.

[7] Sakai, Y., Miya, K., Takahashi, I., and Ando, Y., "Study of Fracture Toughness of Nuclear Pressure Vessel Steels," *Transactions*, Seventh International Conference on Structural Mechanics in Reactor Technology, Vol. G, Chicago, IL, 1983.

[8] Gross, J. H., *Welding Journal*, Vol. 39, 1960, p. 59S.

[9] Willson, A. D., *Transactions of the American Society of Mechanical Engineers, Journal of Engineering Materials and Technology*, Vol. 100, 1978, p. 204.

[10] Irwin, G. R., Kraft, J. M., Paris, P. C., and Wells, A. A., "Basic Aspects of Crack Growth and Fracture," NRL Report 6598, National Research Laboratory, Washington, DC, 21 Nov. 1967.

[11] Pellini, W. S., "Advances in Fracture Toughness Characterization Procedures and in Quantitative Interpretations to Fracture Safe Design for Structural Steels," NRL Report No. 6713, National Research Laboratory, Washington, DC, 1968.

[12] Rolfe, S. T. and Barsom, J. M., "Fracture and Fatigue Control in Structure-Applications of Fracture Mechanics," Prentice-Hall, New York, 1977.

Shinsaku Onodera,[1] *Keizo Ohnishi,*[2] *Hisashi Tsukada,*[3] *Komei Suzuki,*[4] *Tadao Iwadate,*[5] *and Yasuhiko Tanaka*[5]

Effect of Crack-Starter Bead Application on the Drop-Weight NDT Temperature

REFERENCE: Onodera, S., Ohnishi, K., Tsukada, H., Suzuki, K., Iwadate, T., and Tanaka, Y., **"Effect of Crack-Starter Bead Application on the Drop-Weight NDT Temperature,"** *Drop-Weight Test for Determination of Nil-Ductility Transition Temperature: User's Experience with ASTM Method E 208, ASTM STP 919*, J. M. Holt and P. P. Puzak, Eds., American Society for Testing and Materials, Philadelphia, 1986, pp. 34-55.

ABSTRACT: The present paper summarizes several findings in relation to the effect of bead application on the nil-ductility transition (NDT) temperature (NDTT) of drop-weight test specimens.

A series of tests simulating the heat-affected zone (HAZ) under the bead have proved that the overlap of the bead placing in standard specimens exerts a quench and temper effect on the specimen material and produces high toughness values in the HAZ. This HAZ works as a barrier against crack propagation and causes the NDTT to be lower.

It was also found that the toughness of the HAZ depends on the welding conditions, the configuration of the overlapping of the two-pass beads, and the chemical composition of the material.

Further, some embrittled materials were deembrittled by the thermal effect of the welded beads. This problem is specific to temper-embrittled material, and the bead application results in a lower apparent NDTT.

The above-mentioned phenomena are intrinsic to low-alloy and alloy steels. Since the drop-weight test was originally applied to carbon steels, the test method should be reevaluated based on the new findings.

KEY WORDS: nil-ductility transition temperature, drop-weight test, two-pass bead

[1]Associate director, Steel and Heavy Components Division, The Japan Steel Works, Ltd., Head Office, Tokyo, Japan.

[2]General manager, Material Research Laboratory, The Japan Steel Works, Ltd., Muroran Plant, Muroran, Hokkaido 051, Japan.

[3]General manager, Forging Department, The Japan Steel Works, Ltd., Muroran Plant, Muroran, Hokkaido 051, Japan.

[4]Manager, Nuclear Energy Department, The Japan Steel Works, Ltd., Muroran Plant, Muroran, Hokkaido 051, Japan.

[5]General manager, and research engineer, respectively, Research Laboratory, The Japan Steel Works, Ltd., Muroran Plant, Muroran, Hokkaido 051, Japan.

weld, one-pass bead weld, weld bead overlapping, heat-affected zone (HAZ), bead application, temper embrittlement, deembrittlement, ASTM standard E 208

One of the most critical methods of material testing for evaluating the toughness of steels is the drop-weight test [ASTM Method for Conducting Drop-Weight Test to Determine Nil-Ductility Transition Temperature of Ferritic Steels (E 208-81)]. The importance of the test has been increased by the introduction of the linear elastic fracture mechanics (LEFM) concept in the American Society of Mechanical Engineers (ASME) Boiler and Pressure Vessel Code, Section III (1980).

In the drop-weight test, the nil-ductility transition temperature (NDTT) is judged by the extent of propagation of a crack initiated at the brittle weld bead deposited on the specimen to provide a brittle material source for the initiation of a small cleavage crack in the specimen. It seems however, that the variation of NDTT, which is caused by the bead application procedure, may be a serious unsolved problem for the accurate determination of NDTT [*1,2*]. In the case of nuclear steam supply system (NSSS) component materials, such as SA508 Class 3 and SA533 Grade B, Class 1 steels, the variation of NDTT among the different testers for the same heat of material has been a source of controversy.

The possibility of scatter in NDTT results caused by the bead application method is mentioned in ASTM Method E 208-81, which states that anomalous behavior may be expected for material in which the HAZ created by the bead deposition of the crack starter weld is made more fracture resistant than the unaffected material, and that this condition is well developed in quenched and tempered steels of high hardness obtained by tempering at low temperatures. This standard also mentions that the HAZ problem is not encountered with plain structural-grade steels of pearlitic microstructure or with quenched and tempered steels tempered at high temperature to develop maximum fracture toughness.

The anomalous behavior of steels suggested by ASTM Method E 208-81 seems to be more frequently encountered recently with the increasing use of low-alloy quenched and tempered steels, in spite of recent innovations in the steelmaking process.

In the present paper, the effect of the brittle weld bead application on the NDTT in the drop-weight test is investigated using four low-alloy steels. Several findings are discussed.

Material Used

Four low-alloy steels, with the compositions shown in Table 1, were used for the present investigation. The A508 Class 2 and 3 steels are forging-grade materials mainly used for NSSS components. These steels were removed from

TABLE 1—*Chemical composition of the steels used, in weight percent.*

Material	C	Si	Mn	P	S	Ni	Cr	Mo	V	As	Sn	Sb
A508 Class 2	0.20	0.26	0.86	0.005	0.004	0.83	0.35	0.55	<0.01	. . .	. . .	. . .
A508 Class 3	0.20	0.23	1.39	0.008	0.006	0.77	0.17	0.51	<0.01	. . .	. . .	. . .
2.25Cr-1Mo	0.15	0.30	0.50	0.019	0.013	0.18	2.32	1.02	<0.01	0.029	0.022	0.0050
3.5Ni-Cr-Mo-V	0.22	0.34	0.34	0.010	0.009	3.66	1.89	0.42	0.12	0.011	0.013	0.0034

a quarter thickness of a 220-mm-thick forging and a 200-mm-thick forging, respectively. The 2.25Cr-1Mo (in weight percent) steel and the 3.5Ni-Cr-Mo-V steel are typically used for chemical reactors and steam turbine rotor shafts, respectively. These last two steels were manufactured with a comparatively high content of tramp elements, such as phosphorus, arsenic, tin, and antimony, to enhance the susceptibility of these steels to temper embrittlement. The chemical compositions and mechanical properties of these steels are shown in Tables 1 and 2, respectively. To demonstrate the scattering behavior, a carbon-manganese steel was also tested for comparison. As shown in Table 2, some specimens of 2.25Cr-1Mo and 3.5Ni-Cr-Mo-V steels were subjected to step cooling, shown in the first footnote of Table 2, to embrittle the material.

For the brittle crack-starter bead, a Fox Dur 350 or Murex Hardex N welding rod was used.

Experimental Procedure

Test for A508 Class 2 and Class 3 Steels

As mentioned earlier, a variation of NDTT in the same heat of material was sometimes experienced with these steels and the difference often amounted to more than 25°C. Using these steels, the effect of the bead application method on the drop-weight NDTT was investigated.

The configurations and dimensions of the specimens used are shown in Fig. 1. Figure 1*a* shows a standard ASTM P-2 specimen with a two-pass bead

TABLE 2—*Mechanical and impact properties of the steels studied.*

Materials	0.2% Offset Strength, MPa	Tensile Strength, MPa	FATT, °C
A508 Class 2	476	619	−25
A508 Class 3	460	606	−25
2.25Cr-1Mo	651	802	−40
2.25Cr-1Mo[a]	671	784	−15
3.5Ni-Cr-Mo-V	658	812	−120
3.5Ni-Cr-Mo-V[a]	696	854	0
3.5Ni-Cr-Mo-V[b]	666	797	60

[a]Step cooled (cooling rate, 50°C/h) in the following process:

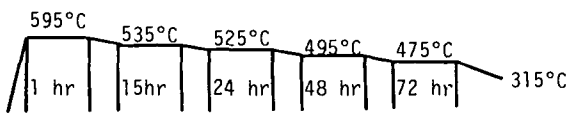

[b]Twice step cooled.

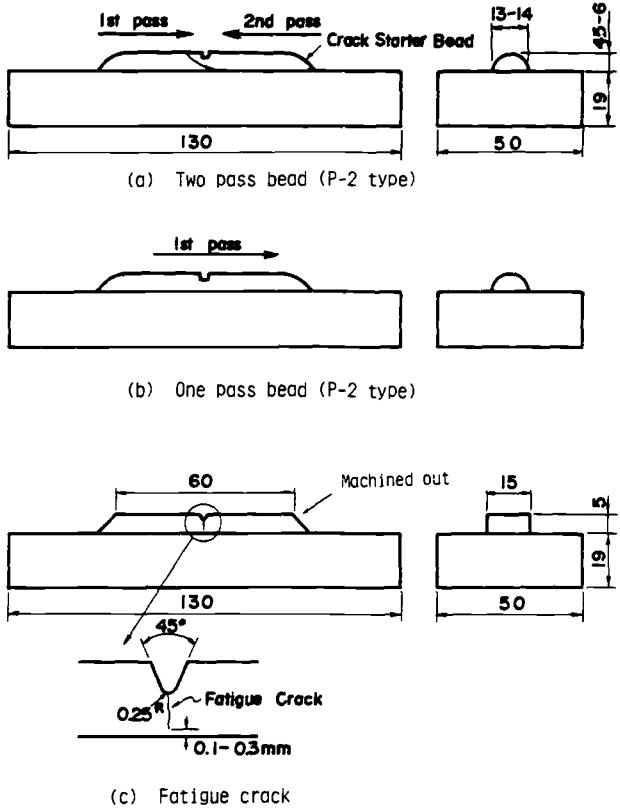

FIG. 1—*Configurations and dimensions of the specimens used.*

application. It should be noted that both the first and second pass beads meet at the center, where a notch is machined. Figure 1*b* shows a standard P-2 size specimen, but with one through-pass bead application. In addition to these specimens, a "fatigue crack specimen" was used, which had a fatigue crack as the crack starter and which was presumed to be free of heat effects brought about by the bead application. The dimensions and configuration of the fatigue crack specimen are shown in Fig. 1*c*.

The welding conditions used were as follows:

Welding voltage:	25 V
Welding current:	160 to 200 A
Travel speed:	15 cm/min

The welding rods were dried at 350°C for 1 h. Preweld and postweld heatings

were not applied. NDTT determination was made in accordance with ASTM Method E 208-81.

Test for 2.25Cr-1Mo and 3.5Ni-Cr-Mo-V Steels

These steels are susceptible to temper embrittlement. To enhance the temper embrittlement, the test materials were subjected to step cooling. The degradation of the fracture appearance transition temperature (FATT) obtained by step cooling is shown in Table 2. These materials were subjected to the drop-weight test as specified in ASTM Method E 208-81, using a standard two-pass bead specimen and also a fatigue crack specimen.

Test Results and Discussion

Effect of Welding Conditions on the Drop-Weight NDTT

Figures 2*a* and 2*b* show the results of the drop-weight test for A508 Class 2 and Class 3 steels, respectively. Significant variation of NDTT, that is, from −45 to −5°C for A508 Class 2 steel and from −45 to −20°C for A508 Class 3 steel, was observed. The differences are noticeable in the two-pass bead application specimens particularly. Low amperage, that is low heat input, during the welding results in lower NDTT. In the cases of one-pass bead application specimens and fatigue crack specimens, identical values of NDTT were observed in both steels, and these specimens gave the highest NDTT. Figure 3 shows an example of propagated cracks in A508 Class 2 steel at NDTT, at 5°C above NDTT, and at 10°C above NDTT for specimens of the two-pass and one-pass bead applications. While the crack propagated deep into the specimen in the no-break specimen in the one-pass bead application, the crack was arrested in the HAZ even at 5°C above the NDTT in the two-pass bead application specimen. Figure 4 shows the cross sections near the notch of a two-pass bead specimen at NDTT and at 5°C above the NDTT. At 5°C above the NDTT, the crack was arrested at the HAZ of the first-pass bead. Moreover, this point corresponds to just under the HAZ of the second-pass bead. Figure 5 shows the distribution of hardness in the HAZ under the notch for two-pass and one-pass bead specimens, respectively. In the two-pass bead specimen, softening of the HAZ of the first-pass bead is marked just under the HAZ of the second-pass bead, whereas the one-pass bead specimen shows no such complicated hardness distribution. The softening of the HAZ of the first-pass bead in the two-pass bead specimen is caused by the tempering resulting from the second-pass bead application. This zone plays an important role as a barrier against crack propagation.

For comparison, the results of tests on the carbon-manganese steel are shown in Fig. 6, where no significant effect of bead application on NDTT is observed.

A508 Cl.2 Steel

Test	Bead	Welding Sequence	Amperage A	Test Temperature, °C											NDTT °C
				-50	-45	-40	-35	-30	-25	-20	-15	-10	-5	0	
A	FOX	2 pass	150/160	●	●	○○		○							-45
B	FOX	2 pass	170/180	●	●	○○		○							-45
C	FOX	2 pass	190/200			●	●	●	○○						-30
D	FOX	1 pass	150/160					●				●	●	○○	-5
E	FOX	1 pass	170/180					●				●	○○	○	-10
F	FOX	1 pass	190/200					●				●	○○	○	-10

FOX : FOX DUR 350 ● Break ○ No break

FIG. 2*a*—*Drop-weight test results for specimens of A508 Class 2 steel prepared with various welding conditions.*

A508 Cl.3 steel

Test	Bead	Welding Sequence	Amperage A	Test temperature, °C											NDTT °C
				-50	-45	-40	-35	-30	-25	-20	-15	-10	-5	0	
A	FOX	2 pass	160		●	○○		○							-45
B	FOX	2 pass	180		●		●○	○○							-35
C	FOX	2 pass	200					●○	●○	○○					-25
D	Murex	2 pass	160		●	●	○○								-40
E	Murex	2 pass	180					●	○○						-30
F	FOX	1 pass	180					●	●	●	○○				-20
G	FOX	1 pass	200					●	●	●	○○				-20
H		Fatigue crack	-				●		●	●	○○				-20

● : Break ○ : No break FOX: FOX DUR 350 Murex: Murex Hardex N

FIG. 2*b*—*Drop-weight test results for specimens of A508 Class 3 steel prepared with various welding conditions.*

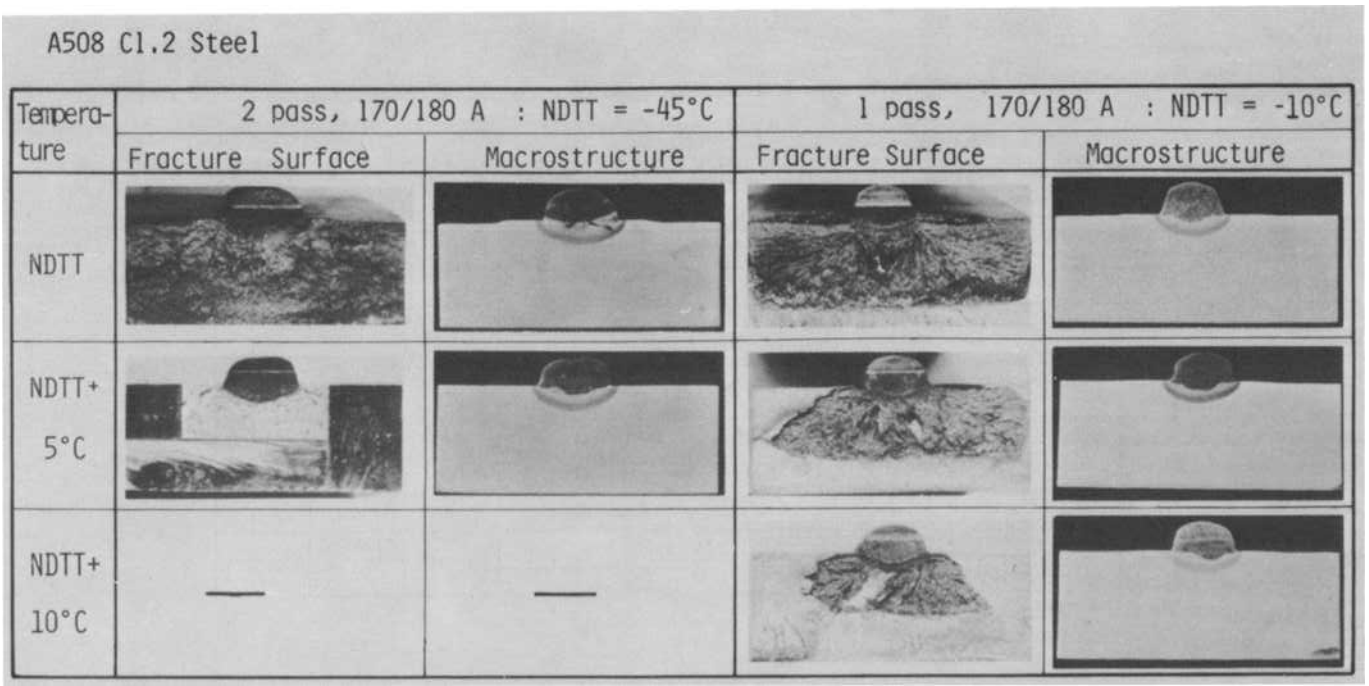

FIG. 3—*Examples of fracture surfaces of A508 Class 2 steel at NDTT, at 5°C above NDTT, and at 10°C above NDTT.*

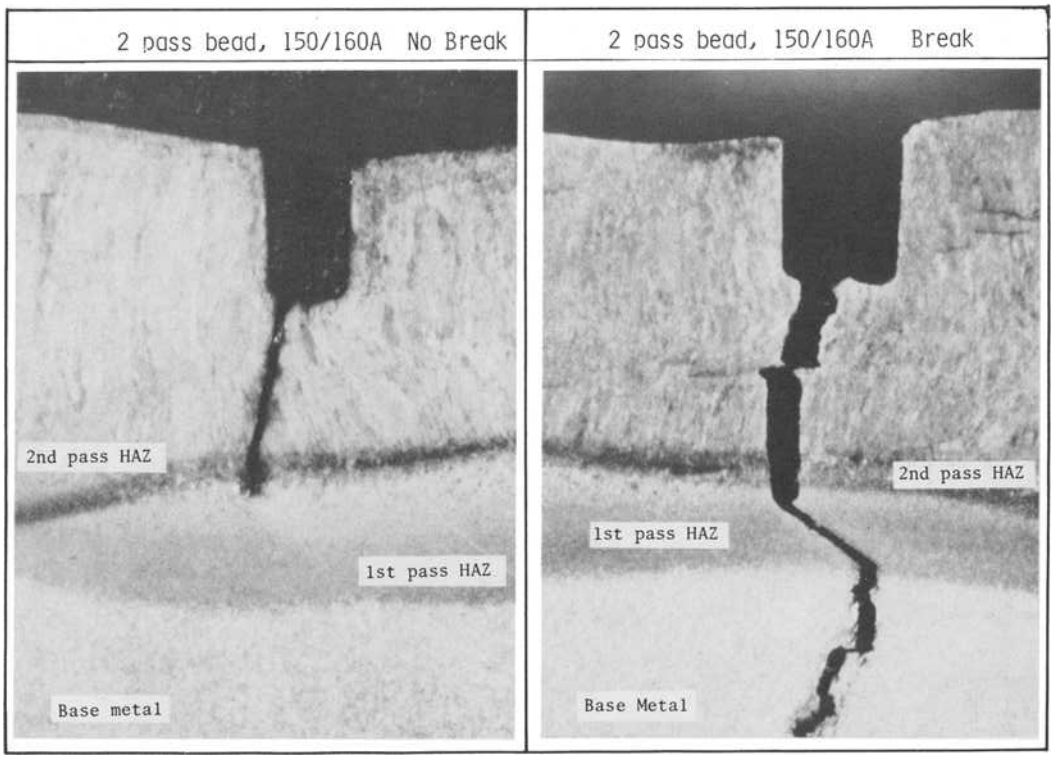

FIG. 4—*Longitudinal cross sections of a two-pass bead specimen of A508 Class 2 steel at NDTT and at 5°C above NDTT.*

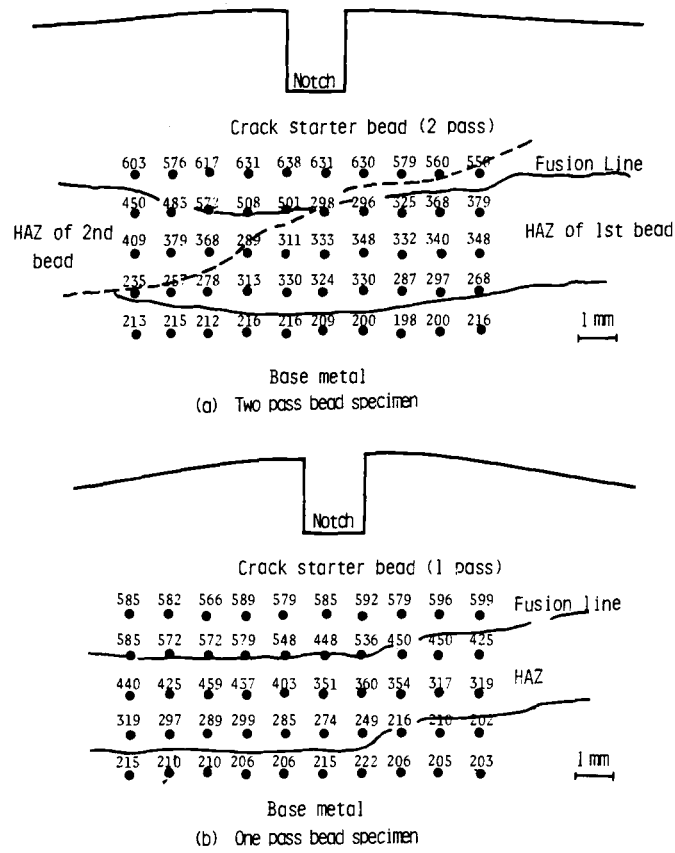

FIG. 5—*Hardness distribution in the HAZ for two-pass and one-pass bead specimens of A508 Class 2 steel.*

Simulation of HAZ

To evaluate the toughness of HAZ under the crack-starter bead, Charpy V-notch testing of simulated HAZ was carried out using an A508 Class 3 steel.

Figure 7 shows the temperature-time relationships of the simulated weld thermal cycles. The peak temperatures of 1350, 1100, and 900°C correspond to the coarse, medium, and fine grain zones in the HAZ, respectively. The cycles peaking at temperatures of 500 to 800°C simulate the second thermal cycle, due to the second-pass bead application. The thermal cycles given to the base material were achieved using induction heating and carbon dioxide gas cooling.

Figure 8 shows the Charpy V notch absorbed energy transition curves from tests on the simulated HAZs. Peak temperatures of the given artificial ther-

0.13%C-0.8%Mn Steel

Test	Bead	Welding Sequence	Amperage A	Test temperature, °C											NDTT °C
				-50	-45	-40	-35	-30	-25	-20	-15	-10	-5	0	
A	FOX	2 pass	160			●		●	●	○○	○	○			-25
B	FOX	2 pass	200			●		●	●	○○	○	○			-25
C	FOX	1 pass	180			●		●	●	○○	○	○			-25

●:Break ○:No break FOX : FOX DUR 350

FIG. 6—*Effect of welding conditions on the NDTT of carbon-manganese steel.*

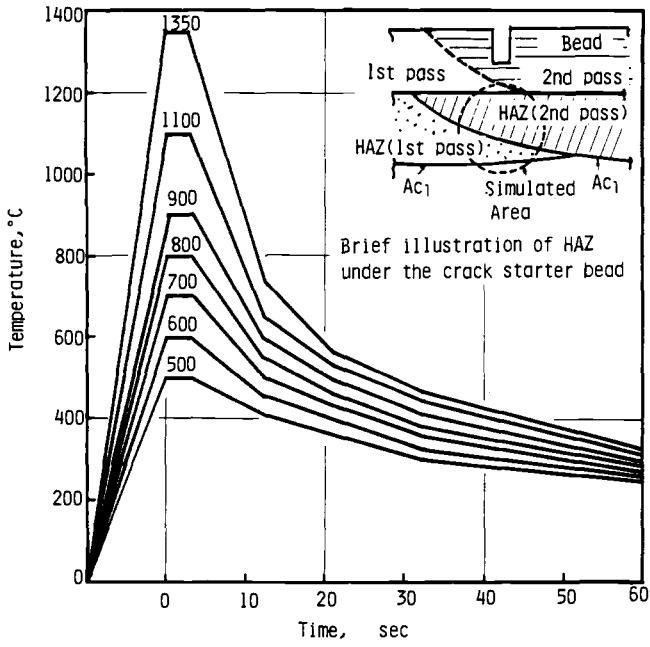

FIG. 7—*Temperature versus time relationships in simulated weld thermal cycles.*

mal cycles are shown. The energy transition temperature of the simulated HAZ formed by the first thermal cycle is higher than that of the base metal and is associated with a low upper shelf energy. The transition curves of the HAZ that received the second thermal cycle of the peak temperature of 700°C appear superior to that of the base metal and give a remarkably low transition temperature with a high upper shelf energy. These results suggest that the highest toughness zone appears in the HAZ of two-pass bead specimens.

Figure 9 shows the effect of peak temperature of the second thermal cycle. The portion of the HAZ reheated up to temperatures between 600 and 700°C by the second thermal cycle is tougher than the base metal.

The cause of the high-toughness region in the HAZ is the quench and temper effect. The HAZ cooled rapidly from the austenite region after the first-pass welding has martensitic structure in both Class 2 and Class 3 A508 steels. When martensite is reheated to 700°C, that is, just below the austenite transformation temperature Ac_1 by the second-pass weld, the HAZ may be tempered to form a high-toughness structure.

In this manner, a high-toughness region is formed in the HAZ of the two-pass bead specimen.

To investigate the effect of the high-toughness HAZ on NDTT results, special drop-weight test specimens were prepared and tested. The material used

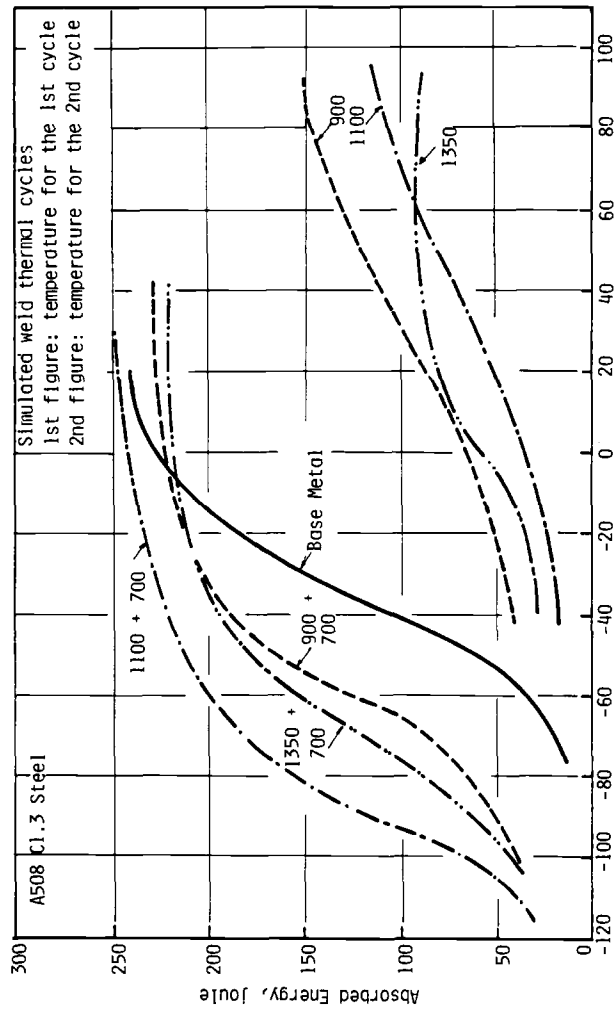

FIG. 8—*Charpy V-notch absorbed energy transition characteristics of simulated HAZ of A508 Class 3 steel. (The peak temperature of the thermal cycle is shown in the figure.)*

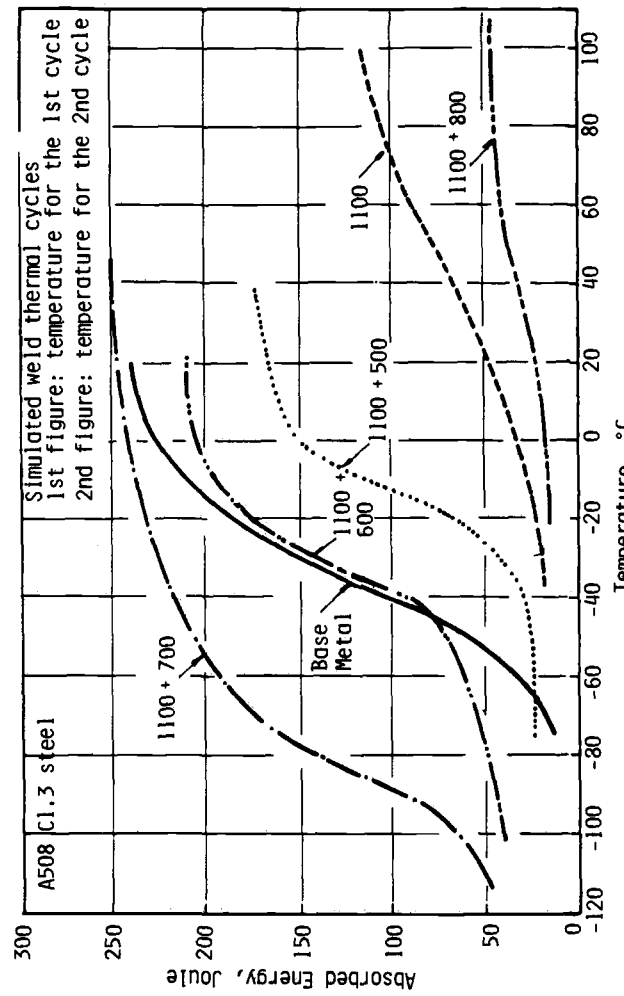

FIG. 9—*Effect of the peak temperature of the second thermal cycle on the Charpy absorbed energy transition of simulated HAZ. (The peak temperature of the thermal cycle is shown in the figure.)*

was A508 Class 2 steel. The crack-starter beads of the specimens were welded by one through pass using currents of 150 to 160 A and 190 to 200 A, respectively. Subsequently, these specimens were heated at 650°C for 2 h to temper the HAZ. This heat treatment tempered the martensite structure in the HAZ. The test results are shown in Fig. 10. Lower NDTTs were observed in the tempered specimens. In them, all the cracks were arrested in the HAZ and a significant effect of HAZ toughness was observed.

Effect of Overlapping

The combinations of the two thermal cycles, which determine the HAZ toughness, are innumerable since a change of heat input or in the amount of overlapping affects the thermal cycle. This uncertainty may cause different NDTT values. The reason the low heat input gives the lower NDTT has not been established, but one theory is that the low heat input results in a rapid cooling rate, which may result in a tough structure in the material during the welding of the first pass. These overlapping profiles of the HAZ depend not only on the welding conditions but also on the welding technique.

Figure 11 shows the effect of change in overlapping on the NDTT for A508 Class 2 steel. To simplify the overlapping conditions and control the overlapping, a special welding sequence was applied. As shown in the lower part of the figure, one through-pass bead was welded on the specimen and machined to a prescribed height of d, then the second through-pass bead was welded on it. The change in the height of the first-pass bead determines the change in overlapping, as shown by the photographs in the lower part of the figure.

The NDTT obtained varies between -35 and -10°C, according to the overlapping conditions of the HAZ.

Scattering of NDTT of the Heavy Section Steels

It should be noted that the NDTT problem may be encountered frequently in the heavy section steels.

Figure 12 shows a graph of continuous cooling transformation (CCT) for an A508 Class 3 steel obtained by simulation of the cooling rate from 890°C. In the case of material removed from a quarter-thickness location of an actual heavy section plate, the cooling rate at the location was limited to a low rate at which bainitic microstructure may be formed, while the surface material subjected to the quenching and faster cooling tends toward a martensitic structure, which can have high toughness values after tempering. Figure 13 shows the Charpy V-notch energy transition behaviors of (*a*) surface material, (*b*) quarter-thickness material, and (*c*) half-thickness material taken from a 300-mm-thick steel. The surface material reveals a low transition temperature, while the inner materials show a higher transition temperature. Similarly, a rapid cooling rate can be expected after the weld bead welding, and conse-

A508 Cl.2 steel

Test	Bead	Welding Sequence	Amperage A	Test Temperature, °C											NDTT °C
				-55	-50	-45	-40	-35	-30	-25	-20	-15	-10	-5	
G	FOX	1 pass + 650 °C*	150/160		●	●	○○		○						-45
H	FOX	1 pass + 650 °C*	190/200	●	○○		○		○						-55
I	FOX	650 °C** + 1 pass	170/180										●	○○	-10

FOX : FOX DUR 350 ● Break ○ No Break

*) The specimens were tempered at 650°C for 2 hrs after the welding of crack starter bead.

**) The specimens were tempered at 650°C for 2 hrs prior to the welding of crack starter bead.

FIG. 10—*Effect of tempering after a one through-pass bead application on the NDTT of A508 Class 2 steel.*

A508 Cl.2 steel

Test	Thickness of First Bead	Amperage A	Test Temperature, °C									NDTT °C
			-40	-35	-30	-25	-20	-15	-10	-5	0	
J	0.5mm	170/180			●		●		●	○○		-10
K	1.5mm				●		●	●	○○			-15
L	2.5mm		●	●	○○							-35

● Break ○ No break

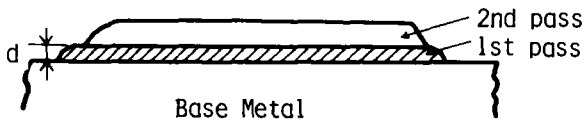

Thickness of 1st bead (after machined)

Fig. (a) d = 0.5mm
Fig. (b) d = 1.5mm
Fig. (c) d = 2.5mm

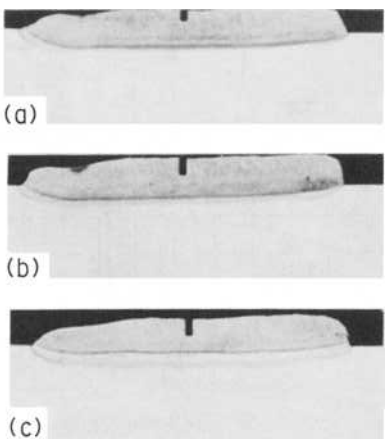

FIG. 11—*Effect of change in bead overlapping on the NDTT of A508 Class 2 steel—a simulation.*

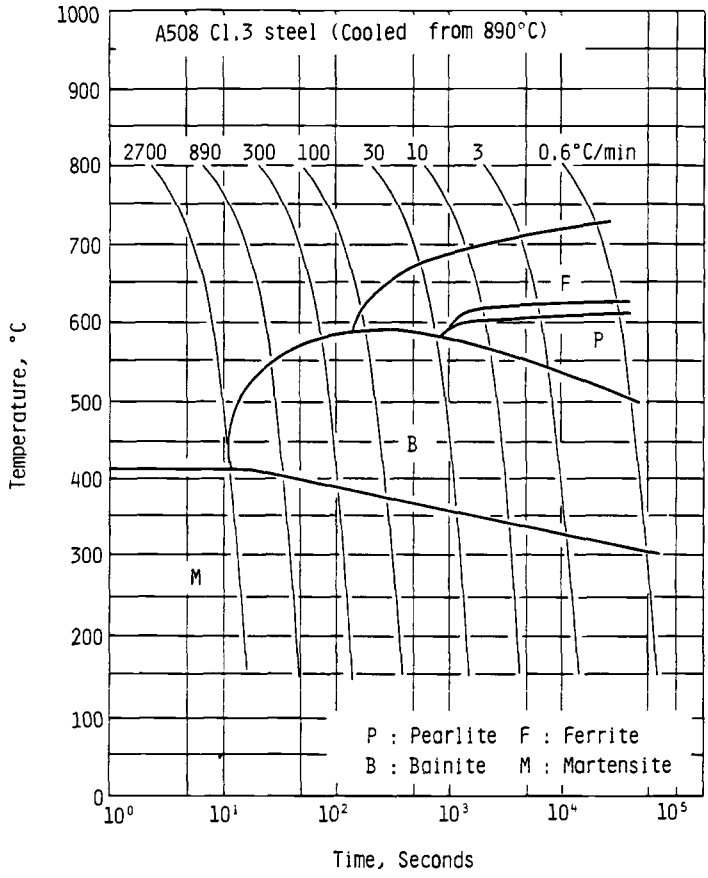

FIG. 12—*Continuous cooling transformation (CCT) graph for an A508 Class 3 steel.*

quently, the HAZ may develop a high-toughness structure, which results in transition curves like those in Fig. 13. If the specimen material is removed from a quarter thickness or a half thickness, an apparent low NDTT may be obtained. The behavior depends largely on the chemical composition of the materials, since the transformation characteristics determine the structure and the toughness of the HAZ.

Effect of Bead Application on Embrittled Materials

Another aspect is the effect of bead application on embrittled materials. In Table 3 are shown the NDTTs of quenched and tempered and step-cooled 2.25Cr-1Mo and 3.5Ni-Cr-Mo-V steels. A significant difference between the NDTTs obtained by the standard specimen and the fatigue crack specimen

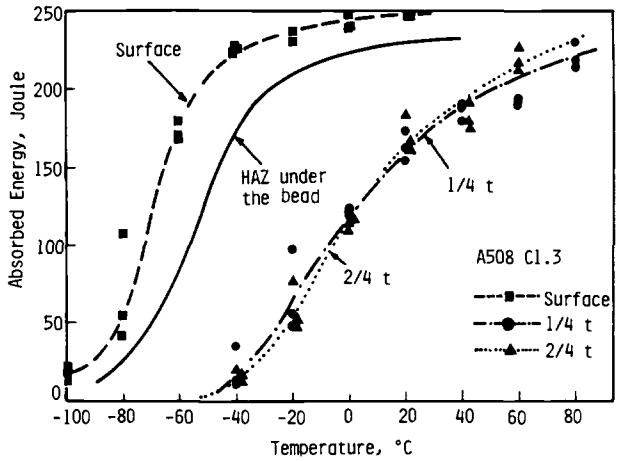

FIG. 13—*Charpy V-notch absorbed energy transition behaviors at various locations in 300-mm-thick A508 Class 3 steel.*

TABLE 3—*Effect of bead application on the NDTT of embrittled steels.*

Test	Material	Treatment	FATT, °C	Type of Specimen	NDTT, °C
A	2.25Cr-1Mo	quenched and tempered	−40	fatigue crack P-2	−25
					−20
B	2.25Cr-1Mo	step cooled	15	fatigue crack P-2	−20
					45
C	3.5Ni-Cr-Mo-V	quenched and tempered	−120	fatigue crack P-2	−130
					−125
D	3.5Ni-Cr-Mo-V	step cooled	0	fatigue crack P-2	−100
					−35
E	3.5Ni-Cr-Mo-V	twice step cooled	60	fatigue crack P-2	−85
					10
F	3.5Ni-Cr-Mo-V	material from Test D + bead application + step cooling	130	P-2	30
G	3.5Ni-Cr-Mo-V	material from Test D + step cooling + bead application	130	P-2	−65

was observed in the embrittled materials. The difference becomes larger in severely embrittled materials. As an example, the NDTT of as-quenched and tempered 3.5Ni-Cr-Mo-V steel is −130°C, using the standard specimen procedure, while in the fatigue crack specimen procedure, the NDTT is −125°C. In the case of step-cooled material, of which the FATT is 60°C, the discrepancy between NDTTs obtained using standard and fatigue crack spec-

imens amounts to 95°C. Scanning electron microscope observation of the fracture of the propagated cracks in these specimens disclosed that the fracture surface of fatigue crack specimens of embrittled steel shows intergranular fracture, whereas the standard specimen with bead application shows the transgranular quasi-cleavage fracture. This result suggests that deembrittlement of the specimen material, which could be produced by the thermal cycle of the bead application, results in a lowered NDTT.

Figure 14 shows the effect of simulated weld thermal cycles on the fracture appearance transition temperature of these steels. The given thermal cycles are the same as those in Fig. 7. The transition temperatures of embrittled steels shift to the lower sides by heating up to about 700°C for a few seconds. The NDTTs of the specimens subjected to step cooling before and after bead application are also shown in Table 3. Though the step cooling was carried out in the same furnace, the variation in NDTTs obtained amounted to 95°C. The results demonstrate the effect of deembrittlement of the specimen material on NDTT.

In the case of neutron irradiation embrittled steels, a similar phenomenon may be expected when the crack-starter bead is welded on the steel.

Summary and Conclusions

The effect of the crack-starter bead application on the drop-weight NDT temperature was investigated using A508 Class 2, A508 Class 3, 2.25Cr-1Mo, and 3.5Ni-Cr-Mo-V steels. The important findings are as follows:

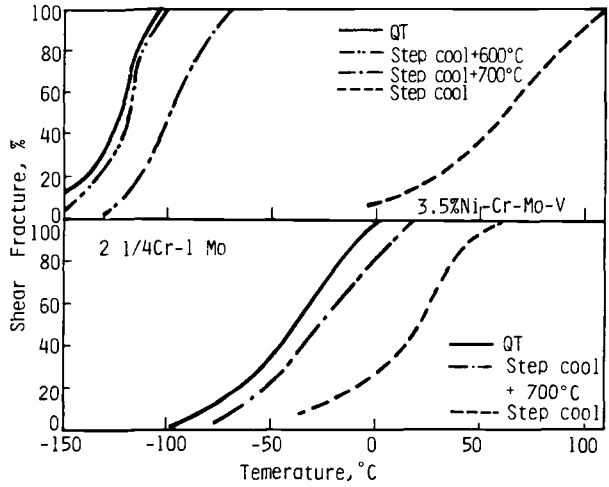

FIG. 14—*Effect of simulated weld thermal cycles on the fracture appearance transition temperature of 2.25Cr-1Mo and 3.5Ni-Cr-Mo-V steels.*

1. The two-pass bead application, as specified by ASTM Method E 208-81, produces a quenching and tempering effect on the materials tested and forms a high-toughness zone, which produces a lower NDTT in all the steels studied.

2. The main factors influencing the toughness of HAZ are the welding conditions, overlapping of HAZs brought by the first and second passes of welding bead, and the chemical composition of the steels.

3. These phenomena are further enhanced for the steels that are susceptible to temper embrittlement, such as 2.25Cr-1Mo steel.

In conclusion, the authors recommend that extensive studies be conducted in order to solve these problems related to the more established test method.

References

[1] Pröger, M. and Langer, R., "Cooperative Test Programme (Round Robin Test) on Toughness Behaviour Judgement within the 'Research Programme Integrity of Components'," *Proceedings*, Fifth Material Prufungs Anstalt Seminar, University of Stuttgart, Stuttgart, West Germany, 1979.

[2] Onodera, S., Tsukada, H., Suzuki, K., Iwadate, T., and Tanaka, Y., "A Study on Pellini Test: Reproducibility and Welding Procedure," *Proceedings*, Sixth Material Prufungs Anstalt Seminar, University of Stuttgart, Stuttgart, West Germany, October 1980.

Carl D. Lundin,[1] *Edwin A. Merrick,*[2] *and Brian J. Kruse*[3]

Influence of the Crack-Starter Bead Technique on the Nil-Ductility Transition Temperature of ASTM A572 Grade 55 Hot-Rolled Plate

REFERENCE: Lundin, C. D., Merrick, E. A., and Kruse, B. J., **"Influence of the Crack-Starter Bead Technique on the Nil-Ductility Transition Temperature of ASTM A572 Grade 55 Hot-Rolled Plate,"** *Drop-Weight Test for Determination of Nil-Ductility Transition Temperature: User's Experience with ASTM Method E 208, ASTM STP 919,* J. M. Holt and P. P. Puzak, Eds., American Society for Testing and Materials, Philadelphia, 1986, pp. 56-68.

ABSTRACT: An investigation of the nil-ductility transition (NDT) temperature of three heats of A572 Grade 55, hot-rolled steel plate, revealed a distinct and decided difference in behavior for specimens fabricated with a single-pass technique in comparison with those fabricated with the two-pass technique, which places the terminal weld crater at the bead center. The single-pass technique resulted in NDT temperatures 11°C (20°F) higher than those for the two-pass technique. Furthermore, the crack behavior was distinctly different at temperatures above the NDT, with the single-pass specimens showing progressively shorter cracks as the temperature was raised. This result is in contrast to that for the two-pass technique, which revealed no crack extension from the starter bead heat-affected zone (HAZ) above the NDT.

The metallurgical reasons for the observed behavior were determined by utilizing optical microscopy, scanning electron fractography, and microhardness methods. The toughness of the various regions of the HAZ and the base metal were correlated with the microstructure and NDT behavior. The differences in the NDT temperature are related to a toughening of the HAZ by the two-pass technique. The effect of this toughened HAZ on crack propagation and crack fracture morphology from the crack-starter bead, through the HAZ, and into the base metal was evaluated.

KEY WORDS: mechanical properties, structural materials, A572 steel plate, nil-ductility transition temperature, fracture toughness, drop-weight test, Charpy V-notch test, ASTM standard E 208

[1]Professor and director of welding research, Materials Science and Engineering Department, The University of Tennessee, Knoxville, TN 37996.
[2]Senior engineer, Tennessee Valley Authority, Knoxville, TN 37902.
[3]Senior engineer, Duke Power Co., Charlotte, NC 28242.

The drop-weight test, conducted in accordance with the ASTM Method for Conducting Drop-Weight Test to Determine Nil-Ductility Transition Temperature of Ferritic Steels (E 208-81), has been used extensively in evaluation of the conditions involved in initiation of brittle fracture in structural steels [*1-4*]. The test has taken on greater importance in recent years since the method and the results are required by the Boiler and Pressure Vessel Code of the American Society of Mechanical Engineers (ASME), together with Charpy V-notch test information, to assure adequate fracture toughness of pressure vessel materials. However, some investigations have shown that the test method can produce considerable data scatter and that the results may not be conservative when certain fabrication test methods are used to prepare the specimens [*5,6*]. While the studies using the test methodology have utilized the quenched and tempered low-alloy steel employed in nuclear pressure vessel construction [Classes 2 and 3 in the ASTM Specification for Quenched and Tempered Vacuum-Treated Carbon and Alloy Steel Forgings for Pressure Vessels (A 508-84)] [*5,6*], the information reported herein suggests that the same concerns should hold true for some of the hot-rolled steels of a ferritic/pearlitic microstructural morphology.

Results and Discussion of Experimental Work

The drop-weight testing of three heats of A572[4] Grade 55 steel was undertaken to evaluate the nil-ductility transition (NDT) temperature, in order to provide a basis for a fracture mechanics assessment of a welded structure. Charpy V-notch (CVN) testing was also conducted in concert with the NDT evaluation to provide additional data relative to the fracture toughness. All testing was performed in accordance with the applicable provisions of ASTM Method E 208-81 and the ASTM Methods for Notched Bar Impact Testing of Metallic Materials (E 23-82). The 38.1-mm (1½-in.)-thick A572 Grade 55 material was in compliance with the specification with regard to composition and mechanical properties and was in the hot-rolled condition.

In the initial testing of the A572 Grade 55 material in accordance with ASTM Method E 208-81, the two-pass (welded from both ends toward the center) crack-starter weld bead technique was used. The electrode was Hardex N and the bead shape was in compliance with the standard. The material was evaluated in both the as-received (hot-rolled) and postweld heat-treated (PWHT) conditions. During testing to determine the NDT temperature, it became apparent that at temperatures above the NDT, the crack initiated in the crack-starter bead did not leave the immediate confines of the crack-starter bead heat-affected zone (HAZ). However, at and below the NDT temperature, the specimen fractured completely by crack propagation through the thickness and to the edges of the test specimen. This behavior was consis-

[4]Based on the ASTM Specification for High-Strength Low-Alloy Columbium-Vanadium Steels of Structural Quality (A 572-84).

tent for all three heats of A572 Grade 55 material for both the hot-rolled and postweld heat-treated (PWHT) conditions. This occurrence prompted a retesting of the three heats of material using a single-pass bead technique (one pass) with the terminal crater positioned at one end of the bead, away from the notch. The single-pass technique used the same welding conditions employed for the two-pass technique, which are identical to those stated in E 208-81: 180 to 200 A, medium arc length, and a travel speed that results in a moderately high crowned bead, without weave or oscillation and employing a 4.5-mm (3/16-in.)-diameter electrode, yielding a bead that is approximately 12.7 mm (1/2 in.) wide and 63.5 mm (2 1/2 in.) long. When the NDT was determined using this crack-starter bead configuration, the NDT temperature was found to be 11°C (20°F) higher than it was with the two-pass technique. The data are given in Table 1. The crack propagation behavior above the NDT temperature was such that the crack extended past the crack-starter bead HAZ and decreased in extent as the temperature was increased above the NDT. This is behavior identical to that encountered by Onodera et al [5] in the testing of SA-508 Class 2 material. The following quote from that work is to be noted at this juncture.

> It is found that there is a significant difference in crack propagation behavior between two pass bead and one pass bead specimens. In two pass bead specimen, the extension of crack in "no break" specimen is very small and the crack is arrested in the HAZ. While, in the one pass bead specimen, the amount of crack extension gradually increases and finally reaches the "break" condition with decreasing temperature.

Based on the behavior apparent in the A572 Grade 55 material and the observations of Onodera et al [5], metallographic, fractographic, and HAZ hardness evaluations were undertaken. Charpy testing was extended to include the HAZ of multiple-pass welds made in one of the three heats of the A572 Grade 55 material. This additional testing permitted an assessment of the behavior and provided insight into the testing parameters, especially the crack-starter weld bead technique.

The results of the Charpy testing, together with the NDT temperatures for

TABLE 1—*NDT determinations for three heats of A572 Grade 55 steel.*

Heat	NDT Temperature, °C (°F)	
	Two-Pass Technique	One-Pass Technique
1	−13 (+8)	−2 (+28)
2	−19 (−2)	−8 (+18)
3	−19 (−2)	−8 (+18)

the one-pass and two-pass crack-starter weld technique in the NDT test, are shown in Fig. 1 for Heat 3. The Charpy specimens were extracted with a longitudinal, notch transverse (LT) orientation from the quarter-thickness ($^1/_4$-T) location in the plate and from the HAZ of a full-penetration shielded metal arc welding (SMAW) multiple-pass weld on the straight side of the single bevel preparation (to ensure a straight, through-thickness HAZ and definitive HAZ location). It is clear from Fig. 1 that the as-welded HAZ toughness far exceeds that of the hot-rolled base material. Furthermore, the difference in the NDT/Charpy energy level correlation varies from approximately 17 J (12 ft · lb) to 39 J (28 ft · lb), depending on whether the one-pass or two-pass crack-starter bead is utilized. These data show that the multiple-pass HAZ in A572 Grade 55 material is tougher than the base plate.

In other work at the University of Tennessee Welding Research Laboratory, Knoxville, Tennessee, the authors of the present paper have repeatedly shown the potential superiority of a multiple-pass HAZ in hot-rolled ferritic/pearlitic structural steel. Table 2 shows some of the data obtained from the Charpy toughness evaluation conducted on simulated HAZs in A36 and A572 material. By examination of Table 2, one can see that the specimens experiencing an intercritical HAZ cycle show improved toughness in comparison with the hot-rolled material and the coarse-grained region of the HAZ. The multiple-cycled (three times) specimens showed even higher toughness in the intercritical (lower temperature) region of the HAZ. Clearly portions of the HAZ of the A572 Grade 55 plate are tougher than the base material, and the actual HAZ toughness measurements on the identical test material (Heat 3) are superior to those of the base material in the as-received, hot-rolled condition. This gives rise to the observation that the crack-starter weld bead HAZ can provide a tougher zone in the crack path during drop-weight testing, especially if the two-pass technique is employed (the two-pass technique produces overlapping or multiple-pass HAZs). This was indeed one of the conclusions drawn by Onodera et al [5] in their work on SA 508 Class 2 material. Quoting again from this work, Onodera et al state, "Anomalous behavior may be expected from materials where the heat-affected zone (HAZ) created by the deposition of the crack-starter weld is made more fracture resistant than the unaffected material."

To investigate further the differences in behavior between the one-pass and two-pass techniques of crack-starter bead deposition, metallographic examinations and hardness evaluations were conducted on the NDT specimens tested. In Fig. 2, the schematic appearance of the one-pass and two-pass technique crack-starter bead is shown with regard to the bead progression and the extent of the HAZ. The two-pass technique produces an overlapping of the HAZs from the two bead segments. This creates two distinct metallurgical conditions: an overlapped HAZ, which was noted earlier (Table 2) as creating tough microstructure in the outer extremities of the HAZ in hot-rolled materials of the A572 Grade 55 type, and a tempering affect, which will toughen any

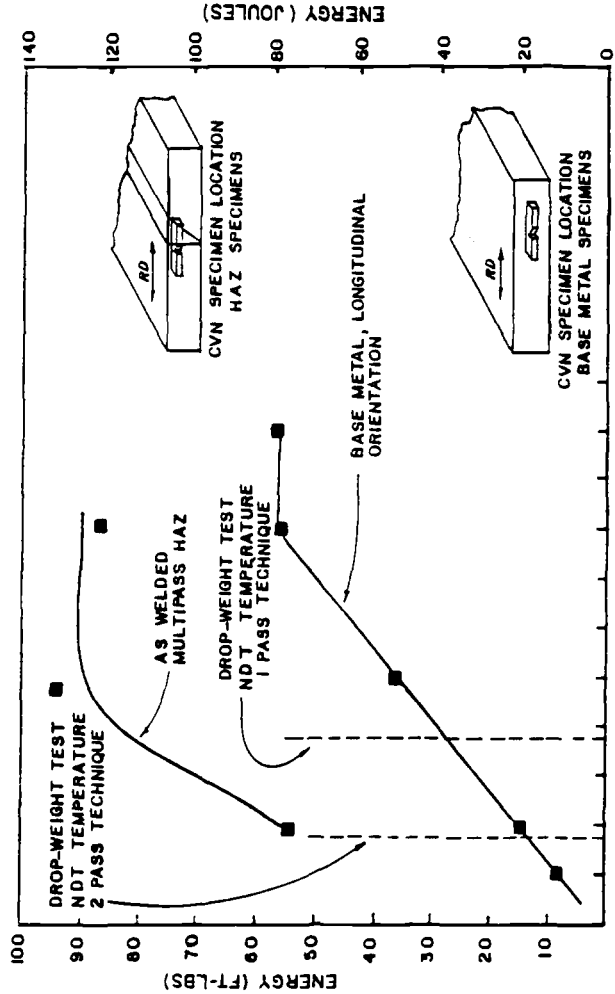

FIG. 1—*Average CVN impact toughness (A572 Grade 55 steel, Heat 3).*

TABLE 2—*Simulated HAZ (Gleeble) toughness Charpy impact values at 0°C (32°F) for A36 and A572 steels.*

Material	Hot-Rolled, J (ft · lb)	Intercritical Region		Grain-Coarsened Region	
		1 Cycle, J (ft · lb)	3 Cycles, J (ft · lb)	1 Cycle, J (ft · lb)	3 Cycles J (ft · lb)
A36	34 (24)	48 (34)	99 (71)	28 (20)	27 (19)
A572	45 (32)	106 (76)	246 (176)	18 (13)	11 (8)

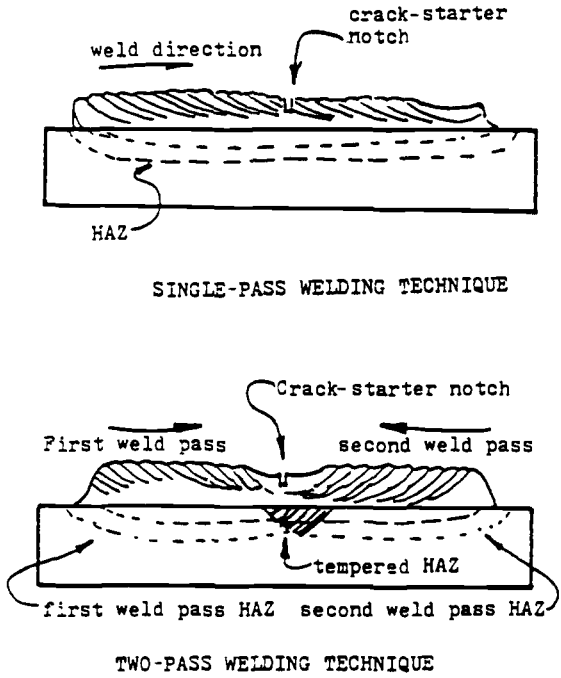

FIG. 2—*Schematic of the single-pass and two-pass welding techniques.*

low-temperature transformation products formed in the upper temperature regions of the HAZ. Both of these factors will influence the propagation of a crack from the hardened crack-starter bead. Microstructurally, the overlapped region can be clearly seen on polished and etched sections made through the weld, HAZ, and base plate. Hardness surveys revealed that the maximum hardness in the single-pass (not-overlapped and not-tempered) HAZ was HRC 30, whereas the maximum hardness in the two-pass (recycled and tempered) HAZ was HRB 98 for the A572 Grade 55 material. These mea-

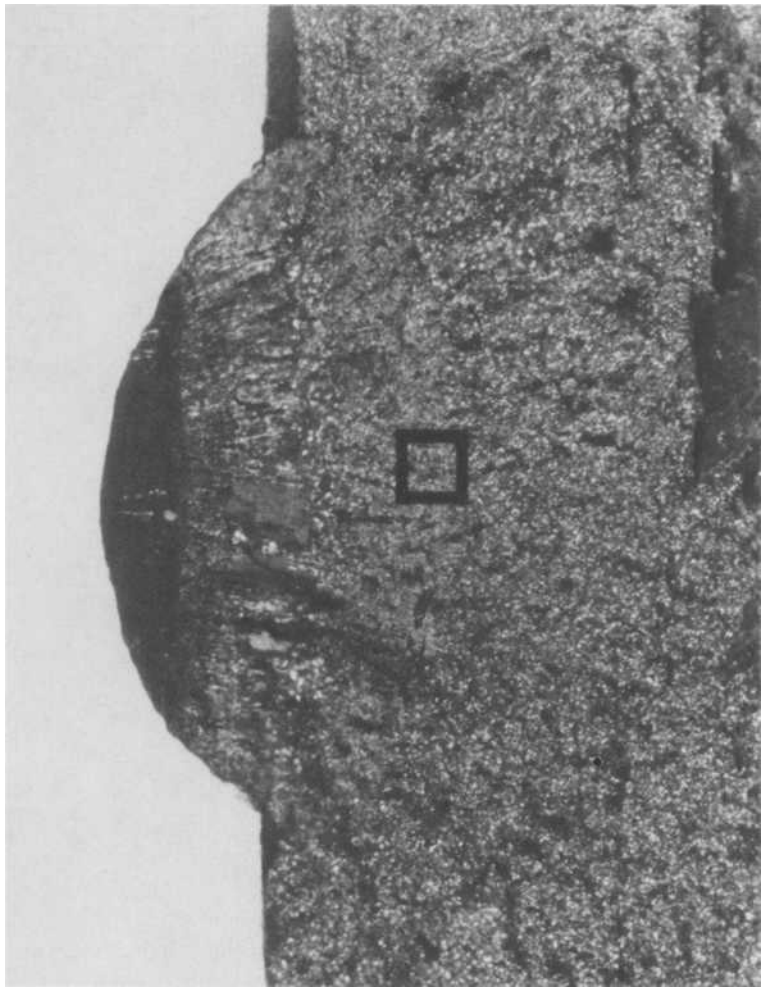

FIG. 3a—*Typical optical fracture appearance of a specimen tested at the NDT temperature after the one-pass technique (×5 magnification). The area within the square is enlarged in Fig. 4a.*

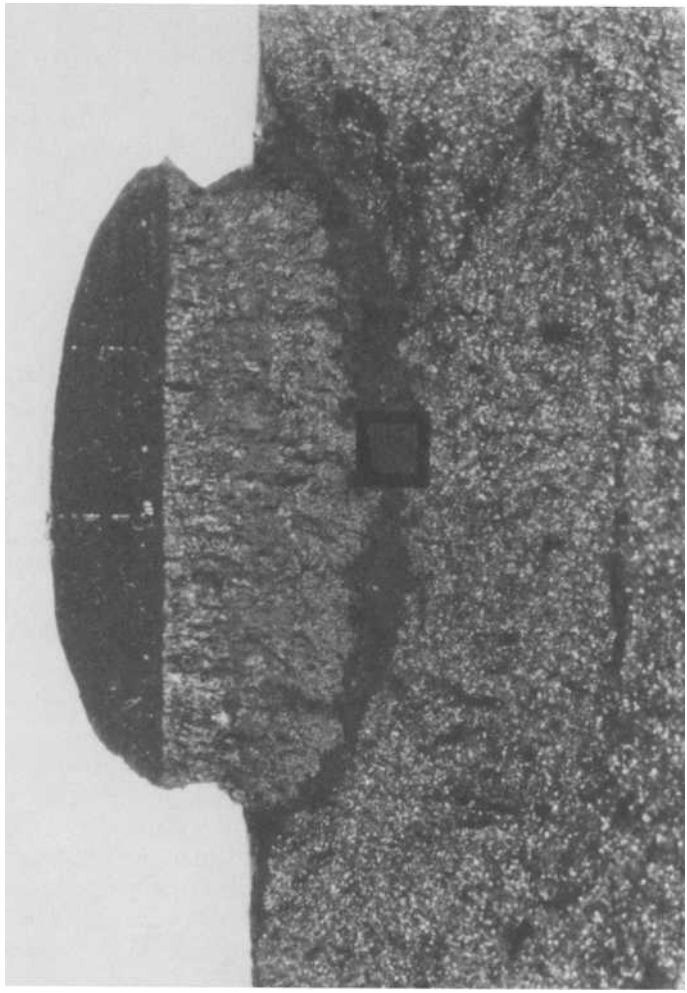

FIG. 3*b*—*Typical optical fracture appearance of a specimen tested at the NDT temperature after the two-pass technique (×5 magnification). The area within the square is enlarged in Fig. 4b.*

surements show the character of the HAZ in terms of the relative ductility (often proportional to toughness) for the two techniques employed.

The fractographic features were evaluated optically to determine the macrofractographic mode and in the scanning electron microscope (SEM), to define the fine-scale, microfractographic features. The optical macrofractographic appearance is shown in Figs. 3*a* and 3*b* at ×5 magnification for specimens typical of the one-pass and two-pass crack-starter techniques tested at the NDT temperature. In the two-pass specimen (Fig. 3*b*), a clearly defined dark-appearing band is noted in the HAZ of the crack-starter bead. The light reflectivity in this band is considerably less than that in the surrounding fracture and thus it appears darker in the optical fractograph. This band is located adjacent to the fine-grained region at the outer boundary of the HAZ. This dark band is conspicuously absent in the one-pass crack-starter bead test specimens. The SEM fractographic appearance of the microfractographic features of the dark band region of the two-pass crack-starter weld and of an identical region in the one-pass crack-starter weld bead are shown in Figs. 4*a* and 4*b*. (The areas are marked on the photomacrographs in Figs. 3*a* and 3*b*.) The dark band fracture features correspond to a ductile tearing, ductile dimple, fracture morphology characteristic of relatively high toughness, whereas the identical region in the one-pass weld shows an entirely cleavage morphology, representative of brittle low-toughness fracture. The typical base metal fracture morphology beneath the crack-starter HAZ for both the one-pass and two-pass sequences is presented in Fig. 5. The fracture is 100% cleavage, the fracture morphology anticipated at or below the NDT. Extensive fractography was performed on several specimens to verify these findings. The fractographic data show that a unique, high-toughness zone is created when the two-pass crack-starter weld bead technique is used. This zone is comparable in location and character (ductility and toughness) to that defined and characterized from the toughness standpoint in the simulated HAZ studies. (See the data in Table 2.)

The authors postulate, therefore, that the differences in NDT temperature and crack propagation behavior between the one-pass and two-pass crack-starter weld bead technique are directly related to, and caused by, the toughening of a segment of the HAZ in the two-pass weld sequence. This toughened band extending around the periphery of the HAZ causes the crack, initiated in the hardened crack-starter bead weld metal, to arrest at temperatures near the NDT, causing lowering of the NDT and limiting crack growth above the NDT temperature. The absence of the toughened band in the one-pass technique results in the presence of a singularly low and uniformly tough region at the NDT temperature, which does not inhibit crack propagation from the crack-starter bead weld metal. Thus, the one-pass technique presents the base metal with a running crack that is not inhibited in its propagation by a toughened region, the requirements of the concept of the procedure in ASTM Method E 208-81 are fulfilled, and the NDT of the base plate is correctly assessed.

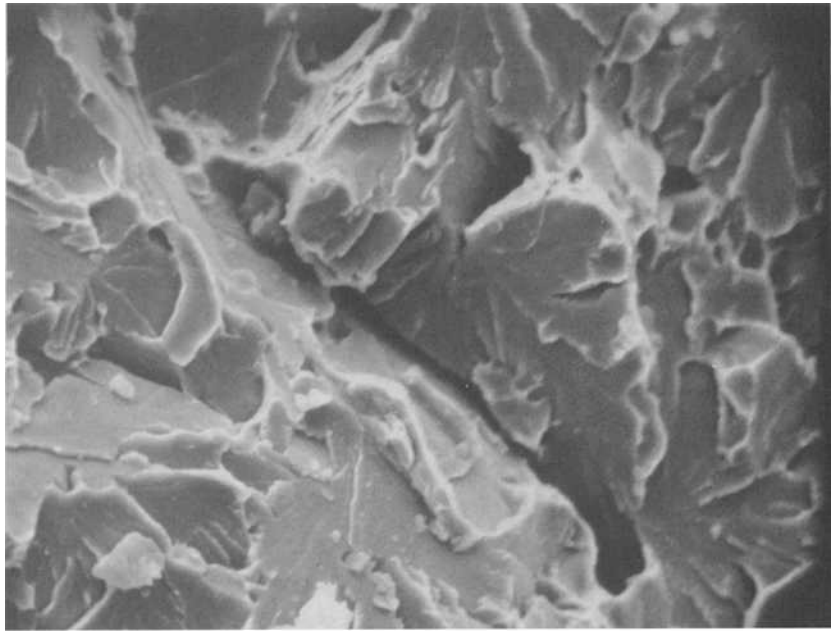

FIG. 4*a*—*SEM fractographic appearance of a one-pass weld in the grain-refined region of the HAZ in Fig. 3a (× 2000 magnification).*

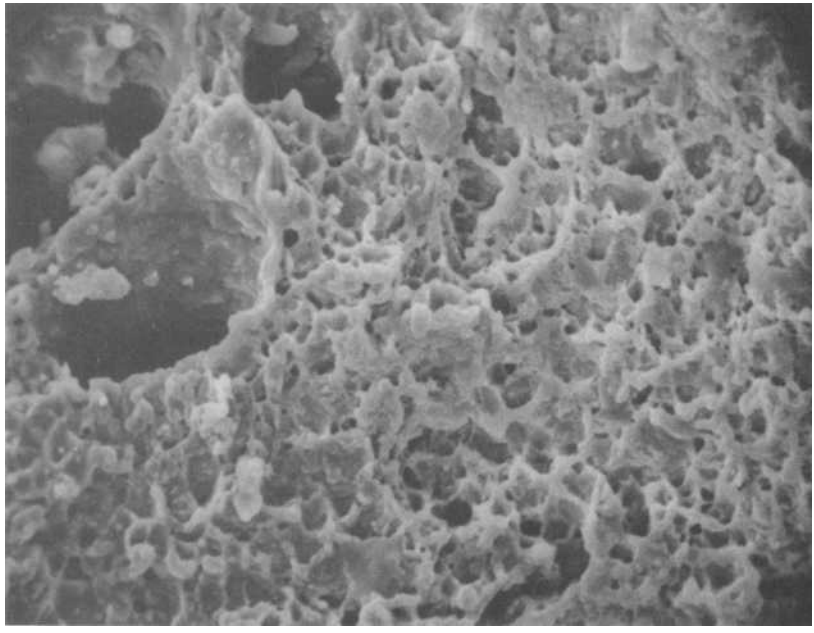

FIG. 4*b*—*SEM fractographic appearance of a two-pass weld in the grain-refined and tempered region of the HAZ (dark-appearing band) in Fig. 3b (× 2000 magnification).*

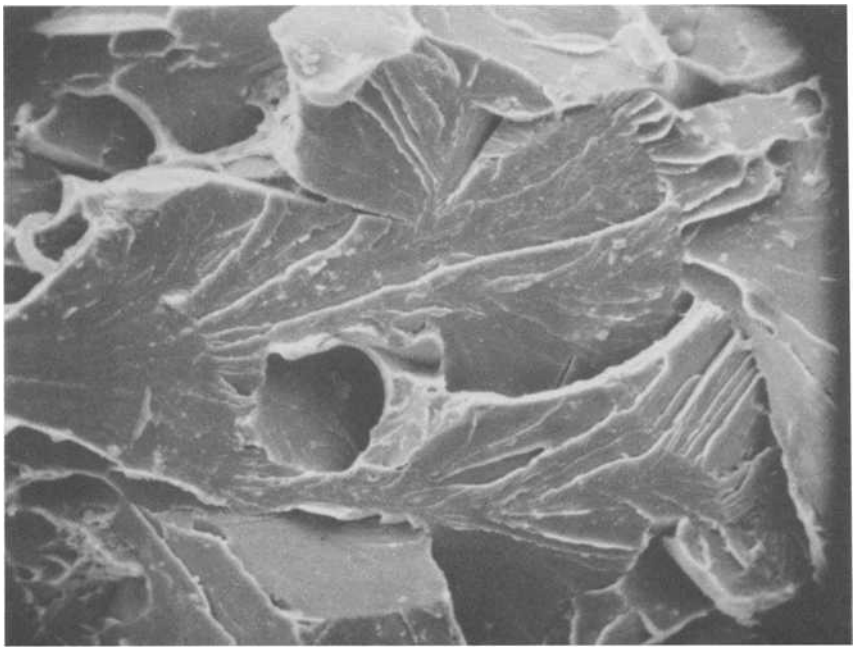

FIG. 5—*SEM fractographic appearance of the base material (× 1000 magnification).*

ASTM Method E 208-81 recognizes the necessity for the test material, the base steel, to be presented with a running crack at all test temperatures. Thus, when the test temperature reaches the NDT, the crack will not be arrested by the test steel and will propagate to the extent necessary to fracture the specimen. The caveat provided by Method E 208-81 is contained in the first paragraph of Section 13, titled Interpretation of Test Results:

> The success of the drop-weight test depends on the development of a small cleavage crack in the crack-starter weld after a minute bending of the test specimen. The test evaluates the ability of the steel to withstand yield point loading in the presence of a small flaw. The steel either accepts initiation of fracture readily under these test conditions and the specimen is broken, or initiation of fracture is resisted and the specimen bends the small additional amount permitted by the anvil stop without complete fracturing.

It is for this reason that the condition of the HAZ of the crack-starter bead is very important, and thus the crack-starter weld must provide a microstructure conducive to ready propagation from the crack-starter bead weld metal, through the HAZ, into the underlying base metal. It is apparent from this study and the work on SA-508 Class 2 material [*5,6*] that the one-pass technique provides the most reliable means of assuring the proper metallurgical

conditions, so that it is the base metal that is evaluated and not the crack-starter bead HAZ.

In addition, there are provisions in ASTM Method E 208-81 that can exacerbate the conditions described for the two-pass technique. For example, Section 7.7 on the Crack-Starter Weld states, "The weld height at the center of the bead should be approximately equal to the height of the bead crown, but any deficiency observed after cleaning the weld can be corrected by adding more metal to the crater-depression." And Section 7.9 states, "Weld beads notched too deeply may be repaired by the deposition of more weld metal after grinding of the notched area without contacting the surface of the specimen." Both of these permissible corrective measures will alter the HAZ microstructure and change the crack propagation resistance in the crack path toward the base metal. The provisions of Section 7.10 allow variations in the crack-starter weld bead, but the deviations are addressed primarily at the crack initiation in the starter bead. There are some admonitions concerning shorter crack-starter weld beads (successfully employed with P-3 specimens but "not recommended" for P-1 specimens). From these concerns presented in Section 7.10, the specification writers apparently have included experience factors to guide in the successful application of the test method.

Conclusions

Based on the foregoing information, the authors suggest that the drop-weight test method, as defined in ASTM Method E 208-81, can be made more definitive for NDT temperature determination, and the scatter in the results can be reduced by incorporating the following procedures:

(*a*) permitting only a one-pass crack-starter weld bead to be used,

(*b*) carefully defining the welding procedures and welding conditions, and

(*c*) eliminating the procedures for correcting deficiencies in the crack-starter bead. (That is, the specimen would be rejected if the original deposition of the crack-starter weld bead deviated from the prescribed conditions.)

The authors are convinced that, if these recommendations are utilized in future versions of the specification, the specification will be strengthened and the test method will be placed on a firmer foundation.

References

[*1*] Puzak, P. P., Eschbacher, E. W., and Pellini, W. S., "Initiation and Propagation of Brittle Fracture in Structural Steels," *Welding Journal,* Vol. 31, No. 12, 1952.

[*2*] Pellini, W. S., Puzak, P. P., and Eschbacher, E. W., "Procedures for NRL Drop Weight Test," NRL Memo Report 316, National Research Laboratory, Washington, DC, June 1954.

[*3*] Puzak, P. P., Schuster, M. E., and Pellini, W. S., "Crack-Starter Tests of Ship Fracture and Project Steels," *Welding Journal,* Vol. 33, No. 9, 1954.

[*4*] Puzak, P. P., Schuster, M. E., and Pellini, W. S., "Supplementary Note on Crack-Starter Tests of Ship Fracture and Project Steels," *Welding Journal,* Vol. 34, No. 4, 1955.

[5] Onodera, S., Tsukada, H., Suzuki, K., Iwadate, T., and Tanaka, Y., "A Study on Pellini Test: Reproducibility and Welding Procedure," R(MS)80-037, Japan Steel Works Ltd., Hokkaido, Japan, 1980.

[6] Tsukada, H., Suzuki, K., Iwadate, T., and Tanaka, Y., R(MS)81-60, "A Study on Drop Weight Test Using A508 CL2 Steel," Japan Steel Works Ltd., Hokkaido, Japan, 1981.

Noriaki Koshizuka,[1] *Teiichi Enami,*[1] *Michihiro Tanaka,*[1] *Toshiharu Hiro,*[1] *Yuji Kusuhara,*[2] *Hiroshi Fukuda,*[3] *and Shigehiko Yoshimura*[2]

Effect of the Heat-Affected Zone at the Crack-Starter Bead on the Nil-Ductility Transition Temperature of Steels Determined by the Drop-Weight Test

REFERENCE: Koshizuka, N., Enami, T., Tanaka, M., Hiro, T., Kusuhara, Y., Fukuda, H., and Yoshimura, S., **"Effect of the Heat-Affected Zone at the Crack-Starter Bead on the Nil-Ductility Transition Temperature of Steels Determined by the Drop-Weight Test,"** *Drop-Weight Test for Determination of Nil-Ductility Transition Temperature: User's Experience with ASTM Method E 208, ASTM STP 919*, J. M. Holt and P. P. Puzak, Eds., American Society for Testing and Materials, Philadelphia, 1986, pp. 69-86.

ABSTRACT: The effect of the heat-affected zone (HAZ) at the crack-starter bead on the nil-ductility transition temperature (NDTT) of drop-weight test specimens of pressure vessel steels was investigated. NDTT varied with changes in thermal cycles in the bead welding and increased linearly with the hardness of HAZ. Using fracture toughness of the base metal and HAZ geometry, NDTT was estimated and compared with the observed NDTT. The difference between the estimated NDTT and the observed NDTT was caused by changes in HAZ hardness. The observed NDTT became lower with softening of HAZ.

KEY WORDS: pressure vessel steels, toughness, fracture toughness, hardness, heat-affected zone, drop-weight test, nil-ductility transition temperature, ASTM standard E 208

The drop-weight test, which was developed by Puzak et al [*1*], has been established as a standard method in the ASTM Method for Conducting Drop-Weight Test to Determine Nil-Ductility Transition Temperature of Fer-

[1]Senior researchers, Iron and Steel Research Laboratories, Technical Research Division, Kawasaki Steel Corp., Kurashiki 712, Japan.
[2]Managers, Mizushima Works, Kawasaki Steel Corp., Kurashiki 712, Japan.
[3]Manager, New York Office, Kawasaki Steel America Inc., New York, NY 10055.

ritic Steels (E 208-81). The nil-ductility transition temperature (NDTT) is an important value in evaluating the toughness of steels, especially for nuclear pressure vessel steels, and is used to determine the reference temperature for nil-ductility transition (RT_{NDT}), which is the standard temperature for the reference fracture toughness K_{IR} given in the Boiler and Pressure Vessel Code, Section III, Appendix G, of the American Society of Mechanical Engineers (ASME); K_{IR} is determined by NDTT and Charpy impact properties.

The drop-weight test specimen has a welded brittle bead to initiate cracks and also a heat-affected zone (HAZ), both of which have mechanical properties different from those of the base metal. The HAZ was generally thought to have no effect on NDTT; however, it has been reported that properties of the HAZ significantly affect NDTT in some steels. For example, in temper-embrittled chromium-molybdenum steel plate, NDTT apparently decreased because the temper-embrittled base metal near the welded bead was toughened by heat from the brittle bead welding [*2*].

In this study, the effect of HAZ under the crack-starter bead on the NDTT of drop-weight test specimens of pressure vessel steels is investigated.

Experimental Procedure

The chemical compositions and mechanical properties of steel plates used are shown in Tables 1 and 2. In this study, three 250-mm-thick ASTM A533 Grade B, Class 1 steel plates, a 70-mm-thick quenched and tempered Mn-Ni-Mo-V steel plate (Japan Industrial Standard No. G3115, SPV-50Q), and a 45-mm-thick ASTM A516 Grade 70 steel plate were used.

The NDTTs of these steel plates were determined by the drop-weight test using Type P-3 specimens, in accordance with ASTM Method E 208-81. The axial direction of the specimens was normal to the rolling direction. In order to investigate the effect of HAZ on NDTT, the methods of welding the crack-starter bead in the drop-weight test specimens were experimentally changed. The crack-starter bead was welded on the center of the test specimen, using a Murex Hardex N electrode under the conditions shown in Table 3. The welding current, voltage, and traveling speed were maintained, in accordance with ASTM Method E 208-81, at a constant 190 A, 20 V, and 2.33 mm/s, respectively. However, the welding sequence, preheating temperature of the specimens, and drying conditions of the electrodes were changed.

In the case of the continuous-weld sequence, after the first half of the bead was welded on the drop-weight test specimen, the second half was welded immediately; for the interrupted sequence, the second half of the bead was welded after the test specimen had cooled to room temperature. Some test specimens were heated at 473 K for 3.6 ks before being welded and others were not preheated. The electrodes were used after being dried at 373 K for 3.6 ks in the electric furnace or were used in the as-received condition.

Thermal cycles in the welding, the size of the bead and HAZ, and the hard-

TABLE 1—*Chemical compositions of the steel plates used.*

Steel		Thickness, mm	Chemical Composition, weight %										
Specification	No.		C	Si	Mn	P	S	Cu	Ni	Cr	Mo	V	Acid-Soluble Aluminum
A533 Grade B, Class 1	A	250	0.19	0.27	1.38	0.008	0.003	0.01	0.63	0.15	0.54	...	0.026
	B	250	0.18	0.27	1.39	0.008	0.004	0.01	0.61	0.15	0.54	...	0.019
	C	240	0.19	0.26	1.37	0.011	0.006	0.01	0.67	0.11	0.54	...	0.019
SPV-50Q	D	70	0.12	0.29	1.26	0.012	0.003	0.14	0.56	0.11	0.20	0.04	0.015
A516 Grade 70	E	45	0.17	0.24	1.19	0.018	0.003	0.14	0.44	0.10	0.05	0.03	0.031

TABLE 2—*Mechanical properties of the steel plates used.*

Sampling Location	Steel No.	Tension Test[a]			Charpy Test[b]	
		Yield Strength, MPa	Tensile Strength, MPa	Elongation, %	50% Shear FATT, K[c]	50 ft · lb Transition Temperature, K[d]
Quarter thickness	A	445	584	28	276	260
	B	488	614	27	270	244
	C	448	595	30	259	223
	D	540	639	31	195	166
	E	327	528	30	248	220

[a] 12.5 ϕ by 50 mm gage length.
[b] 2 mm V-notch.
[c] FATT = fracture appearance transition temperature.
[d] 50 ft · lb = 67 J.

TABLE 3—*Welding conditions for the crack-starter bead.*

Electrode	Murex Hardex N
Current	180 to 200 A
Voltage	20 V
Speed	2.17 to 2.5 mm/s
Welding sequence	continuous, interrupted
Preheat temperature	room temperature, 473K
Drying condition of electrode	as received, dry (373 K)

ness of the weld metal (WM) and HAZ were measured for the test specimens. Fracture surfaces and microstructures of some tested specimens were observed by scanning electron microscope (SEM). The dynamic fracture toughness K_{Id} of the base metal of A533 Grade B, Class 1 steel plates was determined at various temperatures by the precracked Charpy impact test. Dynamic fracture toughness was calculated by using the following equation, in accordance with the ASTM Test for Plane-Strain Fracture Toughness of Metallic Materials (E 399-83).

$$K_{Id} = \frac{PS}{Bw^{3/2}} f\left(\frac{a}{w}\right) \tag{1}$$

where

P = maximum load, N,
S = span length, mm,

B = thickness of the specimen, mm,
w = depth of the specimen, mm, and
a = crack length of the specimen, mm.

In the case of elastic-plastic fracture, K_{Id} was converted from the J value. The J value was calculated by using Eq 2.

$$J = \frac{2A}{B(w - a)} \tag{2}$$

where A is the area under the load-displacement curve up to the maximum load. The conversion of J to K_{Id} was made using the following equation.

$$K_{Id} = \sqrt{\frac{EJ}{1 - \nu^2}} \tag{3}$$

where E and ν are the elastic modulus and Poisson's ratio, respectively.

Results and Discussion

Investigation of the Crack-Starter Bead Weld

In the standard method of preparation of drop-weight test specimens, the first brittle bead weld and the second, succeeding one should overlap at the center of the specimen's length. As the crack-starter notches are machined at the center of the length of the combined weld, the notch root comes near the boundary of these two welded beads. Thus, it can be assumed that the brittle crack mainly initiates and propagates at the weld metal of the first bead. The properties of the weld metal of this first bead, which we call WM-1, are affected by heat input from the second, succeeding bead weld.

The thermal cycles of the fusion line for the first weld bead during welding were measured; Fig. 1 shows some examples. These cycles were measured by using a Chromel-Alumel thermocouple. The solid line is an example of the thermal cycle obtained in the continuous sequence of bead welding. The dotted line is an example of the thermal cycle of the interrupted sequence. The cooling rate at the fusion line of the first bead in the continuous sequence is lower than that in the interrupted sequence. The dot-and-dash line is the thermal cycle of the continuous sequence of bead welding with preheating of the specimen. The cooling time for 1073 to 773 K, $t_{1073\text{-}773}$, of this sequence is 33 s, which is longer than that of the continuous sequence without preheating of the specimen, 14 s.

The hardnesses of WM-1 and HAZ obtained by the bead welding methods described earlier were measured.

The relationship between the mean hardness values and $t_{1073\text{-}773}$ is shown in

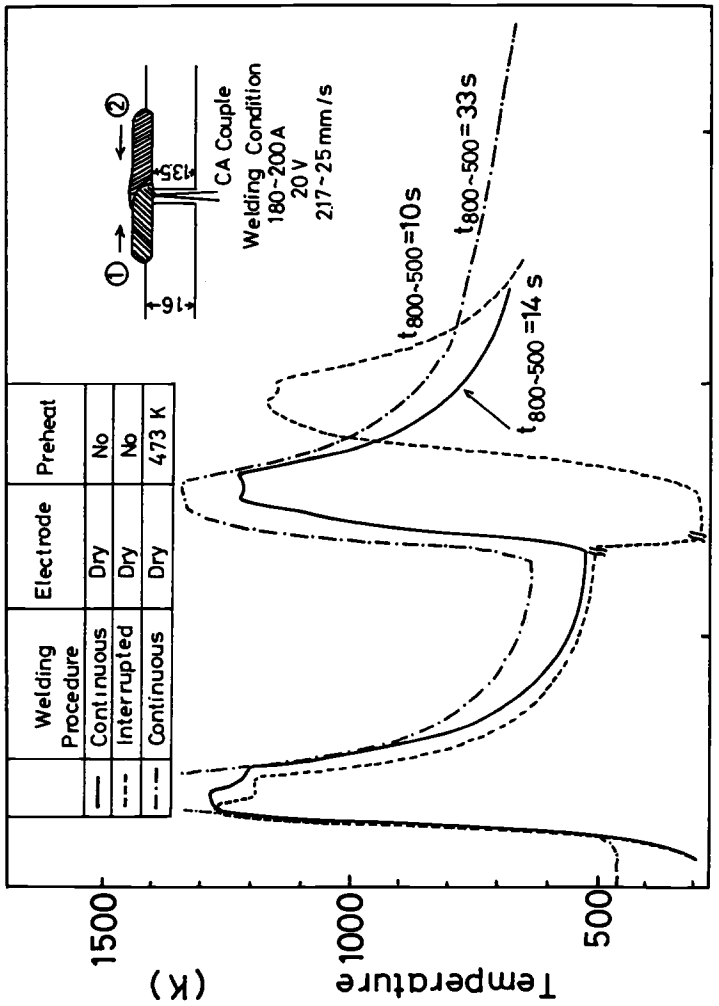

FIG. 1—*Thermal cycles of the fusion line of the first welded bead during bead welding.*

Fig. 2. As shown in Fig. 2*a*, the hardness of WM-1 decreases with increased cooling time because of the welding procedure, but does not vary much with the kind of steel. If the hardness of the crack-starter bead is at an extremely low level, the crack does not start at the test loading. In this case, the test is invalid, as stated in ASTM Method E 208-81. The relationship between the mean hardness of HAZ and the cooling time $t_{1073\text{-}773}$ is shown in Fig. 2*b*.

At the same cooling time, the mean HAZ hardness of A533 Grade B, Class 1 steel plate is higher than that of other steel plates. The mean HAZ hardness of SPV-50Q steel plate is nearly the same as that of A516-70 steel plate. As mentioned earlier, it is clear that the mean hardness of HAZ is dependent on the hardenability of the steel. Therefore, in such a steel as A533 Grade B,

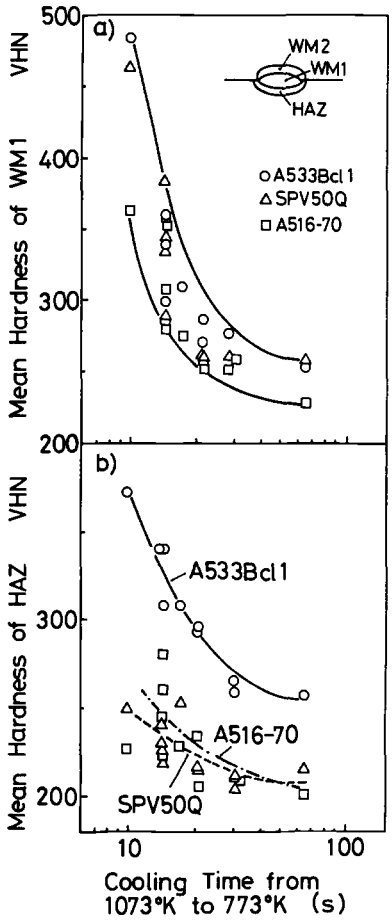

FIG. 2—*Relationship between the cooling time from 1073 to 773 K and the mean hardness of* (a) *the weld metal (WM-1) and* (b) *the heat-affected zone (HAZ).*

Class 1, the hardness of HAZ varies remarkably with the changes in cooling rate in the bead welding.

Relationship Between NDTT and the Hardness of the Welded Bead Zone

The relationship between NDTT and the mean hardness of WM-1 is shown in Fig. 3*a*, and Fig. 3*b* shows the relationship between NDTT and the mean hardness value of HAZ. As shown in Fig. 3*a*, NDTTs of SPV-50Q and A516-70 steel plates do not vary with the increase in hardness of the weld metal, but NDTT of A533 Grade B, Class 1 steel plates varies with the increase in hardness of the weld metal. On the other hand, NDTT increases linearly with the increase in hardness of the HAZ, as shown in Fig. 3*b*. The difference between the NDTTs of SPV-50Q and A516-70 steel plates, is small, because the difference in their HAZ hardness is small. But, in A553B Grade B, Class 1 steel

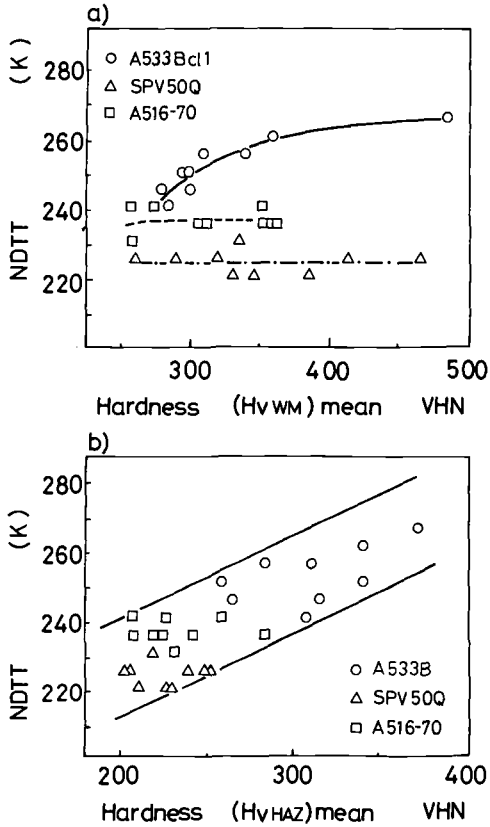

FIG. 3—*Relationship between NDTT and the mean hardness of* (a) *the weld metal (WM-1) and* (b) *the heat-affected zone (HAZ).*

plates, NDTT largely increases with the increase in HAZ hardness. Thus, the authors conclude that the hardness of HAZ under the crack-starter bead strongly affects NDTT, and they assume that the hardness of the weld metal does not affect NDTT if the crack-starter bead is not too ductile and can create a visible crack at the notch.

Effects of the Heat-Affected Zone on NDTT of A533B Grade B, Class 1 Steel Plates

Fractured surfaces and crack paths of specimens tested at the temperature above NDTT are shown in Fig. 4.

After testing, the specimens were completely broken at an extremely low temperature, 77 K. The dark area in both specimens on the left-hand side of Fig. 4 fractured at the test temperature, and the remaining area fractured at 77 K. As shown in the figure, in the specimen tested at the higher temperature, 248 K, the fractured area is small, but it is large in the specimen tested at the lower temperature, 238 K. Moreover, in the specimen tested at the lower temperature, the crack, which propagated a short distance at the surface of the tested specimen, extended to near the side edge at the midthickness area.

The fractured specimens were cut perpendicularly at the line shown in the left-hand side of Fig. 4. The correlation between the crack path and the microstructure is shown in the right-hand side of the figure. This figure also shows that the propagated crack stops at the fine grain zone of the HAZ in the specimen tested at 248 K. At the lower test temperature of 238 K, the crack propagates to the base metal across the HAZ but changes its propagating direction at the HAZ boundary. Therefore, it seems that the HAZ has significant resistance to crack propagation.

The fracture surfaces and microstructures of perpendicular sections in the tested specimens were observed by SEM. As shown in Fig. 5*a*, the crack easily propagates through WM, because the fracture surface of it seems very smooth. The propagated crack through the WM area also easily runs into the coarse grain zone of HAZ across the fusion line, as shown in Fig. 5*b*. The fracture surface of the HAZ 1.2 mm away from the fusion line has fine facets and dimples, as shown in Fig. 5*c*. In this zone, ductile fracture showing a dimple pattern in the fractured surface is observed, so it is assumed that this zone has high resistance to crack propagation. The fine grain zone of the HAZ especially has a large energy absorption effect, which acts against propagation of a crack.

Therefore, the authors have studied the formation of the heat-affected zone during brittle bead welding. It was found that each part of the weld metal and HAZ formed by the first bead welding is affected by thermal cycles of the second, succeeding bead welding. Figure 6*a* schematically shows the geometry of the WM and HAZ of the first and second beads in a longitudinal section

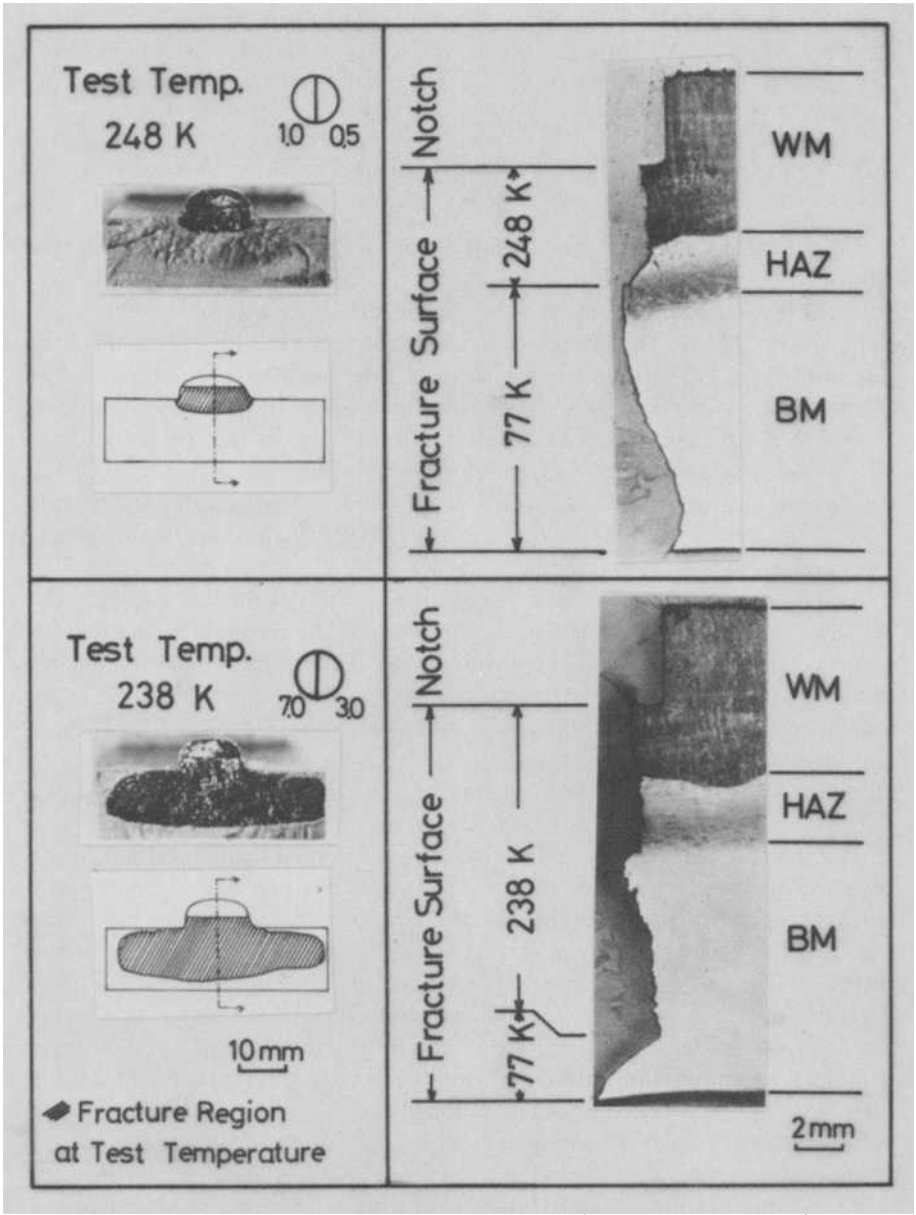

FIG. 4—*Crack paths and microstructures of drop-weight test specimens tested at 248 K* (top) *and 238 K* (bottom).

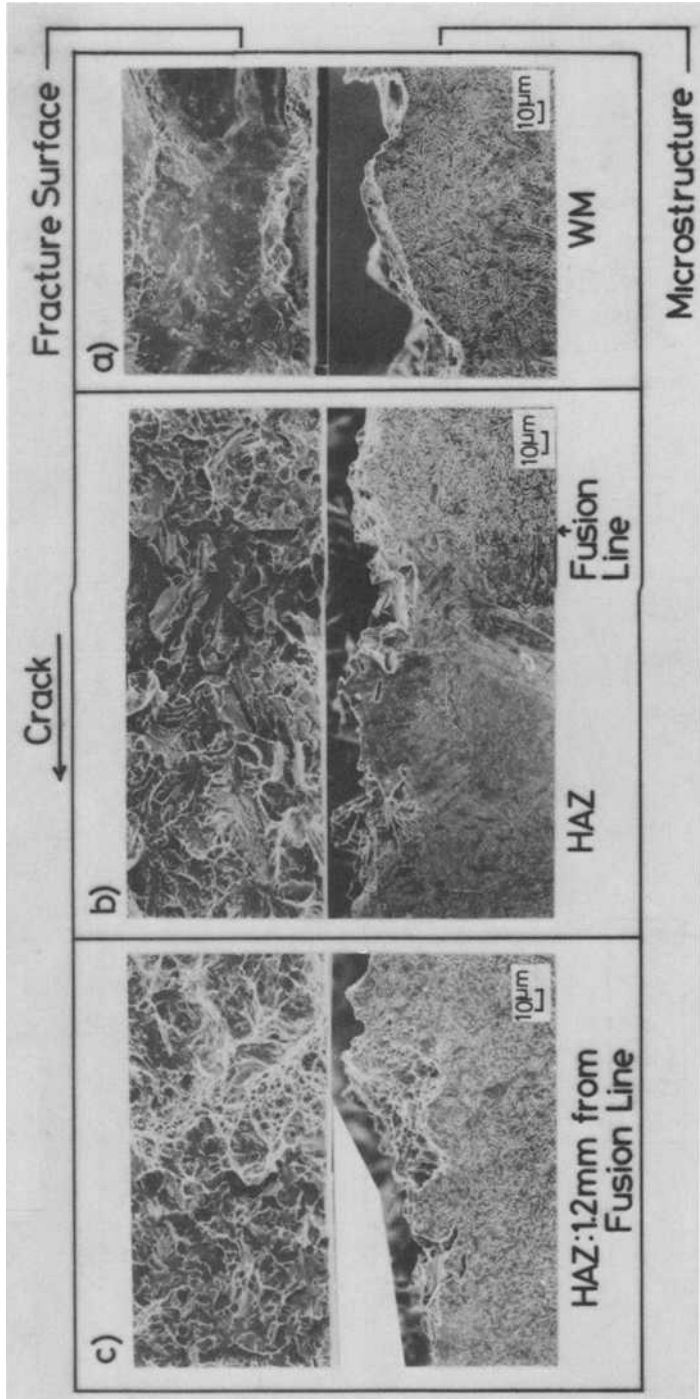

FIG. 5—*Scanning electron photomicrographs of the fracture surface and microstructure near the welded bead for a drop-weight test specimen:* (a) *WM;* (b) *HAZ, near the fusion line;* (c) *HAZ, 1.2 mm away from the fusion line.*

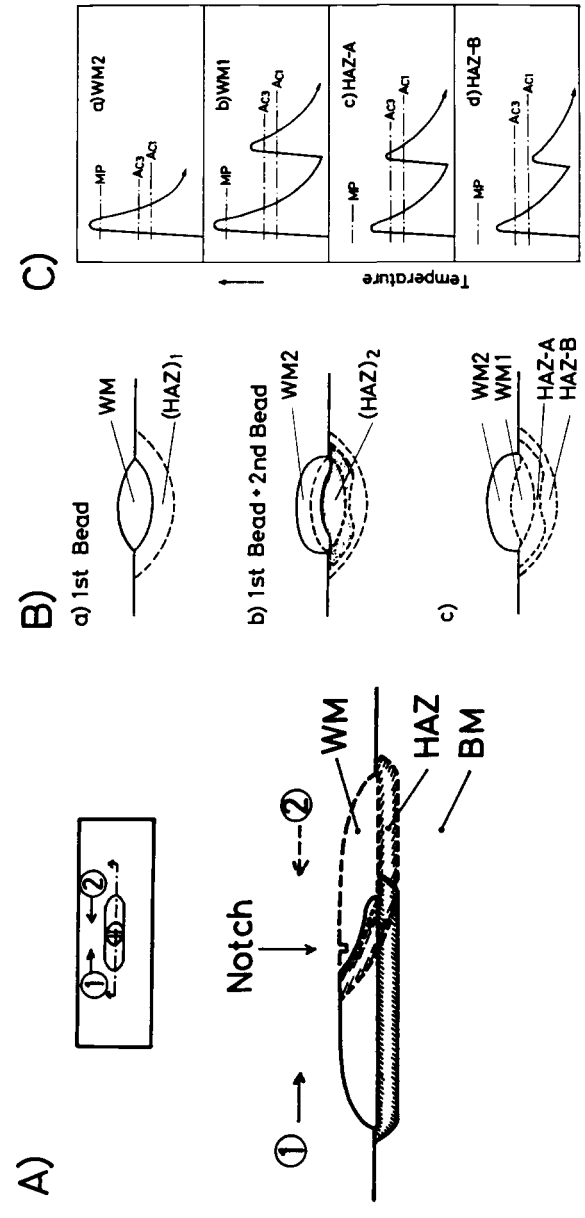

FIG. 6—*Schematic illustrations of the sections and thermal cycles of each zone for a drop-weight test specimen:* (a) *longitudinal section,* (b) *cross section.* (c) *thermal cycle.* Ac_1 *is the starting temperature of ferrite plus cementite to austenite transformation:* Ac_3 *is the finishing temperature of ferrite to austenite transformation: and MP is the melting point.*

of a drop-weight test specimen. Since the notch was cut at the mid-length of the brittle bead, where the first and the second beads overlaped, the area under the notch shows a very complicated microstructure.

Figure 6*b* schematically shows cross sections of a drop-weight test specimen at the center of the bead after welding. The weld metal (WM-1) and HAZ of first bead (HAZ-1) are affected by the heat of the second bead welding. HAZ-1 especially is divided into two zones. One zone (HAZ-A) is heated to a higher temperature than the finishing temperature of ferrite to austenite transformation Ac_3, as shown in Fig. 6*c*.

The strength and toughness of WM-1 and HAZ-A are changed by the cooling rate after the second bead welding. On the other hand, in the HAZ-B zone, the strength is decreased but toughness is increased because of the tempering effect of the sequential welding heat.

In order to evaluate the toughness of these zones in a drop-weight test specimen of A533 Grade B, Class 1 steel plate (Steel C), the Charpy impact test was conducted using specimens simulating the welding thermal cycles of these zones. The comparison of the toughness of the HAZ-A and HAZ-B zones is shown in Fig. 7. From these results, the authors conclude that the HAZ-B zone has a high resistance to crack propagation because of its high toughness values. The HAZ-A zone is also expected to have resistance to crack propagation, if it has low strength and high toughness values, which depend on the cooling rate of second bead welding.

As mentioned earlier, these mechanical property changes of HAZ near the brittle bead are in good agreement with the changes in NDTT and the fracture surface observations.

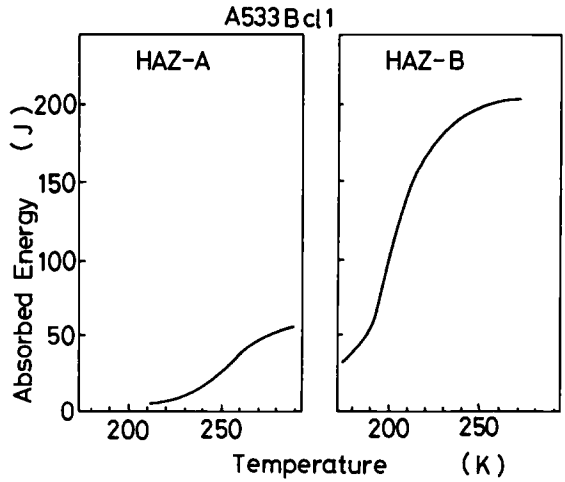

FIG. 7—*Charpy impact transition curves for HAZ-A and HAZ-B zones. The charpy impact test was conducted by using specimens simulating the thermal cycles of these zones.*

Evaluation of the NDTT of A533 Grade B, Class 1 Steel Plates Based on Their Fracture Toughness

In this investigation, NDTT of A533 Grade B, Class 1 steel plates varied remarkably with the welding conditions of the crack-starter bead. On the other hand, NDTTs of SPV-50Q and A516-Grade 70 steel plates varied little, because the hardness of the HAZ in these steel plates is comparatively low, 200 to 250 HV. Also, the hardness values of the HAZ are not influenced so much by welding conditions in drop-weight test specimens.

Using the fracture toughness values, the exact NDTTs of A533 Grade B, Class 1 steel plates were estimated. An assumption was made that the fracture in drop-weight test specimens corresponds to a case in which bending stress is applied to a plate having a semielliptical flaw.

The stress intensity factor K_I for a semielliptical flaw under bending stress is defined in the following equation.

$$K_I = M_{B\alpha}\sigma\sqrt{\frac{\pi a}{Q}} \tag{4}$$

where $M_{B\alpha}$ is a dimensionless magnification factor [*3,4*], σ is applied bending stress, Q is $\Phi^2 - 0.212(\sigma/\sigma_y)^2$, and Φ is the elliptic integral

$$\Phi = \int_0^{\pi/2} \left[\sin^2\phi + \left(\frac{a}{c}\right)^2 \cos^2\phi\right]^{1/2} d\phi$$

where a is the flaw depth, $2c$ is the flaw width, and σ_y is the material yield stress. As the applied stress σ is equal to the dynamic yield stress σ_{yd} at drop-weight test conditions [*5*], it is possible to calculate the K_I value using Eq 4, if the flaw depth a and its width $2c$ are given.

When the welding condition of the crack-starter bead are suitable, K_{Id} of HAZ is smaller than that of the base metal. Therefore, the authors conclude that unstable fracture initiates and propagates if K_I at the flaw tip is equal to or larger than K_{Id} of the base metal, as shown in Eq 5.

$$K_I \geqq K_{Id}(T) \tag{5}$$

where $K_{Id}(T)$ is the dynamic fracture toughness of the base metal at temperature T.

K_{Id} values of the base metal of A533 Grade B, Class 1 steel plates were determined by the instrumented precracked Charpy test. K_{Id} values obtained by this method sometimes produce questionable values because of the small specimen size. But the test is reliable at the low nil-ductility temperature. An example of the temperature dependence of K_{Id} values of the base metal is shown in Fig. 8.

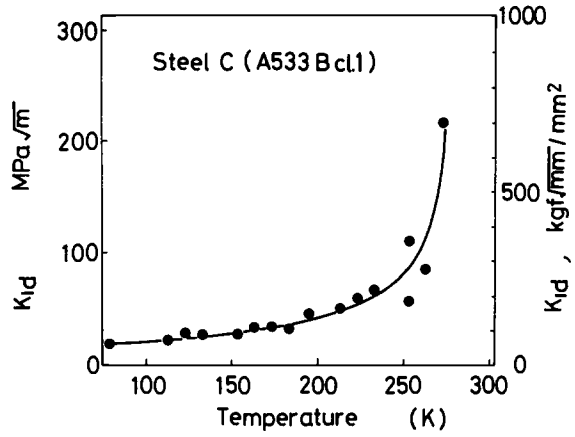

FIG. 8—*An example of the temperature dependence of the dynamic fracture toughness* K_{Id} *of the base metal for A533 Grade B, Class 1 steel plate (Steel C).*

Since cracks easily propagate in the coarse grain zone of HAZ, as stated earlier, it is assumed that the flaw depth is one third of the HAZ and its width is equal to the crack-starter bead width. The σ_{yd} of the base metal was estimated in accordance with the procedure described in Ref 5 because σ_{yd} had not been measured yet. The calculated NDTT was estimated by using Eq 4, provided that K_I is equal to K_{Id} of the base metal at NDTT. These calculated NDTTs are compared with the observed NDTTs in Fig. 9. The observed NDTTs are lower than the calculated NDTTs. Differences between the calcu-

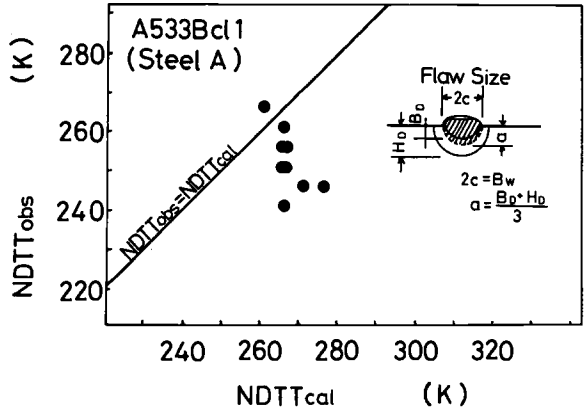

FIG. 9—*Relationship between the estimated NDTT* ($NDTT_{cal}$) *and the observed NDTT* ($NDTT_{obs}$) *of A533 Grade B, Class 1 steel plates.*

lated NDTTs and the observed NDTTs, $\Delta NDTT = NDTT_{cal} - NDTT_{obs}$, were calculated. The relationship between $\Delta NDTT$ and the mean hardness values of HAZ is shown in Fig. 10. The $\Delta NDTT$ increases with the decrease in HAZ hardness. The lower the HAZ hardness, the lower the observed NDTT is.

Consequently, this large difference between the observed and calculated NDTTs is caused by the lower hardness of HAZ under the crack-starter bead. Therefore, in order to obtain the exact NDTT of steel plate, it is important that drop-weight test specimens have hard and brittle HAZ around the welded bead to create the crack easily. Thus, by using specimens with brittle weld metal and HAZ, the NDTT values of three kinds of A533 Grade B, Class 1 steel plates (Steels A, B, and C) were determined and are tabulated in Fig. 11, which compares the NDTT and estimated NDTT, (NDTT)*. The (NDTT)* was obtained as follows. At NDTT, Pellini and Loss [5] obtained the following relationship

$$\frac{K_{Id}}{\sigma_{yd}} = 0.4 \text{ to } 0.7\sqrt{\text{in.}} = 2.0 \text{ to } 3.5\sqrt{\text{mm}}$$

The temperature dependence curves of K_{Id}/σ_{yd} in these steels are shown in Fig. 11. NDTTs estimated by using the relationship of Pellini and Loss are in good agreement with the observed NDTTs.

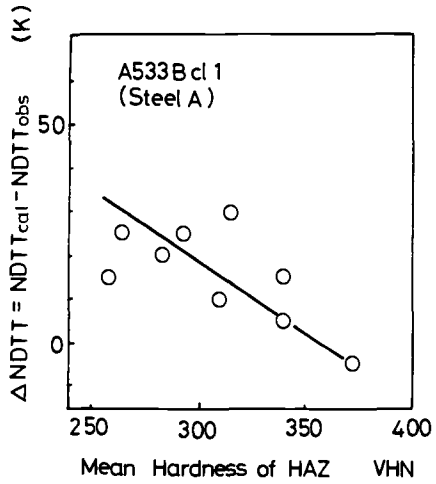

FIG. 10—*Relationship between ΔNDTT, the difference between the observed NDTT and the calculated NDTT, and the mean hardness of the HAZ for A533 Grade B, Class 1 steel plates.*

Steel	NDTT	(NDTT)*
A	263 K	253 K
B	248	248
C	228	228

* Temperature at $K_{Id} / \sigma_{yd} = 25\sqrt{mm}$

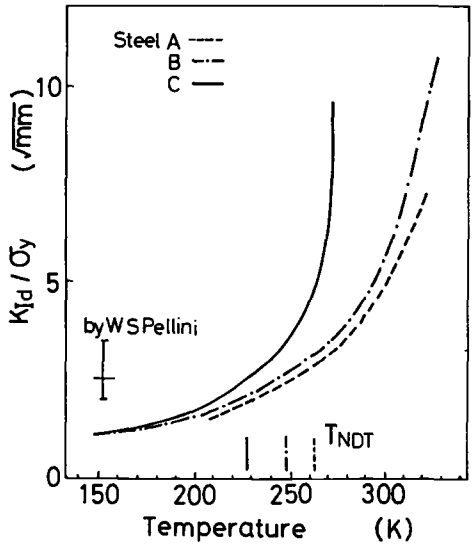

FIG. 11—*Relationship between the temperature dependence of* K_{Id}/σ_{yd} *and the observed NDTTs for A533 Grade B, Class 1 steel plates. The observed NDTT and the estimated NDTT, (NDTT)*, of these steels are tabulated in the table of this figure.*

Conclusions

The effect of the heat-affected zone (HAZ) under the crack-starter bead on the nil-ductility transition temperature (NDTT) in drop-weight test specimens of pressure vessel steels was investigated. The following results were obtained:

1. The NDTT becomes higher by increasing the hardness of HAZ. It varies remarkably in A533 Grade B, Class 1 steel plate but little in SPV-50Q and A516-70 steel plates.

2. Ductile fracture is observed in the fine grain zone of HAZ near the crack-starter bead. This zone appears to have a high resistance to crack propagation.

3. In A533 Grade B, Class 1 steel plates, the observed NDTT, which is determined by using specimens with brittle weld metal and HAZ, is in good agreement with the estimated NDTT calculated by using K_{Id}.

References

[1] Puzak, P. P., Eschbacker, E. W., and Pellini, W. S., *Welding Journal*, Vol. 31, 1952, p. 561S.

[2] Ohnishi, K., Tsukada, H., Suzuki, K., Murai, M., and Tanaka, Y., *Tetsu to Hagané*, Vol. 64, 1974, p. 831.

[3] Shah, R. C. and Kobayashi, A. S. in *Stress Analysis and Growth of Cracks, ASTM STP 513*, American Society for Testing and Materials, Philadelphia, 1972, pp. 3-21.

[4] Marrs, G. R. and Smith, C. W. in *Stress Analysis and Growth of Cracks, ASTM STP 513*, American Society for Testing and Materials, Philadelphia, 1972, pp. 22-36.

[5] Pellini, W. S. and Loss, F. J., NRL Report No. 6900, Naval Research Laboratory, Washington, DC, 1969.

Carl E. Hartbower[1]

Drop-Weight NDT Temperature Test Results for Five Heats of ASTM A517 Steel

REFERENCE: Hartbower, C. E., **"Drop-Weight NDT Temperature Test Results for Five Heats of ASTM A517 Steel,"** *Drop-Weight Test for Determination of Nil-Ductility Transition Temperature: User's Experience with ASTM Method E 208, ASTM STP 919*, J. M. Holt and P. P. Puzak, Eds., American Society for Testing and Materials, Philadelphia, 1986, pp. 87-107.

ABSTRACT: This paper describes the results of drop-weight (DW) nil-ductility transition (NDT) temperature testing (according to the ASTM Method for Conducting Drop-Weight Test to Determine Nil-Ductility Transition Temperature of Ferritic Steels [E 208-69(1975)]) of "as fabricated" surfaces as well as quarter-point (subsurface) material from five plates of ASTM A517 steel, each plate from a different heat of steel. The steel was from two California bridges, one of which developed brittle fracture of a main-load-carrying flange during erection of the bridge. The five plates were characterized by Charpy V-notch impact, precracked Charpy impact, dynamic tear, and plane-strain fracture toughness testing; these results were compared with the results obtained from the drop-weight test. One plate showed 66.7°C (120°F) difference between the NDT temperatures for surface and subsurface material. Heat tinting "unbroken" drop-weight specimens revealed further complications in using ASTM Method E 208, including cracked tension surfaces not revealed in evaluation by the ASTM test and specimens with uncracked corners (and therefore rated "unbroken" by the ASTM test) but with virtually completely fractured cross sections. Both the dynamic tear and precracked Charpy impact tests were evaluated for usefulness in estimating the drop-weight NDT temperature; the correlation of test results was made uncertain, if not precluded, by through-thickness inhomogeneity and complications in the ASTM DW test method. Recommendations are made to improve ASTM Method E 208 by heat tinting. The five heats of ASTM A517 steel were shown to have widely variable fracture characteristics.

KEY WORDS: nil-ductility, transition temperature, ASTM standard E 208, drop-weight test, dynamic tear test, Charpy V-notch impact test, precracked Charpy impact test, thickness toughness gradient, A517 Grade F steel, A517 Grade H steel, failure analysis

On June 13 1970, a large, steel, box-girder bridge under construction at Bryte Bend, west of Sacramento, California, developed a brittle fracture in

[1]Consultant welding engineer, Fair Oaks, CA 95628.

one of three tension flanges as the concrete deck was being placed. The failure occurred catastrophically across the full width of a 762-mm (30-in.)-wide by 57.2-mm (2¼-in.)-thick flange and was arrested about 101.6 mm (4 in.) down the web of the girder (Fig. 1).[2] The ambient temperature was 14.4°C (58°F). The steel was ASTM A517 Grade H modified. Although Grade H is normally limited to a 50.8-mm (2-in.) thickness, for this bridge, Grade H was allowed in thicknesses up to 57.2 mm (2¼-in.). Following this failure, an

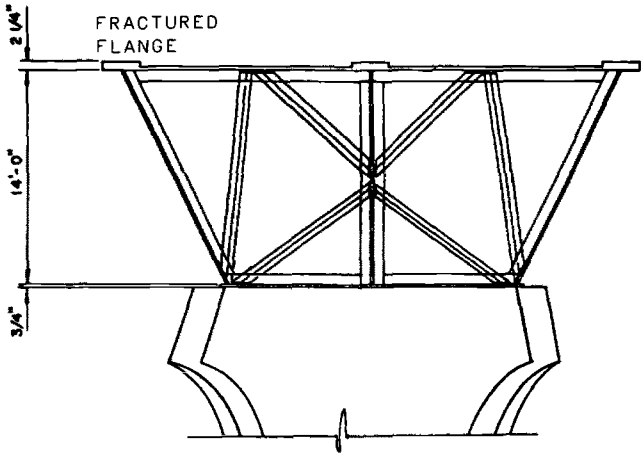

FIG. 1*a*—*Typical section of steel box girders in the Bryte Bend Bridge.*

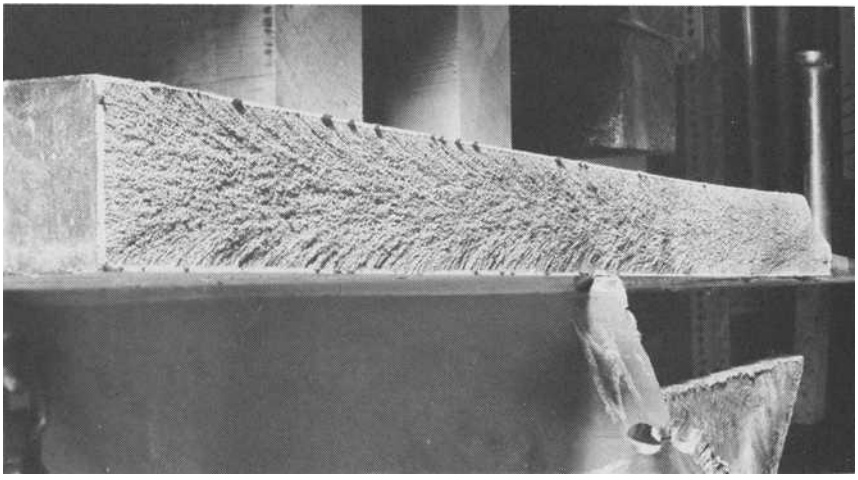

FIG. 1*b*—*Fractured flange, 57.15 mm (2¼ in.) thick by 762 mm (30 in.) wide.*

[2]The original measurements were made in English customary units.

FIG. 1*c*—*Fracture origin at the weld between the flange and the cross bracing.*

extensive investigation of the cause was initiated by the California Department of Transportation [*1*]. The data presented in this paper are part of the fracture testing done in the bridge failure analysis.

The fracture tests performed were the following:

(*a*) Charpy V-notch impact (CVN) test [ASTM Methods for Notched Bar Impact Testing of Metallic Materials (E 23-72(1978)];

(*b*) precracked Charpy impact (PCI) test [*2–4*];

(*c*) compact tension (CT) fracture toughness test [ASTM Test for Plane-Strain Fracture Toughness of Metallic Materials (E 399-72)];

(*d*) dynamic tear (DT) test [ASTM Test for Dynamic Tear Energy of Metallic Materials (E 604-77)];

(*e*) Drop-weight (DW) nil-ductility transition (NDT) temperature test [ASTM Method for Conducting Drop-Weight Test to Determine Nil-Ductility Transition Temperature of Ferritic Steels (E 208-69(1975))].

This paper compares the NDT temperature obtained from the DW test with those predicted from the other tests, and the shortcomings of the DW test procedure are discussed.

Materials and Experimental Work

Fifty-two plates of ASTM A517 steel were investigated; however, drop-weight NDT temperature tests were performed on only five of them. These five plates include the casualty plate (identified as Plate CK); two plates that exhibited CVN properties similar to those expected for the grade (Plates D

and Y) (Fig. 2*a*); and two plates that exhibited atypical CVN properties, where the transition from brittle to ductile behavior occurred at temperatures higher than expected for the grade (Plates A and AL) (Fig. 2*b*). CVN tests were also performed on Plate AL using specimens taken from various positions through the thickness; these results (Fig. 3) show that CVN notch toughness varies through the thickness. No brittle-to-ductile transition was observed for tests of Plate CK compact tension specimens (Fig. 4). (All CT test results shown were valid based upon 2.5 $(KQ/\text{yield strength})^2$ and P_{max}/P_q criteria). The results of dynamic tear tests are shown in Table 1; as can be seen in Table 1 and Fig. 5, a through-thickness DT-toughness gradient exists. The chemical composition and the tensile properties of Plates A and D are shown in Tables 2*a* and 2*b*, along with the corresponding values specified by the ASTM Specification for Pressure Vessel Plates, Alloy Steel, High-Strength, Quenched and Tempered (A 517 Grade F) at the time the plates were ordered.

Discussion

ASTM E 208 NDT Temperatures in Fractured Plate CK

Table 3*a* gives the drop-weight NDT temperature test results obtained for the top and bottom surfaces of the 57.2-mm (2½-in.)-thick Grade H flange plate. ASTM Method E 208-69(1975) specifies that:

> Products thicker than the standard specimen thickness shall be machine-cut to standard thickness from one side, preserving an as-fabricated surface unless otherwise specified, or agreed to, in advance by the purchaser. The as-fabricated surface so preserved shall be the welded (tension) surface of the specimen during testing.

It should be recalled from Fig. 5 that the dynamic tear (DT) test showed that the surface of Plate CK was somewhat tougher than the midthickness material. According to the ASTM Method E 208-69(1975), the NDT temperature has not been reached until the specimen is fractured to one or both edges of *the tension surface*. If the microstructure in the plate surface (the tension side of the test specimen) is relatively tough, the specimen may be nearly completely fractured and yet be "unbroken" because the corners of the tension surface are not fractured.

The correlation between the DT test and the drop-weight NDT test results is good, with the *surface* DT test indicating an NDT temperature of 15.6°C (60°F), in comparison with the drop-weight-measured value of 26.7°C (80°F). The precracked Charpy impact (PCI) test indicated little or no difference between the surface and center of the CK plate, with the steel showing consistently low toughness, irrespective of the thickness position. The PCI data plotted as a straight line out to 160°C (320°F) with no evidence of an inflection in the transition curves and, therefore, provided no indication of

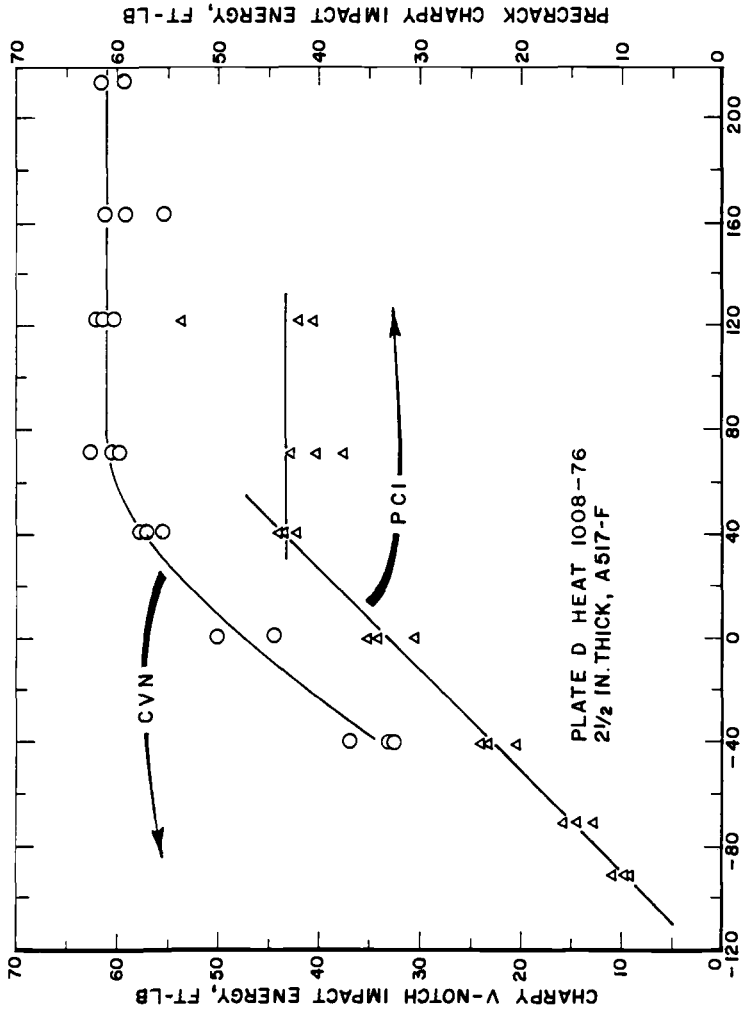

FIG. 2a—*Typical CVN results for A517 Grade F steel.*

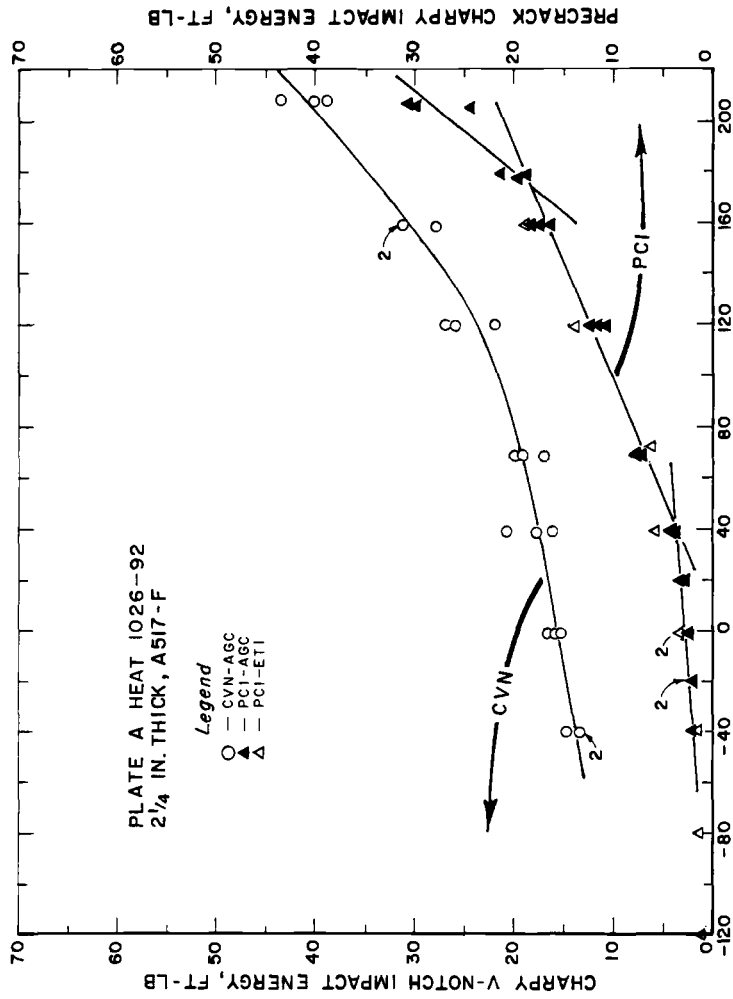

FIG. 2*b*—*CVN results for an atypical heat.*

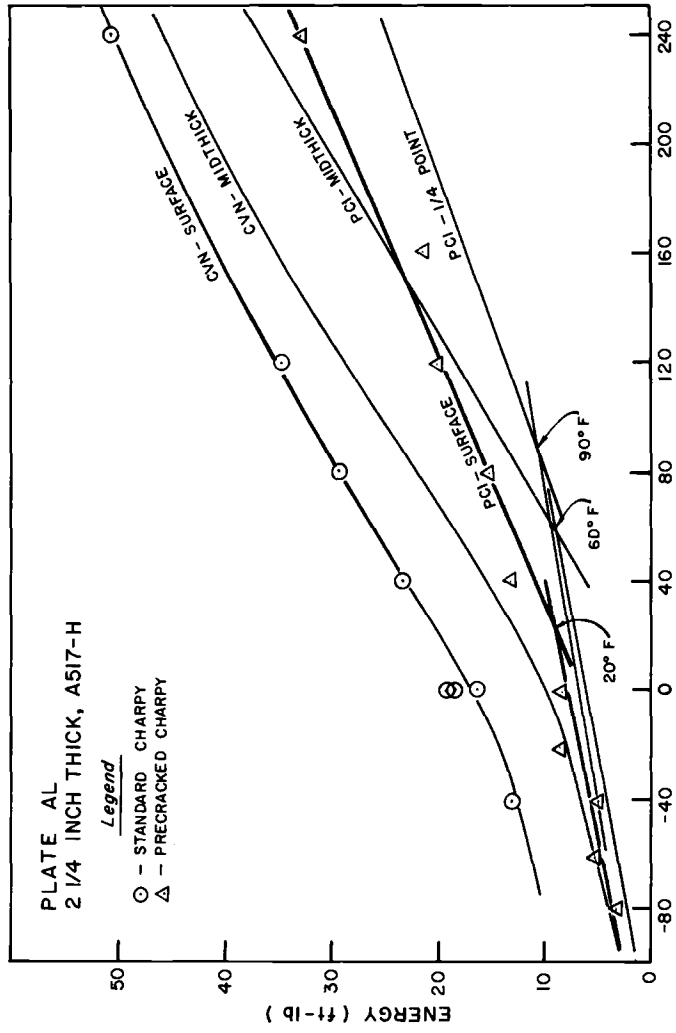

FIG. 3—*Charpy test results as a function of the thickness position.*

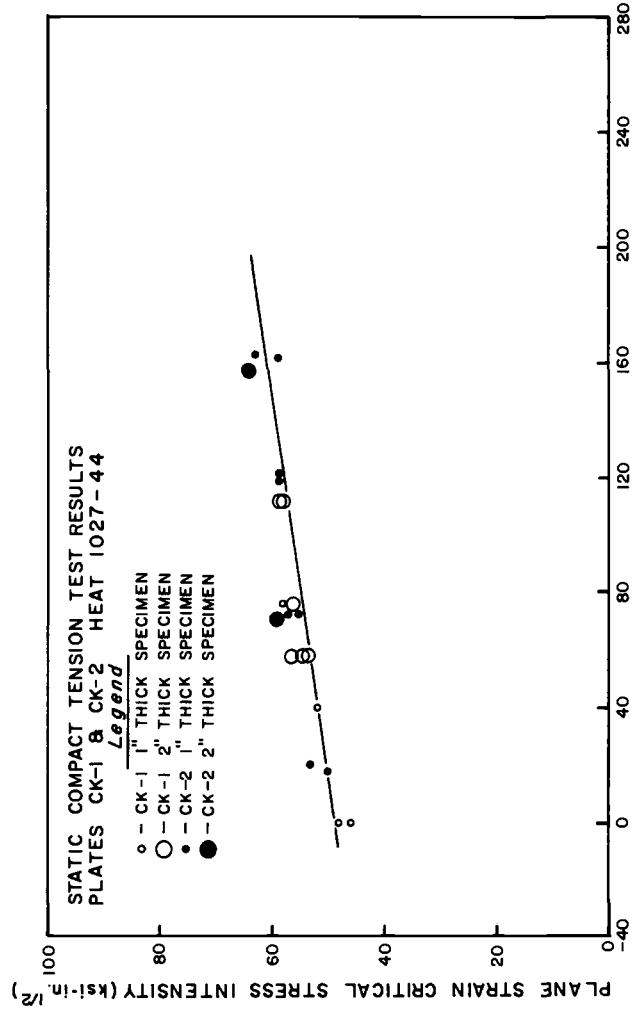

FIG. 4—*Static compact tension test result for Plates CK1 and CK2.*

TABLE 1—*Dynamic tear test results.*

Test Temperature, °F[a]	Plate Data, ft · lb						
	Plate D, A517 Grade F	Plate A, A517 Grade F	Plate AL, A517 Grade H	Plate Y, A517 Grade H	Plate CK, A517 Grade H, Thickness Position		
					Top	Center	Bottom
−100	92	...	...	...	...	...	...
−80	101	...	...	...	...	...	...
−60	147	...	...	...	...	...	...
−40	246	...	...	...	...	...	...
−20	...	...	80[b]	72[b]	...	...	...
0	515	59[b]	67[b]	68[b]	59	58	55
20	...	88	96	108	...	...	...
40	569	67[b]	126	141	...	61	76
60	...	99	168	...	76/68/70	57/51/53	70/66/69
80	...	121	207	204	99	65	84
100	...	...	...	...	105	65	97
120	...	123/124	265	301	105/112	71/79	104/109
140	...	...	...	...	...	...	...
160	...	271	349	399	143	111	131
180	...	...	...	...	...	...	...
200	...	224/234	303/386	448	157/150	128/126	180/165
220	...	...	...	...	...	...	...
240	...	...	...	479	...	...	...
270	...	...	...	...	214	194[c]	205
330	...	...	...	...	263	251	261[d]

[a] °C = (°F − 32)/1.8.
[b] A single spike from a force-time trace provides the estimate of NDT temperature.
[c] Tested at 123.3°C (254°F).
[d] Tested at 162.8°C (325°F).

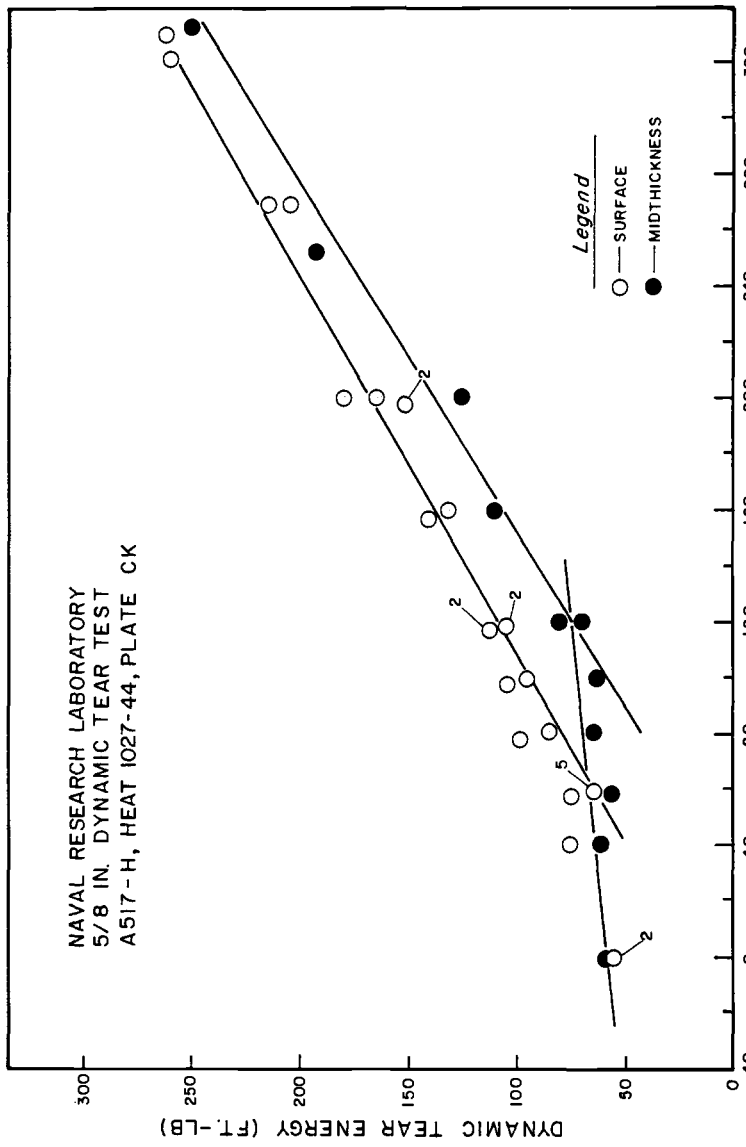

FIG. 5—*Dynamic tear test results for surface and midthickness positions.*

TABLE 2*a*—*Mechanical properties of Plates A and D.*

Plate	Yield Strength, ksi[a]	Tensile Strength, ksi	Elongation, %	Reduction of Area, %
D	124.8	133.2	19.0	60.5
A	113.5	127.1	20.0	57.7
ASTM Specification A 517[b]	100.0	115.0	16.0	45.0

[a]1 ksi = 6.8948 MPa.
[b]At the time the plates were ordered.

TABLE 2*b*—*Chemical analysis of Plates A and D, in weight percent.*

Plate	C	Mn	P	S	Si	Cu	Ni	Cr	Mo	V	B
D	0.17	0.89	0.010	0.016	0.24	0.23	0.80	0.49	0.45	0.04	0.002
A	0.15	0.78	0.015	0.015	0.24	0.29	0.80	0.52	0.45	0.06	0.003
ASTM Specification A 517[a]	0.08 to 0.22	0.55 to 1.05	0.035 max	0.040 max	0.13 to 0.37	0.12 to 0.53	0.67 to 1.03	0.36 to 0.69	0.36 to 0.64	0.02 to 0.09	0.002 to 0.006

[a]At the time the plates were ordered.

TABLE 3*a*—*Drop-weight nil-ductility transition temperature data for the casualty plate.*[a]

Steel Code	Top Surface Position			Bottom Surface Position		
	Temperature, °F[b]	Break	No Break	Temperature, °F	Break	No Break
1027/44CK	60	X		60	X	
A517 Grade H	80	X (NDT)		70		0
Plate CK	90		0	80		0
	100		0	90		0
	120		0	100		0
	200		0	120		0

[a]Using ASTM Method E 208-81 Type P2 specimens, with a weight of 17 kg (60 lb), dropped from a height of 1.83 m (6 ft).
[b]°C = (°F − 32)/1.8.

the NDT temperature. In typical steels, two intersecting straight lines nicely fit the data at the junction of the lower shelf and the transition region (see Fig. 2*b*); the point of intersection is generally taken to be an approximation of the drop-weight NDT temperature).

NDT Temperatures in Plates A, D, AL, and Y

Table 3*b* gives the results obtained in the midthickness and the surface positions of two heats of A517 Grade F steel and two heats of A517 Grade H steel. These are the same heats and plates tested with the DT test. Note that the tests indicated a marked difference between the surface and midthickness values. Except for Plate D, the midthickness position had the higher NDT temperature. A517 Grade F Plate A was a flagrant example of this, with a 66.7°C (120°F) shift between the NDT temperatures for the surface and midthickness. In testing a steel like Plate A, ASTM Method E 208-69(1975) is seriously unconservative when the specimen is cut from the plate surface position.

Figures 6 and 7 show graphically the differences in plate thickness position and the differences between plates. Because of differences between the surface and midthickness positions in these plates, comparisons between test methods can be made only at a given position with respect to thickness. For the midthickness positions note that, in Plate A, the dynamic tear and the precracked Charpy tests were in agreement, indicating that the NDT temperature was 44.4°C (80°F) lower than the the NDT temperature in ASTM Method E 208-69(1975). This anomalous result cannot be explained as a crack-starter-weld heat-affected-zone (HAZ) complication in ASTM Method E 208 NDT testing; when the HAZ has an effect on the test results, it usually causes the E 208 NDT temperature to be fictitiously low. Also, in Plate D, the

TABLE 3*b*—*Drop-weight nil-ductility transition temperature data for four steel plates.*[a]

Steel Code	Midthickness Position			Plate Surface Position		
	Temperature, °F[b]	Break	No Break	Temperature, °F	Break	No Break
1026/92A	40	X		0°F	X (NDT)	0
A517 Grade F	60	X		10		0
Plate A	80	X		10		0
	100	X		20		0
	120	X (NDT)		40		0
	160		0			
1020/46AL	0	X (NDT)		−40	X (NDT)	
A517 Grade H	10		0	−30		0
Plate AL	10		0	−30		0
	20		0	−20		0
	60		0	0		0
				60		0
1008/76D	−90	X		−100	X	
A517 Grade F	−80	1/2 X (NDT)		−80	X	
Plate D	−80		0	−60	X	
	−70		0	−50	1/2 X (NDT)	
				−50		0
				−40		0
1024/91Y	−20	X (NDT)		−60		0
A517 Grade H	−10		0	−40		0
Plate Y	−10		0	−40		0
	0		0	−20		0
	60		0	0		0
				60		0

[a]Using ASTM Method E 208-81 Type P2 specimens, with a weight of 27 kg (60 lb), dropped from a height of 1.83 m (6 ft).

[b]°C = (°F − 32)/1.8.

dynamic tear and precracked Charpy test results were in agreement and, again, the indicated NDT temperature was lower than the ASTM E 208 NDT temperature. However, in this plate the difference between the estimated NDT temperature and the ASTM E 208 NDT temperature was only about 11.1°C (20°F).

In Plate D, the microstructure throughout the thickness was found to consist of a uniform, dense, dispersion of fine carbide particles in a tempered martensite matrix.[3] The steel was almost entirely (95%) tempered martensite. This fine-scale, uniform microstructure is known to possess excellent fracture toughness. In Plate A, on the other hand, at a depth of only 6.35 mm (1/4 in.) below the plate surface, the microstructure was found to consist of 50% intermediate-temperature transformation product (a ferrite-carbide aggregate resembling upper bainite).[3] Moreover, at a distance of 28.58 mm (1 1/8 in.) be-

[3]Pellissier, G. E., personal communication, 10 March 1975.

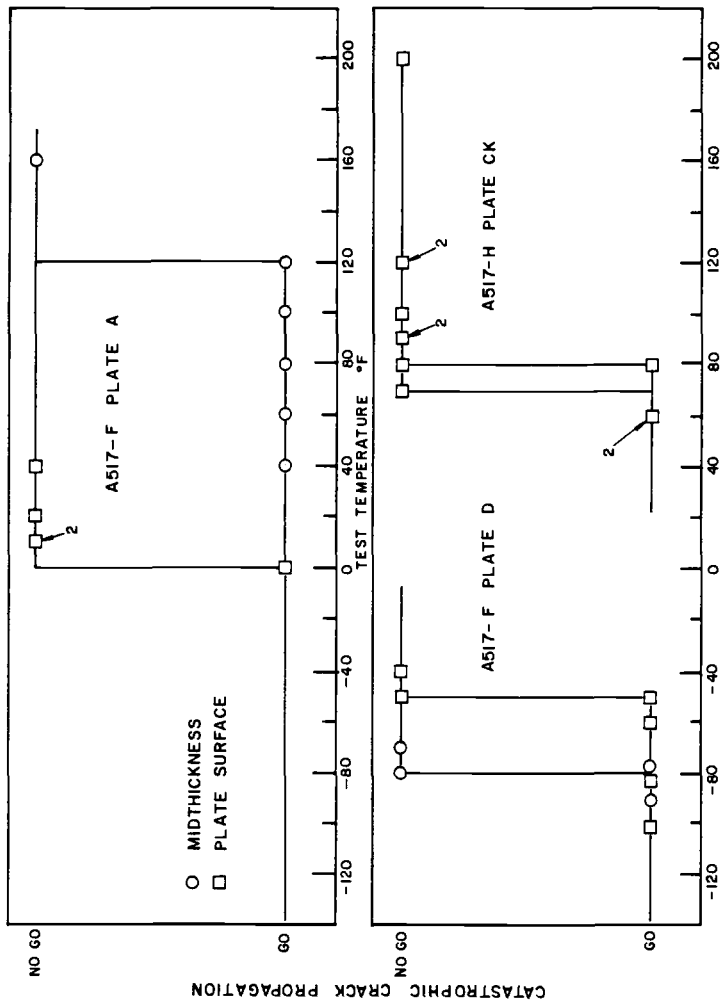

FIG. 6—*ASTM Method E 208 drop-weight test results for the surface and midthickness positions for Plates A, D, and CK.*

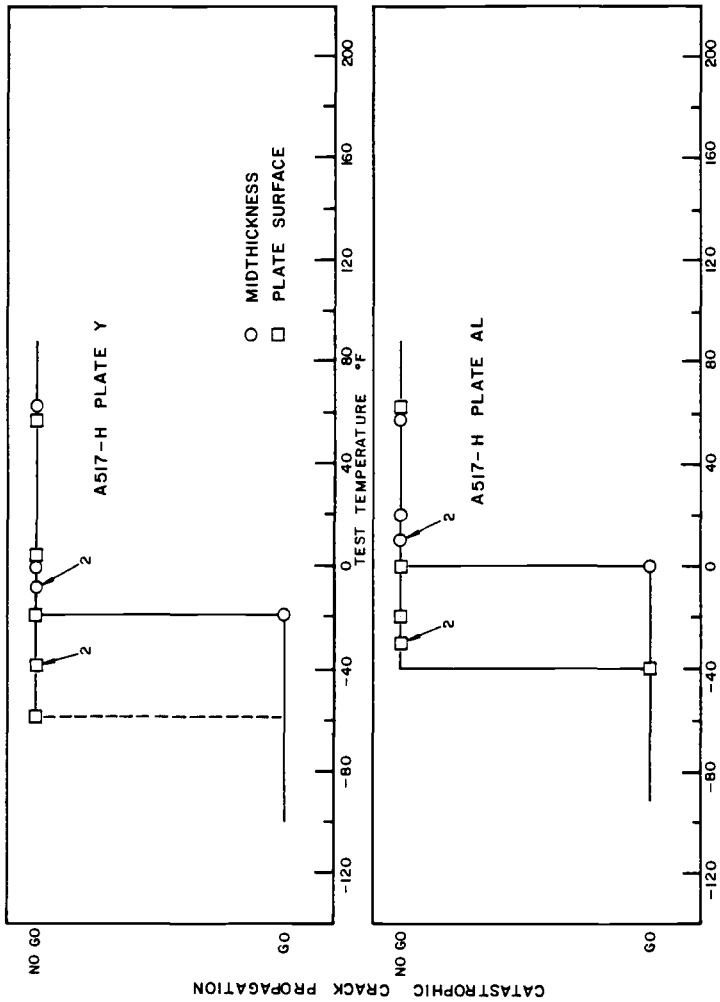

FIG. 7—*ASTM Method E 208 drop-weight test results for the surface and midthickness positions for Plates AL and Y.*

low the plate surface (midthickness) the microstructure contained islands of ferrite in combination with pools of martensite of higher than average carbon content. At midthickness, there was less than 5% tempered martensite. Thus, in A517 Grade F Plates A and D, the quantitative agreement between the dynamic tear and precracked Charpy NDT temperatures was consistent with the relatively uniform microstructures that existed throughout the center section of each plate. In Plate A, the center section was uniformly poor (low-toughness upper bainite), and in Plate D, it was uniformly good (tempered martensite). The fact that, in Plate A, the PCI NDT temperature was the same at the quarter-point and midthickness positions was consistent with the fact that upper bainite extended from the midthickness position to within about 6.35 mm (1/4 in.) of the plate surface.

In this connection, Fig. 8 shows the relative position of each specimen type with respect to thickness and microstructure in Plate A. Note that for the 19.05-mm (3/4-in.)-thick ASTM E 208 Type P-2 NDT specimen at midthickness position, the tension surface (which determines a break or no-break performance) was approximately at the quarter-point position in 57.15 mm (2 1/4-in.)-thick plate.

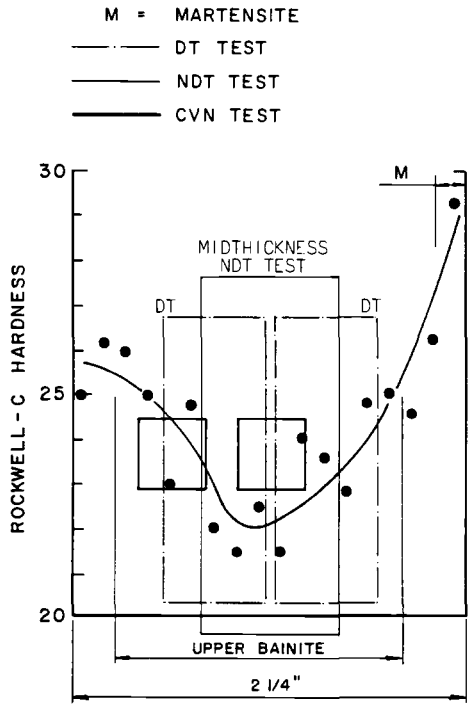

FIG. 8—*Hardness and microstructural gradient from the surface to the midthickness position for Plate A. Heat 1026-92. 57.2-mm (2 1/4-in.)-thick A517 Grade F steel.*

In A514/A517 Grade H Plates AL and Y, the microstructural and attendant hardness gradients precluded correlation between specimen types. When *surface* Charpy specimens were machined from Plate AL, the precracked Charpy impact NDT temperature was −6.7°C (20°F) (see Fig. 3). When the tension surface of the E 208 NDT test specimen contained tough, tempered martensite, one would expect a low NDT temperature [for example, −40°C (−40°F) in Plate AL and −51.1°C (−60°F) in Plate Y], whereas the Charpy specimen, which integrates the resistance to crack propagation over a 10-mm (0.394-in.)-thick surface layer, encompasses both the shallow martensite surface and the less tough intermediate transformation products below the surface. Apparently the mixed structures (martensite plus a ferrite-carbide aggregate resembling upper bainite) at the quarter-point position were even more brittle than the midthickness microstructure.

Heat Tinting in ASTM Method E 208 Testing

Because of the obvious complication introduced by a gradient of microstructure (toughness) from the surface to the midthickness position, the drop-weight NDT specimens that were classified by ASTM Method E 208-69(1975) as "no break" were placed in a furnace at 482.2°C (900°F), heat tinted, and then broken apart at low temperature to determine the extent of the original fracture inside the test piece. At 482.2°C (900°F) the original fracture surfaces were tinted dark blue, and the new fracture produced in breaking the specimen apart (for purposes of viewing the fracture surfaces) was bright and readily distinguished from the heat-tinted, original fracture. The findings confirmed the earlier observations that the present ASTM E 208 NDT test method is not conservative in steels with a surface-to-midthickness gradient of toughness.

Figure 9*a* is a photograph of the fracture surface in Plate AL midthickness specimens. Note that at temperatures *above* the E 208 NDT temperature there was extensive interior fracturing. In fact, at −6.7°C (20°F) there was only a tiny corner of unfractured metal, which disqualified the specimen as a "break." It should be recalled (Fig. 8) that the tension surface of the "midthickness" NDT specimen is approximately at the quarter-point position with respect to thickness.

Likewise in the Plate AL surface specimens, there was extensive interior fracturing at temperatures up to 11.1°C (20°F) above the E 208 NDT temperature. Also it was discovered that one of the −34.4°C (−30°F) test specimens (Specimen AL6) was in fact a "break" by ASTM Method E 208 definition. Unmistakable blueing of the original crack-propagation fracture surface revealed complete separation on one side of the crack-starter weld and only a tiny unfractured corner on the other side. Thus, visual inspection of the test pieces failed to reveal what must have been a hairline crack extending across one corner of the specimen.

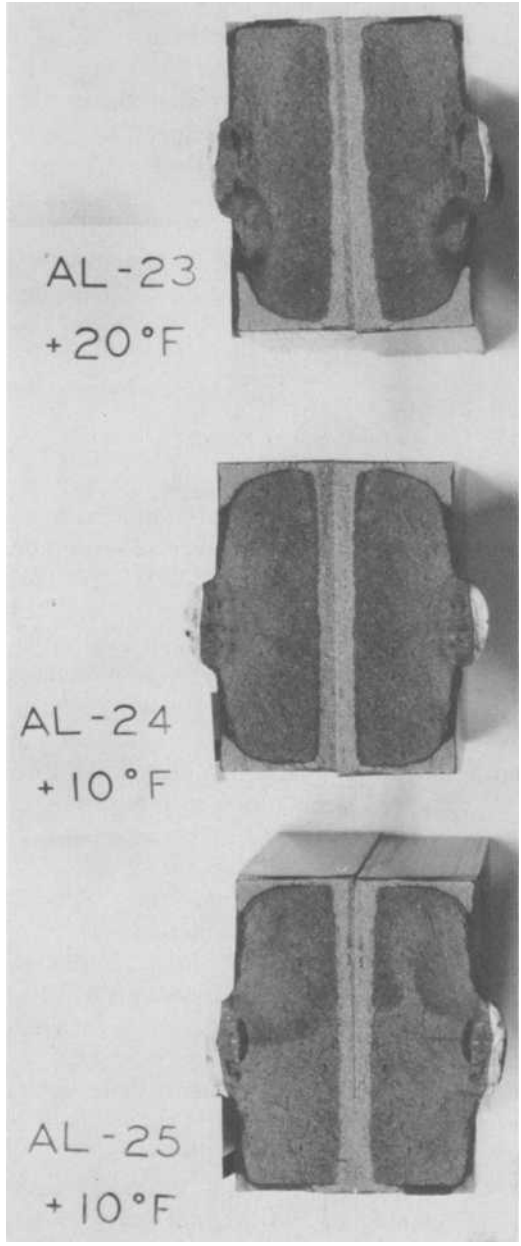

FIG. 9*a*—*Results of testing midthickness material in Plate AL NDT specimens heat tinted and broken apart to show the extent of fracture in the NDT testing. [The ASTM Method E 208 NDT temperature was −17.8°C (0°F)].*

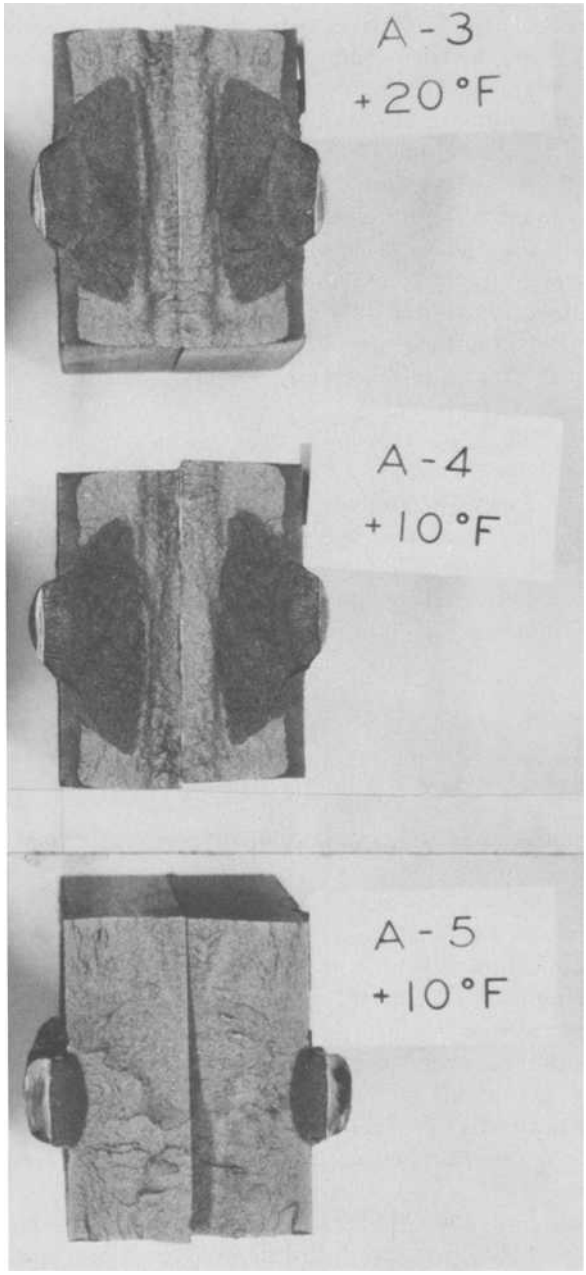

FIG. 9*b*—*Results of testing surface material in Plate A NDT specimens heat tinted and broken apart to show the extent of fracture in the NDT testing. [The ASTM Method E 208 NDT temperature was −17.8°C (0°F).]*

Plate Y also developed extensive interior fracturing at temperatures up to 22.2°C (40°F) above the E 208 NDT temperature in surface testing and up to 11.1°C(20°F) above the NDT temperature in "midthickness" testing.

Another anomaly was discovered in the heat tinting experiments; specimens were found with the crack-starter weld deposit fractured but with arrest of the crack at the fusion line. In other words, the weld heat-affected zone prevented the brittle weld-metal crack from entering the parent metal.

Figure 9*b* is an example of this behavior in Plate A surface specimen A5. In connection with this figure, it should be recalled that the "midthickness" NDT test specimens fractured at temperatures up to 48.8°C (120°F). Thus, it appears that the crack-starter-weld heat-affected zone formed in the microstructure at the plate surface arrested the brittle weld crack and was partially responsible for the anomalously great different between the two specimen positions.

Figure 9*b* also illustrates hairline surface cracking that escaped detection with the unaided eye (Specimen A3 and A4) at −12.2 and −6.7°C (10 and 20°F), where specimens had cracked across the entire specimen width, but the cracking was not observable when ASTM Method E 208 was used. Based on the ASTM E 208 test method, these specimens should have been classified as "broken" test pieces, raising the NDT temperature for plate surface material from −17.8 to −6.7°C (0 to 20°F).

Conclusions

The most significant findings relative to the ASTM Method E 208 are the following:

1. When there is a steep toughness gradient from the surface to the quarter point in the plate thickness, the drop-weight test specimen may almost completely fracture and yet be "unbroken" because the corners of the tension surface remain unfractured.
2. The complication of a through-thickness toughness gradient can be resolved by the simple device of heat tinting at 482.2°C (900°F) and then rating those specimens as fractured when 80% or more of the fractured surface is heated tinted; that is, when the initial drop-weight testing fractures 80% or more of the cross section.
3. Surface specimens were found to be completely cracked across the tension surface, with the cracks unseen by the unaided eye but clearly shown by heat tinting.
4. Heat tinting was found to serve another important purpose: when the crack-starter-weld HAZ arrested the brittle weld crack, the arrest was clearly defined by heat tinting. In such cases the apparent NDT temperature can be assumed to be fictitiously low.
5. In the casualty plate (Plate CK), the correlation between Method E 208 testing and dynamic tear testing was excellent for surface material; midthick-

ness E 208 testing was not performed. The NDT temperature was 21.1°C (70°F); the service failure occurred at 14.4°C (58°F).

6. An atypical plate of A517 Grade F (Plate A) had upper bainite throughout most of its cross section; DW NDT testing at the surface and at midthickness (tension surface at approximately the quarter point) indicated a 66.7°C (120°F) difference between the two positions. Method E 208 testing at the plate surface (quenched-and-tempered martensite) gave an NDT of −17.8°C (0°F), whereas testing at approximately the quarter point gave an NDT of 48.9°C (120°F). At the plate surface where the microstructure was tempered martensite, in some specimens the crack-starter weld HAZ completely arrested the crack.

7. In Plate A, both dynamic tear and precracked Charpy impact testing predicted the midthickness NDT temperature to be 4.4°C (40°F); the E 208 test method (modified) gave a quarter point NDT temperature of 48.9°C (120°F). This discrepancy cannot be explained by weld-HAZ crack arrest.

8. In a typical plate of A517 Grade F steel (Plate D) both the dynamic tear and the precracked Charpy impact testing estimated the NDT temperature to be below −73.3°C (−100°F) at the midthickness plate position; Method E 208 testing at the quarter-point position gave an NDT temperature of −62.2°C (−80°F).

Acknowledgments

The author is indebted to Peter P. Puzak of the U.S. Naval Research Laboratory, to Philip Crimmins and Walter Reuter of Aerojet General Corp., and to Charles B. Kendrick, Jr., and Roger D. Sunbury of the California Department of Transportation, all of whom made major contributions to the collection and reporting of the data presented in this paper.

References

[1] Hartbower, C. E. and Sunbury, R. D., "Variability of Fracture Toughness in A514/517 Plate," Report No. FHWA-RD-78-110, Federal Highway Administration, Washington, DC, December 1975.

[2] Hartbower, C. E., "Crack Initiation and Propagation in V-Notch Charpy Impact," *Welding Journal*, Vol. 36, No. 11, November 1957, p. 494.

[3] Orner, G. M. and Hartbower, C. E., "The Low-Blow Transition Temperature," *ASTM Proceedings*, Vol. 58, 1958, p. 623.

[4] "Properties of Welding Joints," *Welding Handbook*, 5th ed., Section 1, Fundamentals of Welding, Chapter 6, "Properties of Welded Joints," American Welding Society, New York, 1963, pp. 6.2-6.51.

Samuel R. Low[1] *and James G. Early*[2]

Drop-Weight Testing of Nonstandard Geometries

REFERENCE: Low, S. R. and Early, J. G., **"Drop-Weight Testing of Nonstandard Geometries,"** *Drop-Weight Test for Determination of Nil-Ductility Transition Temperature: User's Experience with ASTM Method E 208, ASTM STP 919*, J. M. Holt and P. P. Puzak, Eds., American Society for Testing and Materials, Philadelphia, 1986, pp. 108-128.

ABSTRACT: The test requirements contained in the standard test method for drop-weight testing, the ASTM Method for Conducting Drop-Weight Test to Determine Nil-Ductility Transition Temperature of Ferritic Steels (E 208-81), generally limit its applicability to flat products or to products with at least one flat surface; this is done because of the shape of the standard test specimens and the need for the tension surface of the specimen to be an as-fabricated surface. Difficulties arise in the application of ASTM Method E 208-81 to steel products whose fabricated shapes are not flat, for example, piping and pressure vessels. For products with curved surfaces, some of the testing requirements must be violated; these include keeping the as-fabricated surface as the tension surface, uniform specimen thickness, a flat compression surface, and uniform stress on the tension surface. In this study, the nil-ductility transition (NDT) temperature was determined as a function of test specimen geometry for two carbon/manganese structural steel grades. The specimens were extracted from the head plates of railroad tank cars and were curved in two orthogonal directions. The sensitivity of the test results to variations in test specimen geometry has been determined as is reported here.

KEY WORDS: AAR M128 steel, ASTM A212 steel, crack initiation, curved products, drop-weight test, fracture, nil-ductility transition temperature, specimen geometry effects, ASTM standard E 208

The drop-weight test was developed at the Naval Research Laboratory, Washington, DC, [*1*] in the early 1950s and has been standardized by the procedures and requirements set forth in the ASTM Method for Conducting Drop-Weight Test to Determine Nil-Ductility Transition Temperature of Ferritic Steels (E 208-81). The test is designed to determine the temperature at

[1]Mechanical engineer, Fracture and Deformation Division, Institute for Materials Science and Engineering, National Bureau of Standards, Gaithersburg, MD 20899.

[2]Deputy chief, Metallurgy Division, Institute for Materials Science and Engineering, National Bureau of Standards, Gaithersburg, MD 20899.

which a ferritic steel loses its ability to deform more than a minute amount in the presence of a sharp notch. This temperature is defined as the nil-ductility transition (NDT) temperature.

The test requirements contained in ASTM Method E 208-81 limit its applicability to flat products or products with at least one flat surface. This restriction results from the flat geometry requirements of the standard test specimens and the additional requirement of preserving an as-fabricated surface for the welded or tension surface of the specimen. Difficulties arise in the application of Method E 208 to steel products whose fabricated shapes are not flat, for example, piping and pressure vessels. For products with curved surfaces, some of the testing requirements must be violated; these include keeping an as-fabricated surface as the tension surface, uniform specimen thickness, a flat compression surface, and uniform stress on the tension surface. The sensitivity of the test results to variations in test specimen geometry and the interpretation of such results based on the crack-starting requirements, are not addressed by Method E 208-81, but are the basis for this study.

In two previous studies [*2,3*] at the National Bureau of Standards (NBS), research was conducted in which the NDT temperature was determined for steel products manufactured as curved plate. Both studies involved the examination of plate specimens taken from the end or head plates of railroad tank-car pressure vessels, which are curved in two orthogonal directions. The tank car plates were constructed of carbon/manganese structural steels, one of ASTM A212 steel and the other of American Association of Railroads (AAR) M128 steel. In these previous NBS studies, specimens with the nonstandard geometry of a curved as-fabricated tension surface and a flat machined compression surface were prepared and tested. This geometry of specimens is designated Group A.

For this study, the NDT temperatures were determined by testing three additional specimen geometries prepared from the same two tank-car headplates. The additional geometries were the following: Group B specimens had a curved as-fabricated tension surface and a curved as-fabricated compression surface; Group C specimens had a flat machined tension surface and a curved as-fabricated compression surface; and Group D specimens had a flat machined tension surface and a flat machined compression surface. The four specimen geometries are shown schematically in Fig. 1. The sensitivity of the test results to these four variations of test specimen geometry is reported here.

Materials

All the materials for this study were extracted from the head plates of two railroad tank cars, one that had been involved in an accident and one that had been used in switchyard impact tests. The test specimens for this work came from undamaged portions of the head plates. The compositions of the

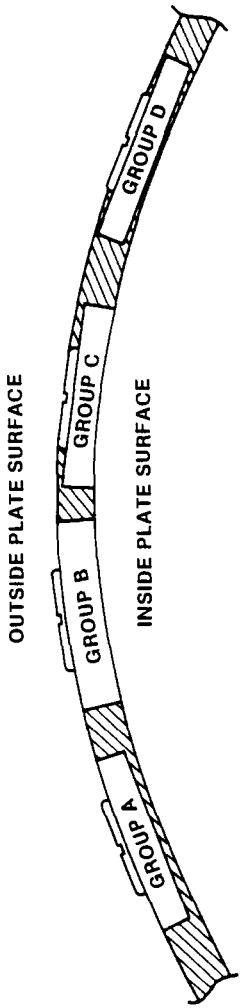

FIG. 1—*Schematic drawing of a head-plate cross section showing the geometries of the four specimen groups and the location on the head plate from which each group was machined. Note that the radius of curvature shown has been greatly exaggerated for clarity.*

two steels, AAR M128 and ASTM A212, are given in Table 1. Previously reported mechanical properties for these two steels are given in Table 2. These steel plates were selected because of the large difference between them in their ductile-to-brittle transition temperature behavior, as measured by the Charpy impact test (Figs. 2 and 3). As previously reported [*2,3*], the 20-J (15-

TABLE 1—*Chemical composition of head plate specimens of ASTM A212 and AAR M128 steels, in weight percent.*

Element	Specification Ladle Analysis	Check Analysis
	ASTM A212-65-B	
Carbon	0.31 max	0.24
Manganese	0.90 max	0.73
Phosphorus	0.04 max	<0.005
Sulfur	0.05 max	0.026
Silicon	0.13/0.33[a]	0.26
Copper	[b]	<0.05
Nickel	[b]	<0.05
Chromium	[b]	0.07
Molybdenum	[b]	<0.05
Vanadium	[b]	<0.01
Aluminum	[b]	<0.01
	AAR M128-69 GRADE A	
Carbon	0.25 max	0.23
Manganese	1.35 max	1.15
Phosphorus	0.04 max	0.01
Sulfur	0.05 max	0.017
Silicon	0.30	0.19
Copper	[b]	0.02
Nickel	[b]	0.20
Chromium	[b]	0.09
Molybdenum	[b]	0.05
Vanadium	0.02 min	0.026
Aluminum	[b]	0.02

[a]Check analysis.
[b]Element not specified.

TABLE 2—*Mechanical properties of ASTM A212 and AAR M128 steels.*[a]

Material	Ultimate Tensile Strength, MPa	Yield Strength, 0.2% Offset, MPa	Elongation, in 1 in., %[b]	Reduction in Area, %	Charpy Upper-Shelf Energy, J	Charpy Transition Temperature, °C
A212	468	227	37.4	61.4	98	19
M128	582	380	31.7	63.2	80	−50

[a]The data are from longitudinal specimens.
[b]1 in. = 25.4 mm.

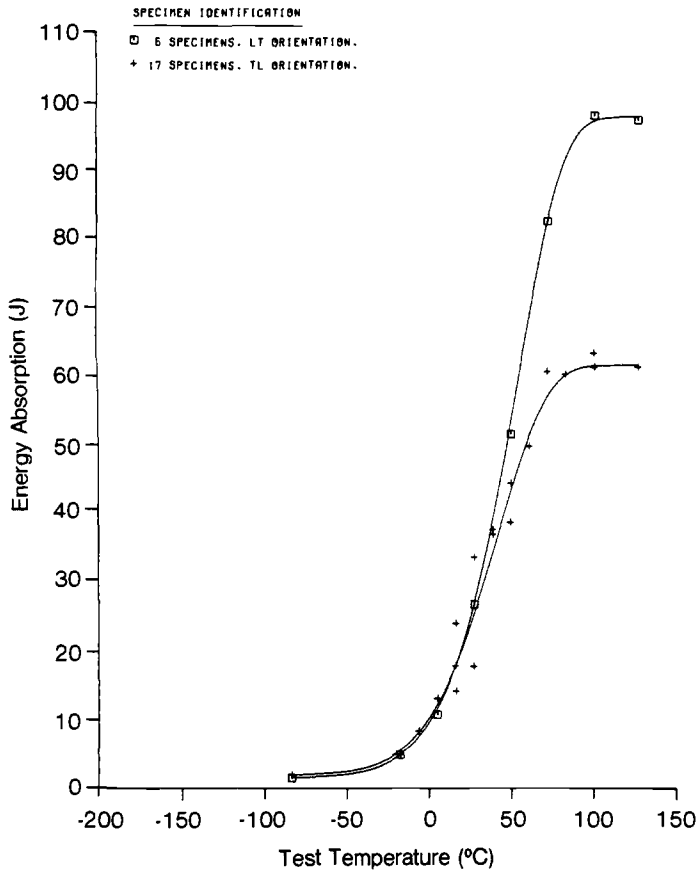

FIG. 2—*Charpy impact test results for head plate specimens taken from ASTM A212 steel.*

ft · lb) transition temperatures were approximately +19°C (66°F) and −50°C (−58°F), respectively, for the A212 and AAR M128 head plates, a difference of 69°C (124°F).

Typical microstructures of the two steels are shown in Figs. 4 and 5. The AAR M128 microstructure is typical of carbon/manganese steel in the hot-rolled condition and consists of a mixture of proeutectoid ferrite and pearlite. A montage of the longitudinal plane microstructure across the plate thickness (Fig. 4) shows the existence of extensive banding with alternate layers (parallel to the plate surface) of ferrite and pearlite. Overall, the banded microstructure is quite uniform from the outside plate surface to the midthickness. The ferrite grain size is ASTM No. 10½ (average grain diameter = 9.4 μm), as determined by the circular intercept method from the ASTM Methods for Determining Average Grain Size (E 112-84). The fine ferrite grain size is one of the factors which promote low impact transition temperatures.

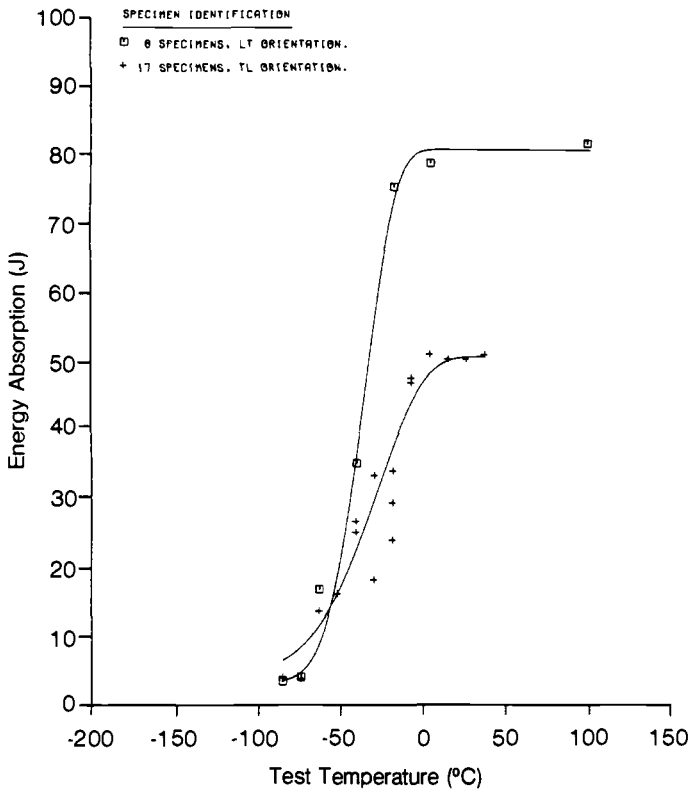

FIG. 3—*Charpy impact test results for head plate specimens taken from AAR M128 steel.*

The cross-sectional montage also reveals the presence of a microstructural anomaly near the inside plate surface. The regularity of the banded structure (Fig. 6*a*) has been disrupted, resulting in local areas of large pearlite colonies and large proeutectoid ferrite grains (Fig. 6*b*). Since the inside plate surface is always the compression surface, this anomaly should have no effect on the NDT results reported here.

The microstructure of A212 steel consists of large pearlite colonies and ferrite grains with little evidence of banding. There is a high degree of variability across the plate thickness (Fig. 5) with three distinct zones. The first zone (Zone 1) consists of a narrow decarburized layer, about 0.5 mm thick, located on both the inside and outside surfaces. Proceeding inward, the second zone (Zone 2), about 5 mm thick, contains large pearlite colonies, within which are found acicular or Widmanstatten side plates of ferrite. The pearlite colonies are observed to be generally surrounded by proeutectoid ferrite located on the prior austenite grain boundaries, as shown in Fig. 7*a*. The third zone, (Zone 3), a large region about 9 mm thick centered on the plate midthickness loca-

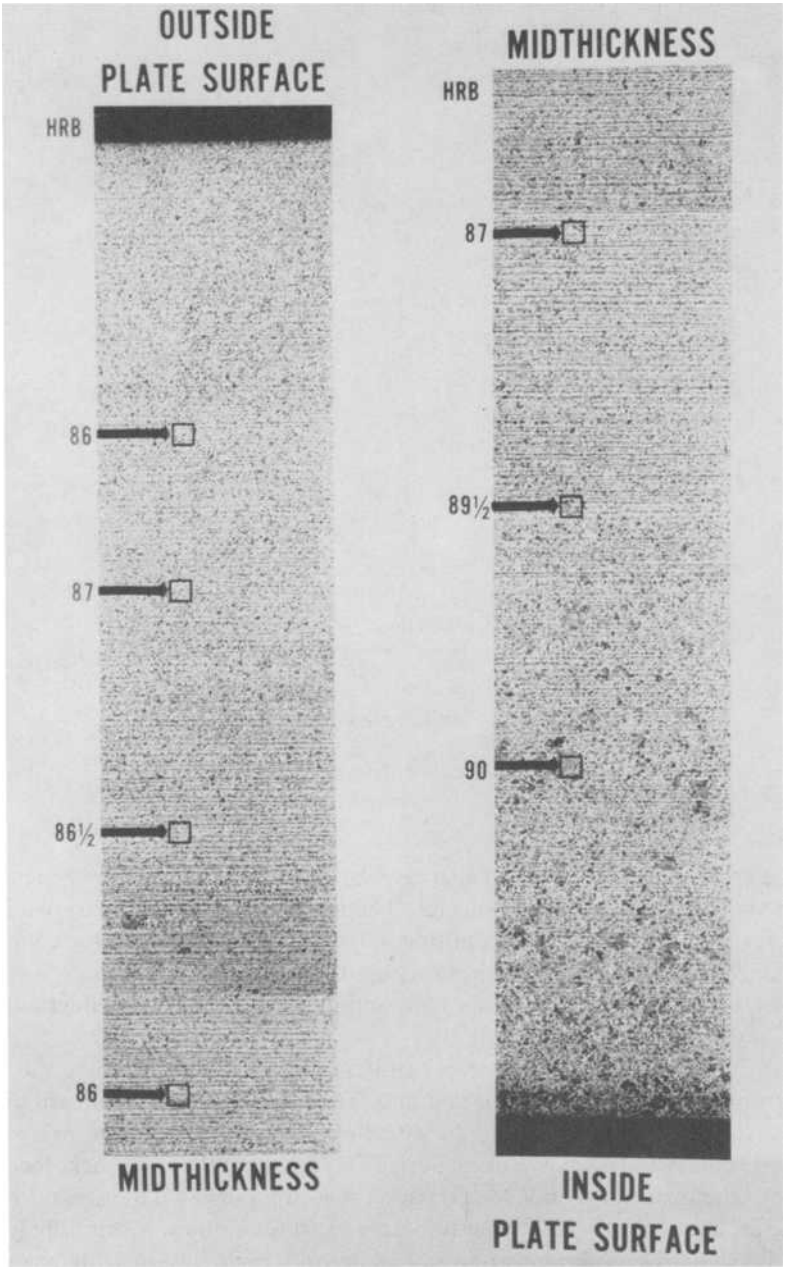

FIG. 4—*Montage of microstructure through the cross section of AAR M128 steel plate. The hardness values are representative of the locations shown. The etch is 1% nital.*

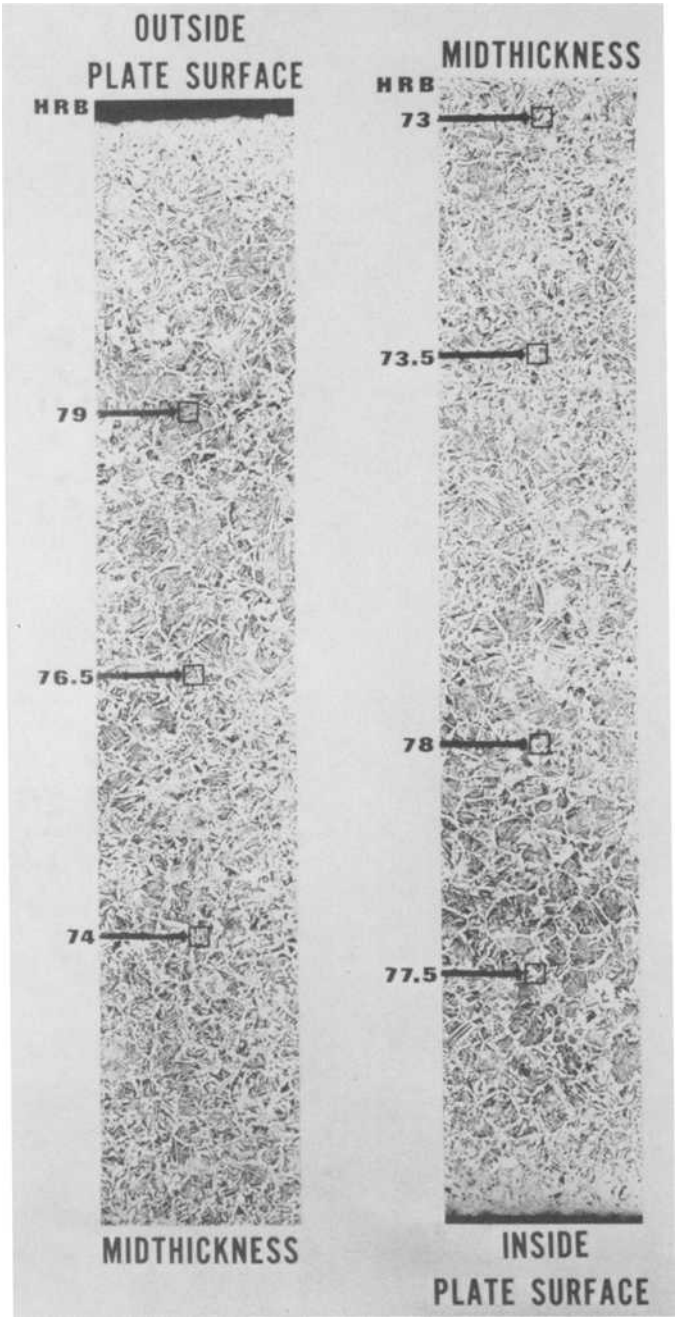

FIG. 5— *Montage of microstructure through the cross section of ASTM A212 steel plate. The hardness values are representative of the locations shown. The etch is 5% nital.*

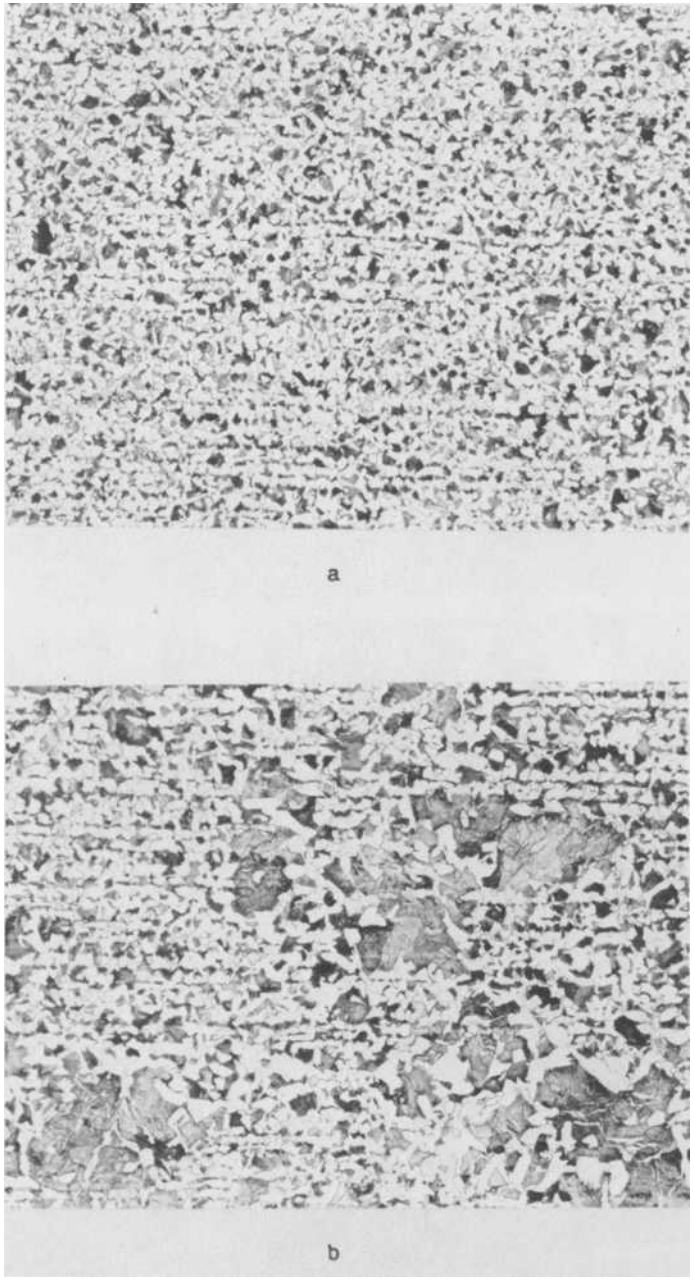

FIG. 6—*Photomicrographs of typical microstructure on longitudinal planes of AAR M128 steel:* (a) *near the outside plate surface;* (b) *near the inside plate surface. The etch is 4% picral; the magnification is* $\times 85$.

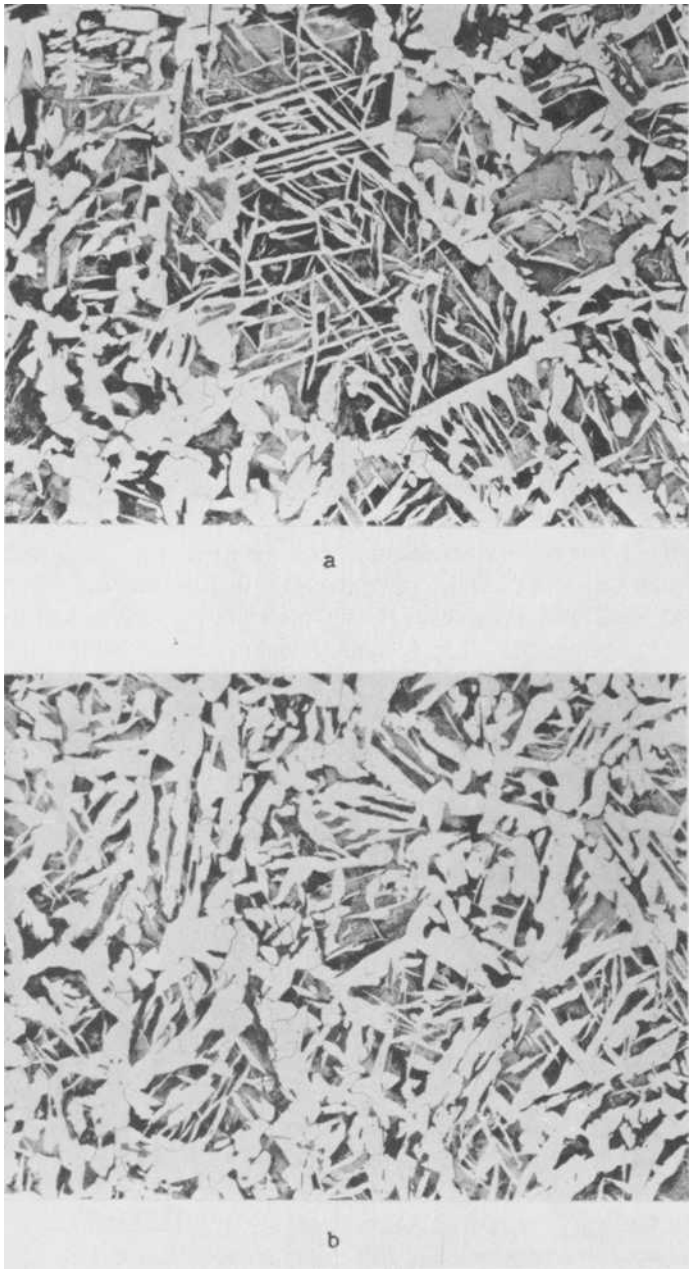

FIG. 7—*Photomicrographs of typical microstructure of ASTM A212 steel:* (a) *Zone 2—pearlite colonies, surrounded by ferrite grains on prior austenite grain boundaries, containing Widmanstatten ferrite;* (b) *Zone 3—large amounts of ferrite mask prior austenite grain boundaries; the Widmanstatten ferrite has greatly thickened. The etch is 4% picral; the magnification is* $\times 85$.

tion, contains a large amount of proeutectoid ferrite, often masking the prior austenite grain boundaries, as shown in Fig. 7*b*. The ferrite grain size of the non-Widmanstatten ferrite was ASTM No. 7 (average grain diameter = 32 μm). Large pearlite colonies and a coarse ferrite grain size are two factors that promote high impact transition temperatures.

The inclusion content of each steel, as determined by a quantitative television microscope (QTM) method, is reported in Table 3. These results indicate that the cleanliness of the two steels is similar and thus the inclusion content will not affect the NDT results.

Test Variables

Three standard specimen types—Types P-1, P-2, and P-3—of varying length, width, and thickness dimensions are specified in ASTM Method E 208-81. The dimensions of the blank size required for each type are shown in Fig. 8. When choosing a particular specimen type for testing, the primary factor to consider is the thickness of the original plate from which specimens will be taken. The three standard specimen geometries are designed for testing flat plates with thicknesses of 25 mm (1.0 in.), 19 mm (0.75 in.), and 16 mm (0.62 in.). Products thicker than the standard specimens must be machine-cut to one of these three specimen thicknesses. An additional requirement states that at least one as-fabricated surface of the original plate must be preserved on the test specimen, and that this surface should be the welded or tension surface of the specimen during testing. Specimen Type P-3 was chosen as the standard specimen size for testing the ASTM A212 and AAR M128 steels for all four geometries. The decision to use the P-3 specimen type for both steels was based on the fact that the AAR M128 steel plate thickness of 17.8 mm (0.7 in.) does not meet the specification for a Type P-2 specimen. However, the ASTM A212 steel plate thickness of 19 mm (0.75 in.) could satisfy the P-2 requirements, and thus one set of specimens with the Group B geometry was tested with the Type P-2 deflection.

In the initial NBS studies of the two steels, the as-fabricated outside surface of the tank-car head plate was preserved. This resulted in the Group A specimens having a convex surface on the welded or tension side of the specimen. The impacted or compression surface was machined flat, thus achieving the required Type P-3 specimen thickness dimension only at the center of the specimen under the notch. From the center point, the thickness diminished in all directions.

For the Group B test specimens, both of the curved as-fabricated plate surfaces were preserved, producing full-thickness specimens. The curvature of the specimen, however, violates the flat specimen requirement. Specimens prepared from the ASTM A212 steel plate satisfied the thickness dimension for Type P-2 standard specimens, while specimens prepared from the AAR M128 steel plate with this geometry did not meet the thickness dimension

TABLE 3—*QTM inclusion content rating of head plate specimens from ASTM A212 and AAR M128 steels.*

Head Plate Steel	Effective Magnification	QTM Ratings, Percentage of Inclusion Area						
		Number of Fields with Inclusion Area ≥0.5[a]	Quarter Thickness Position (25 Fields)	Mid-thickness Position (50 Fields)	Three-fourths Thickness Position (25 Fields)	Overall Average (100 Fields)	Worst Field[b]	
							Quarter Thickness	Mid-thickness
ASTM A212	×100	6	0.29	0.32	0.24	0.29	0.54	0.79
AAR M128	×100	0	0.17	0.22	0.24	0.21	0.40	0.46

[a]Per 100 fields.
[b]Per 50 fields.

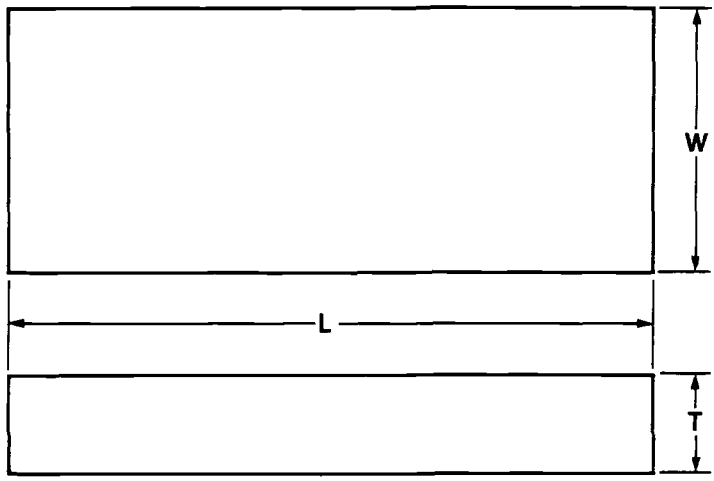

Specimen Type	Thickness, T	Length, L	Width, W
P-1	25 ± 2.5 mm (1.0 ± .012 in)	360 ± 10 mm (14.0 ± 0.5 in)	90 ± 2.0 mm (3.5 ± 0.1 in)
P-2	19 ± 1.0 mm (0.75 ± 0.04 in)	130 ± 10 mm (5.0 ± 0.5 in)	50 ± 1.0 mm (2.0 ± 0.04 in)
P-3	16 ± 0.5 mm (0.62 ± 0.02 in)	130 ± 10 mm (5.0 ± 0.5 in)	50 ± 1.0 mm (2.0 ± 0.04 in)

FIG. 8—*Standard drop-weight test specimen dimensions.*

specification for any of the three standard specimen types. Although all the Group B specimens violated the specifications of ASTM Method E 208-81 for Type P-3 specimens, they were nevertheless tested using a P-3 anvil stop in a manner identical to that used for the other three groups.

The surface strain developed at the tension surface of a specimen during the test event is dependent on the specimen width and thickness, the bending span, and the amount of deflection in the specimen. During the development of the drop-weight test, the Naval Research Laboratory tested a variety of plate thicknesses and specimen dimensions to establish corresponding deflections that would obtain a constant level of strain for different specimen sizes [*4*]. When testing Type P-2 and P-3 specimens, ASTM Method E 208-81 specifies specimen deflections of 1.50 mm (0.060 in.) and 1.90 mm (0.075 in.), respectively. When testing Group B specimens with thicknesses of 17.8 mm (0.70 in.) and 19.0 mm (0.075 in.) on a P-3 anvil, the specimen experiences a larger deflection than is appropriate for these thicknesses and thus

creates higher surface strains than those used for a standard test. To understand this effect better, a few Group B specimens of AAR M128 steel were also tested on a P-2 anvil. A comparison of these results is also reported.

The Group C specimens were machined so that the tension and compression surfaces were reversed from the Group A geometry. For this group, the tension surface was machined flat, and the inside surface of the tank-car head plate was retained as the as-fabricated plate surface on the compression side of the specimen. Again, the thickness dimension specification for Type P-3 specimens was achieved only at the center of the specimen. From the center point, the specimen thickness increased in all directions.

The fourth and final set of specimens, Group D, was prepared by machining both plate surfaces flat to a uniform thickness of 16 ± 0.5 mm (0.62 ± 0.02 in.), thus satisfying this dimension for the P-3 standard specimen. For this group however, the requirement of preserving an as-fabricated surface was violated.

ASTM Method E 208-81 requires that a particular specimen type be tested by supporting it on an anvil designed only for that type of specimen. The anvil used for this study is shown schematically in Fig. 9. The anvil is constructed with stops designed to prevent the specimen, when impacted, from deflecting more than a specified amount. When Group A and Group B specimens are placed on a standard anvil, the curvature of the tension surface allows the

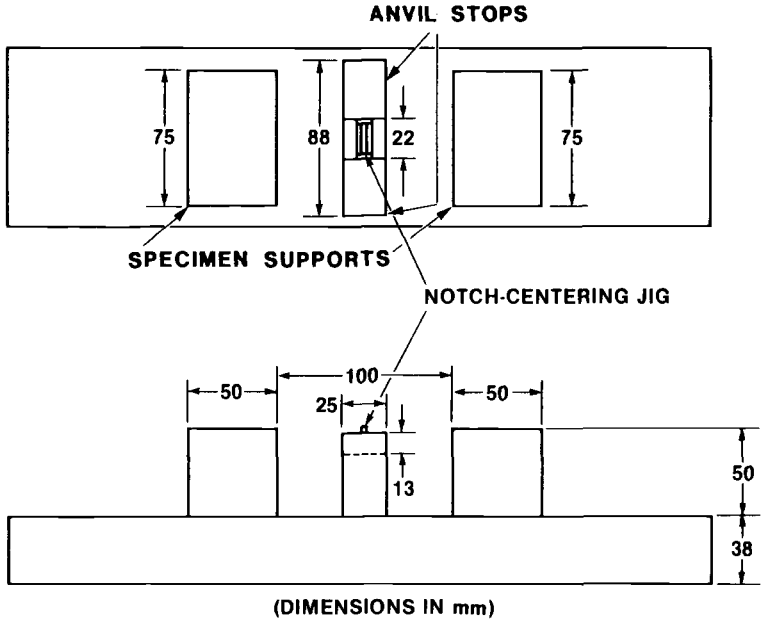

FIG. 9—*Schematic of the anvil used in this study for the drop-weight test.*

center portion of the specimen to lie in a position too close to the anvil stops. If tested in this manner, the specimen would not deflect the required distance specified by Method E 208-81. To remedy this problem, two methods were employed for adjusting the displacement of the specimen in relation to the anvil stops. Both methods involved placing metal shims beneath the specimen to raise it to the proper position.

The first method, used when testing the Group A specimens, involved measuring the specimen thickness at four locations, calculating the tension surface curvature, and using appropriate shims to adjust for that curvature. These measurement locations were the two points where the specimen came in contact with the inside edges of the specimen supports and the two points at which the specimen would come in contact with the inside edges of the anvil stops after impact. To adjust for the curvature, from one to three shims were placed in position on the anvil prior to a test. The test proceeded normally by placing the specimen on the anvil and on top of the shims, which raised the specimen to the appropriate deflection height.

A second method using shims for adjusting the specimen deflection was used for the Group B specimens. The geometry of the Group A specimens, which had one flat machined side, allowed the thickness to be measured at different locations with respect to a common plane. The two curved surfaces of the Group B specimen geometry prohibited using this measurement technique. A second method was devised whereby two shims with a thickness equal to the anvil deflection displacement were temporarily placed on the anvil stops. This brought the effective height of the anvil stops level with the specimen supports. A specimen was then placed on the anvil in the position for testing. Shims of increasing thickness were placed between the specimen ends and the specimen supports until the appropriate size of shim thickness, that which would support the specimen at each end while not raising it off the anvil stops, was determined. These two shims were the only ones used during an actual test. The two used to adjust the height of the anvil stops were removed prior to the test. Both methods equally accomplish the tasks of adjusting the specimen displacement to allow for the proper amount of deflection and to support the specimen adequately in that position.

In addition to the test requirements that were deliberately violated in this study, there were some additional factors that did not remain constant. First, although the welding electrodes used for the crack-starter weld were the approved type and from the recommended manufacturer, they were from different lots. Next, the crack-starter welds were prepared by two welders following the same welding procedure. For all specimens, the last weld metal to freeze was in the center of the weld at the notch location. Last, the crack-starter notch widths ranged from 1.15 mm (0.045 in.) up to the specification maximum of 1.57 mm (0.062 in.). However, these variations are the type routinely encountered (unless otherwise forbidden) and thus were assumed to play a minor role.

Test Procedure

The quantity of material available for testing was limited, which thus restricted the number of specimens that could be extracted from each tank-car head plate. A total of seven to ten specimens of each steel was prepared in each of the four groups.

The testing was conducted on a commercial drop-weight tower having a one-piece drop weight of 39 kg (86 lb). The weight and striking tup are released by an electrically controlled air-pressure release mechanism. The free-falling weight is guided by two vertical rails rigidly supported at the base of the test machine. The anvil, designed with a spring-loaded notch-centering jig to aid in specimen alignment, was securely bolted to the test machine base. For all of the reported tests, the weight and striking tup were dropped from a height of 416 mm (16.4 in.) above the compression surface of the specimen. This provided 159 J (117 ft · lb) of available impact energy. Although this energy level is below the minimum of 350 J (250 ft · lb) recommended by ASTM Method E 208-81 for the yield strength levels of these steels, 159 J proved to be a sufficient energy level to deflect all specimens to the anvil stops, thus validating the drop height.

On impact with a test specimen, the drop weight often rebounded upward and resulted in multiple impacts with the specimen. A shortcoming of this test machine is the lack of a brake mechanism to restrain the drop weight after the initial impact to prevent the specimen from being struck additional times. The lower drop-weight energy level used for these tests helped reduce the drop-weight rebound, although it was not eliminated.

Results and Discussion

The NDT temperatures for the two steels were determined for each of the specimen geometries of Groups A, B, and C and are summarized in Table 4. In the case of the Group D geometry, the supply of specimens of both steels was exhausted before the NDT temperatures could be determined. For these data sets, Table 4 gives a temperature value that was determined to be equal to or below the actual NDT temperature. Specimens of both steels tested at these temperatures exhibited a "break" result as well as a "no break" result, indicating that these values are near to the actual NDT temperatures. For the discussion that follows, these temperatures are assumed to be the actual NDT temperatures from the Group D geometries. Test results for the individual specimens are given in Appendixes I and II.

The AAR M128 Group B specimens that were tested on a P-2-type anvil were also too few in number to determine the NDT temperature adequately. The tests, however, did exhibit "no break" results for specimens tested at −29°C (−20°F), with no instances of a "break" result at that temperature or above. This indicates that the NDT temperature would have been determined

TABLE 4—*Results of NDT drop-weight tests.*

Specimen Geometry	NDT Temperatures, °C (°F)	
	ASTM A212	AAR M128
Group A, P-3 deflection	−1 (30)	−29 (−20)
Group B, P-3 deflection	4 (40)	−18 (0)
Group B, P-2 deflection	not determined	≤ −29 (≤ −20)
Group C, P-3 deflection	4 (40)	−12 (10)
Group D, P-3 deflection	≥ 10 (≥ 50)	≥ −18 (≥ 0)

to be −29°C (−20°F) or somewhat lower. The result, stated as an NDT temperature less than or equal to −29°C (−20°F), is included in Table 4 for this set of specimens.

The varying test results presented in Table 4 indicate that the four specimen geometries did affect the determination of the NDT temperatures for the two steels tested. It should be recognized, however, that the test method established in ASTM Method E 208-81 restricts the accuracy of the NDT temperature to no better than 5°C (10°F). For the A212 steel, the results of the four specimen geometries fell within a range of about 11°C (20°F), and for the AAR M128 steel, the results are spread within a 17°C (30°F) range. Viewing the data in this way, the results for the A212 steel fall outside the error band for an NDT temperature of 4°C (40°F) by only ±0.5°C (±1°F), and the AAR M128 steel results fall outside the error band for a NDT temperature of −15°C (5°F) by only ±3°C (±5°F). The results are discussed in this manner only to illustrate the magnitude of the inherent inaccuracies associated with conducting a drop-weight test. This level of inaccuracy must be fully appreciated when interpreting the results of this test method. Even with the inaccuracies considered, the results of this study nevertheless show trends to suggest that the different specimen geometries may have an effect on the determination of the NDT temperatures for these steels.

The results indicate that the NDT temperatures determined for the Group A specimens of each steel are below those determined for the Group C and Group D geometries. Although the NDT temperatures determined for the Group B specimens appear to be similar to the Group C and Group D results, they must be interpreted with caution. The Group B NDT temperatures that were determined by tests conducted using a P-3-type anvil are probably high. Subjecting these thicker (P-2-type) specimens to the more severe deflection allowed by the P-3 anvil results in greater surface strain at the tension surface than for a P-3-type specimen. These higher strain levels would be expected to promote crack propagation in the material at temperatures higher than the actual NDT temperature. This bias is evidenced by the results of additional tests of the AAR M128 Group B specimens conducted with a P-2-type anvil. The deflection allowed by the P-2 anvil closely approximates the correct deflection necessary for a specimen having a thickness of 17.8 mm (0.7 in.). The

results of these tests indicate that the NDT would occur at or below −29°C (−20°F), 11°C (20°F) below the P-3 anvil results and would be similar to the Group A results. Therefore, test results for these two steels have indicated that similar NDT temperatures occur for Group A and B geometries and for Group C and D geometries, and that Group A and B NDT temperatures will be lower than those for the Group C and D geometries.

This effect may be attributed to a combination of the specimen having a curved tension surface and the necessity of shimming this curved surface. When these specimen geometries were tested, steel shims were placed between the specimen and the test anvil. As a test proceeds, the specimen is impacted by the drop weight, deflecting the central portion of the specimen toward the anvil stops. As a result of the bending of the specimen during the test, there is a simultaneous inward movement of the specimen relative to the specimen supports of the anvil fixture. The inward movement, although slight, allows the specimen to drop with the curvature of the tension surface and reduces the amount of deflection that occurs in comparison with a standard flat specimen test. In addition, the steel shims may experience a compressive deformation (as does the specimen) during the impact event, which also reduces the amount of deflection experienced by the tension surface. Any combination of these actions could have contributed to a less severe deflection of the specimen than is required and thus resulted in lower measured NDT temperatures. A detailed examination of the effect of shimming a test specimen, however, was not conducted for this study.

Summarizing previously reported material properties [*2,3*], the higher hardness and tensile strength data for the M128 steel is consistent with the strengthening effect from the higher manganese content in this steel. The higher Charpy upper-shelf energy for the A212 steel correlates with the lower yield strength for A212 steel, in agreement with data reported for other steels [*5*]. The higher Charpy transition temperature found for the A212 steel is caused primarily by its larger ferrite grain size. The results of the NDT measurements (Table 4) reveal that the AAR M128 steel always exhibited lower NDT temperatures than the ASTM A212 steel, independent of specimen geometry, and this finding is an agreement with the observed lower Charpy transition temperature found for the M128 steel. More importantly, however, the observed trends in the NDT temperature as a function of changes in geometry are essentially the same for each steel, although of differing magnitudes, and thus an effect of microstructural differences within a steel or a lack thereof was not detected.

Conclusions

To determine the NDT temperature of a curved steel product by conducting drop-weight tests, one or more of the standard test requirements and procedures as specified in ASTM Method E 208-81 must be violated. The results for specimens of ASTM A212 and AAR M128 steels showed trends in how the

different specimen geometries affect the determination of the NDT temperature. These trends are summarized as follows:

1. Retaining the curved as-fabricated plate surface on the tension side of the specimen, which necessitates shimming the specimen during testing, results in a lower NDT temperature determination than that for specimens having a flat machined tension surface.
2. The geometry or surface on the compression side of the specimen does not affect the NDT temperature determination.
3. Full-thickness specimens must be tested on an anvil having the appropriate deflection stop depth for the plate thickness to be tested.
4. A shift in NDT temperature resulting from specimen geometry may be masked by the inaccuracy associated with ASTM Method E 208-81.

Acknowledgment

The authors wish to express thanks to the Federal Railroad Administration for their support of this project through Contract No. DTFR53-84-X-00023 and to D. E. Harne for his assistance in the specimen preparation and testing aspects of this study.

APPENDIX I

Individual Specimen Results for ASTM A212 Steel

Group and Type	Temperature (°C)	Break	No Break	No Test
Group A, P-3 deflection (NDTT = −1°C)	−34			X
	−23	X		
	−12	X		
	−7		X	
	−1		X	
	−1	X		
	4		X	
	4		X	
Group B, P-3 deflection (NDTT = 4°C)	−1	X		
	4			X
	4	X		
	4		X	
	10		X	
	10		X	
Group B, P-2 deflection (NDTT = not determined)		no data		

Individual Specimen Results for ASTM A212 Steel—*Continued*

Group and Type	Temperature (°C)	Break	No Break	No Test
Group C, P-3 deflection (NDT = 4°C)	−7	X		
	−1		X	
	−1			X
	−1	X		
	4	X		
	10		X	
	10		X	
Group D, P-3 deflection (NDTT = ≥10°C)	−1	X		
	4			X
	4	X		
	10	X		
	10		X	
	10			X
	10			X

APPENDIX II

Individual Specimen Results for AAR M128 Steel

Group and Type	Temperature (°C)	Break	No Break	No Test
Group A, P-3 deflection (NDTT = −29°C)	−46	X		
	−34	X		
	−34		X	
	−29	X		
	−29		X	
	−23		X	
	−23		X	
Group B, P-3 deflection (NDTT = −18°C)	−18	X		
	−12			X
	−12	X		
	−12	X		
Group B, P-2 deflection (NDTT = ≤−29°C)	−29		X	
	−23		X	
	−23			X
	−18		X	
	−12			X
	4		X	
Group C, P-3 deflection (NDTT = −12°C)	−18	X		
	−12	X		
	−12		X	
	−7			X

Individual Specimen Results for AAR M128 Steel—*Continued*

Group and Type	Temperature (°C)	Break	No Break	No Test
	−7		X	
	−7		X	
Group D, P-3 deflection	−40	X		
(NDTT = ≥0°C)	−34	X		
	−34		X	
	−34			X
	−34			X
	−29	X		
	−29		X	
	−23	X		
	−18	X		
	−18		X	

References

[1] Puzak, P. P., Schuster, M. E., and Pellini, W. S., "Crack Starter Tests of Ship Fracture and Project Steels," Appendix: Procedures for NRL Drop Weight Test, *Welding Journal*, Vol. 33, No. 10, October 1954, pp. 481-s-495-s.

[2] Early, J. G., "A Metallurgical Analysis of an ASTM A212-B Steel Tank-Car Head Plate," Report No. 9, NBSIR 78-1582, National Bureau of Standards, Washington, DC, September 1978, NTIS PB81/20598, FRA OR&D 81/32.

[3] Early, J. G. and Interrante, C. G., "A Metallurgical Evaluation of Two AAR M128 Steel Tank Car Head Plates Used in Switchyard Impact Tests," Report No. 10, NBSIR 80-2039, National Bureau of Standards, Washington, DC, December 1979.

[4] Puzak, P. P. and Babecki, A. J., "Normalization Procedures for NRL Drop-Weight Test," *Welding Journal*, Vol. 38, May 1959, p. 209.

[5] Gross, J. H., "The Effective Utilization of Yield Strength," ASME Paper No. 71-PVP-11, *Journal of Engineering for Industry*, 1971, pp. 962-968.

William Oldfield[1] *and William L. Server*[2]

NDTT, RT_{NDT}, and Fracture Toughness: A Study of Their Interrelationships Using a Large Data Base and Computer Models

REFERENCE: Oldfield, W. and Server, W. L., **"NDTT, RT_{NDT}, and Fracture Toughness: A Study of Their Interrelationships Using a Large Data Base and Computer Models,"** *Drop-Weight Test for Determination of Nil-Ductility Transition Temperature: User's Experience with ASTM Method E 208, ASTM STP 919*, J. M. Holt and P. P. Puzak, Eds., American Society for Testing and Materials, Philadelphia, 1986, pp. 129-141.

ABSTRACT: The nil-ductility transition temperature (NDTT) test has been used extensively in naval ferritic steel applications since World War II. The use of the test results in fracture-safe design has extended into other structural steel industries, most notably those covered by the American Society of Mechanical Engineers (ASME) Boiler and Pressure Vessel Code. The construction of nuclear reactor pressure vessels, in accordance with the ASME code, requires material specifications that utilize both the NDTT and Charpy V-notch test data; coupling the NDTT and Charpy V-notch data results in a "reference" temperature (RT_{NDT}), which is either greater than or equal to the NDTT. [The RT_{NDT} is defined as being greater than or equal to the NDTT; at RT_{NDT} plus 33°C (60°F), three Charpy V-notch specimen results must exhibit a minimum of 68 J (50 ft · lb) of absorbed energy and 0.89 mm (35 mil) of lateral expansion. The energy requirement generally governs except for irradiated materials.] Interestingly, some materials generally have an RT_{NDT} based upon the NDTT, while others have an RT_{NDT} consisently greater than the NDTT since the RT_{NDT} is governed by the Charpy V-notch data; (that is, the temperature at 68 J (50 ft · lb) minus 33°C (60°F) is greater than the NDTT). For example, the RT_{NDT} for SA533B-1 plate steel is generally set by the Charpy data, but the RT_{NDT} for SA508-2 forging steel (which is similar to SA533B-1) is typically controlled by the measured NDTT.

The science of fracture mechanics has also evolved since World War II, but the matching of transition temperature test results (NDTT, and RT_{NDT}) with actual material fracture toughness (stress intensity) values is still uncertain. However, considerable progress in matching Charpy data with fracture toughness values has been made in recent years through the development of a large material property data base, which includes transition temperature and fracture toughness data. The work described in this paper builds on this research, and uses the same data base to examine the relationship between other transi-

[1]President, Materials Research and Computer Simulation, Inc., Santa Barbara, CA 93110.
[2]Manager, Materials Engineering, Robert L. Cloud Associates, Berkeley, CA 94710.

tion temperature and toughness parameters. Computer modeling using stochastic procedures was employed to develop probability distributions which, by simulating the measurement of NDTT, clarify the interrelationships between NDTT, RT_{NDT}, and fracture toughness. Predictions by the model of NDTT and RT_{NDT} from dynamic fracture toughness data are in excellent agreement with measured values.

KEY WORDS: nil-ductility transition temperature, fracture, Charpy test, test method interrelationships, drop-weight test, ASTM standard E 208

The historical development of fracture-safe design concepts for ferritic steels has led to an array of fracture toughness approaches that are not easily interrelated. Impact testing, using procedures such as the Charpy V-notch (CVN) test, was one of the earliest procedures to be employed for determining a ductile-brittle transition temperature. For a number of reasons, impact testing has sometimes been judged to be insufficient to ensure fracture-safe structures. In the wartime emergency of World War II, structural failures in welds in Liberty Ships led to the development of the nil-ductility transition temperature (NDTT) test [ASTM Method for Conducting Drop-Weight Test to Determine Nil-Ductility Transition Temperature of Ferritic Steels (E 208-81)]. In this test, a brittle weld bead is placed in the center of a bend test specimen using specified procedures. The specimen is then subjected to a controlled impact deflection. When the weld bead cracks, and the crack extends to reach one of the top edges of the specimen, it is said to have broken. The test temperature is then increased by 5.5°C (10°F), and repeated. The break temperature, below which two tests do not result in a break, is defined as the NDTT.

Subsequently, attempts were made to reconcile the NDTT test with the CVN test and to develop a procedure that combined the advantages of both procedures. The reference temperature (RT_{NDT}) procedure was the result [*1*]. As defined in ASTM Method 208-81, this measurement uses the most conservative (highest temperature) of the NDTT and a somewhat complex measurement of transition temperature based on the CVN test.

The scientific revolution that has taken place since World War II has produced new insights into fracture behavior. The brittle fracture concepts proposed by Griffith [*2*] have been developed, and, in particular, the critical stress intensity factor [*3*] concept has been introduced. In this approach, crack initiation depends on the magnitude of the stress intensity at the tip of a flaw, and the ability of the material to resist crack initiation is defined by its critical stress intensity value, termed its fracture toughness.

During the past several years, a substantial body of fracture data has been accumulated in a computer data base for nuclear pressure vessel steels, maintained by Materials Research and Computer Simulation (MRCS) under the acronym PVS [*4*,*5*]. This data base has enabled studies to be made of the interrelationships between the measured toughness values. In particular, different measures of fracture toughness (static, intermediate-rate dynamic,

high-strain-rate dynamic, and arrest) have been shown to be related to each other and to features of the CVN energy-temperature behavior [*6*]. The relationship between these quantities and NDTT and RT_{NDT} temperatures has so far only proved to be a weak one at best. Therefore, it seemed appropriate to make a more informed attempt to discover any relationships that might exist by using computer modeling methods to demonstrate the use of practical insights concerning these tests. In addition, this approach might help explain why the RT_{NDT} for SA533B-1 plate steel is generally controlled by the CVN energy data (that is, $RT_{NDT} > NDTT$) while the RT_{NDT} for SA508-2 forging steel is typically controlled by the NDTT (that is, $RT_{NDT} = NDTT$). Table 1 shows how the RT_{NDT} was controlled for several different materials.

An NDTT Test Model

Since a large data base was available to the authors, a new relationship between high-rate dynamic fracture toughness K_{Id} and the NDTT parameter was sought. The data base included several hundred heats of a wide range of ferritic low-alloy and carbon steels, for which a relationship between K_{Id} and temperature was available, as well as an NDTT measurement. Using these data, the value of K_{Id} at the NDTT temperature could be determined. This value, the dynamic fracture toughness value at NDTT, is termed K_N. Not all estimates had the same value; there was a distribution of K_N results centered on 60 MPa $\sqrt{m}$ (55 ksi $\sqrt{in.}$). The distribution is shown in Fig. 1. It is skewed, with a tail lying toward the higher temperatures.

Several years ago, a computer model for the NDTT test was developed using a Monte Carlo (stochastic) procedure applied to Heavy Section Steel Technology (HSST) Plate 02 (SA533B-1 steel) [*7*]. Starting at a temperature below any reasonable NDTT and using actual details of a set of high-strain-

TABLE 1—*Controlling factor for determining* RT_{NDT}.

Material	Numbers of Heats		Fraction set by CVN Data, %
	Set by NDTT[a]	Set by CVN Data	
SA533B-1 plate	12	26	68.4
SA508-2 forging	12	6	33.3
SA302B plate	0	4	100
SA508-3 forging	8	5	38.5
SA516-70 plate	5	2	28.6
SA533A-2 plate	3	1	25
Manual-arc weld metal[b]	10	4	28.6
Submerged-arc weld metal[b]	15	9	37.5

[a]Note that several heats were set identically by both the NDTT and the CVN data, but these cases are listed under NDTT since it is the first test in determining RT_{NDT}.

[b]Typical production welds on the materials listed in this table.

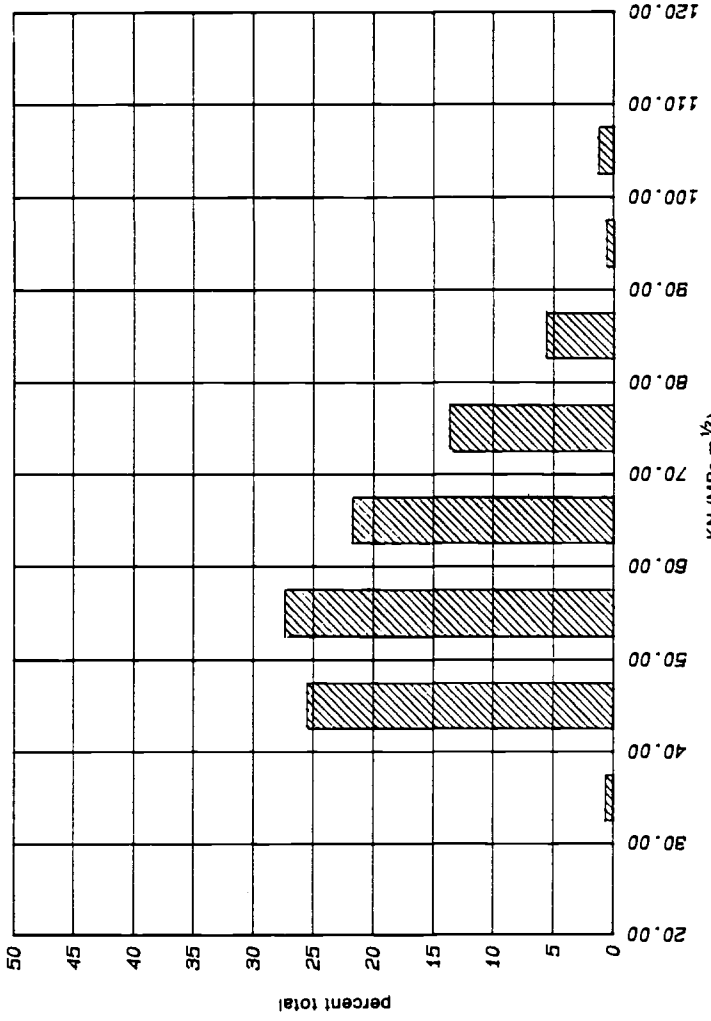

FIG. 1—*Distribution of* K_N *for the total PVS data base.*

rate dynamic test data (instrumented precracked Charpy test), the data were examined to determine whether the fracture toughness (K_{Id}) was above some predetermined level. This level was set at 60 MPa $\sqrt{m}$ (55 ksi $\sqrt{in.}$), which was determined from the data base (Fig. 1). If the fracture toughness at the temperature was below this level, the specimen was assumed to have broken, and the temperature was increased by an increment of 5.5°C (10°F). If the fracture toughness was above the required level, a "no-break" condition was assumed, and a second test was "run". If two "no breaks" results occurred, the temperature was said to be the NDTT. The variability of fracture toughness was taken into account by taking a random number in the range from zero to one. This random number was then used as the probability in the normal distribution to find the deviate from the mean fracture toughness at the temperature. The normal deviate multiplied by the standard deviation of data about the curve gave a random deviate from the best-estimate fracture toughness. (If the random number was less than 0.5, the deviate was negative.) By repeating simulated NDTT tests in this way, a probability distribution was built up which represented the results that would be obtained from a large number of tests on the same material. The spread of the simulated NDTT results over a range of temperatures revealed the effects of the variation in material properties.

The model was then applied to SA508-2 steel, Heat A, from the PVS data base [*4*]. A K_{Id}-temperature relationship had been developed for this heat of material using the instrumented precracked Charpy test, which permitted the model to use actual test data. These data were considerably more variable than results obtained for SA533B-1 steel, as were other SA508-2 results. (The authors offer no explanation for this observation.) The model was not immediately successful. While the peak of the distribution (of NDTT with temperature) was at approximately the correct temperature, the tail toward the low temperature was highly exaggerated. An analysis of the problem revealed that it was caused by the assumption in the model that the fracture toughness had a uniform variance. In reality, it has been shown that the variance of these data is much lower on the lower shelf than in the transition region, with a fairly constant value for all heats [*8*]. With a high variance, high fracture toughness values were being predicted in the lower shelf region, where in fact they could not occur. The problem was corrected making the assumption that the lower shelf variance was about 250 (MPa $\sqrt{m}$) [*1*]. Encouraging results were immediately forthcoming, as is shown in Fig. 2. The predicted NDTT values for many thousands of simulated tests gave a skewed distribution, with a peak (maximum probability) value that corresponded closely to the measured result. Note the skewness of the distribution toward lower temperature values. This skewness is caused by the curvature of the K_{Id}-temperature relationship as it approaches the lower shelf.

For each NDTT, there is a corresponding "best estimate" fracture toughness. This value was determined from the simulated NDTT results shown in

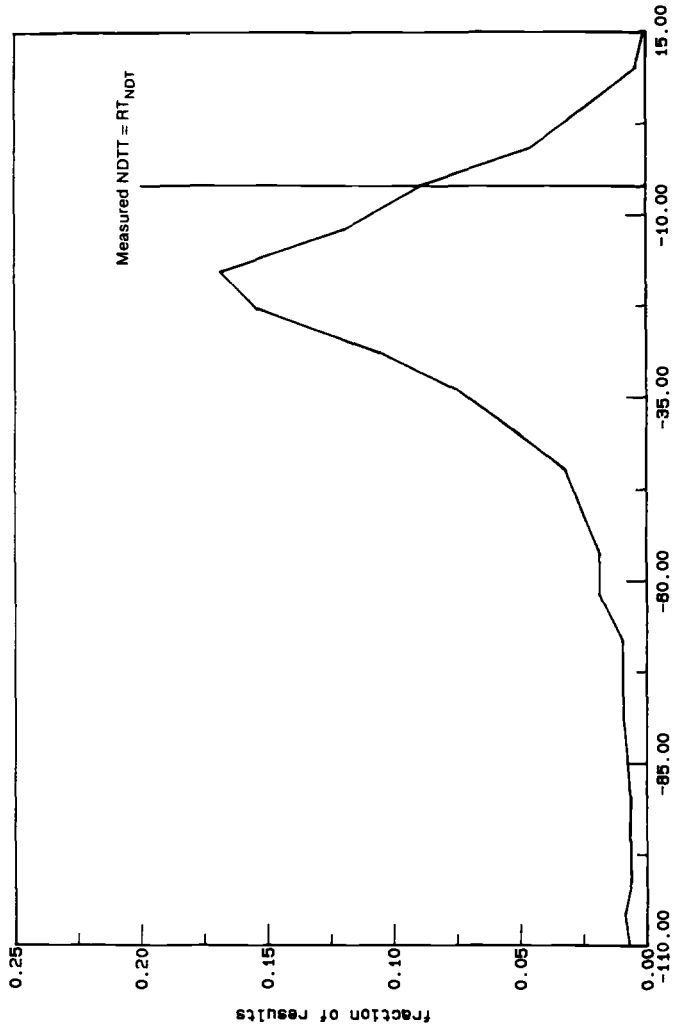

FIG. 2—*Predicted NDTT for SA508-2 steel.*

Fig. 2. The results are shown in Fig. 3. They compare well with those developed for the overall data base, shown in Fig. 1. Note particularly the reversal of the skewness. Whereas the NDTT results are skewed toward lower temperatures, the predicted K_N data are skewed toward higher fracture toughness. This result is also shown in Fig. 1.

The simulation procedure was repeated with a heat of SA533B-1 material characterized in the PVS data base. As already mentioned, the instrumented precracked Charpy fracture toughness data were much less variable for this material. Consequently the NDTT, and to a lesser extent the K_N (best estimate K_{Id}), results were less scattered, as is shown in Figs. 4 and 5, respectively. The simulated NDTT results show the measured value (again close to the peak probability level for the simulation) and the higher RT_{NDT} results developed from CVN data.

CVN Energy and RT_{NDT}

The definition of RT_{NDT} in the Boiler and Pressure Vessel Code of the American Society of Mechanical Engineers (ASME) calls for the modification of the NDTT result by features of the CVN data [*1*]. [The RT_{NDT} is defined as being greater than or equal to the NDTT; at RT_{NDT} plus 33°C (60°F), three Charpy V-notch specimen results must exhibit a minimum of 68 J (50 ft · lb) of absorbed energy and 0.89 mm (35 mil) of lateral expansion. The energy requirement generally governs except for irradiated materials.] The lateral expansion requirement almost never enters into the setting of RT_{NDT} for pressure vessel steels [*9*].

A requirement for three specimens to exceed 68 J (50 ft · lb) obviously is a more stringent requirement than requiring that the mean CVN energy be at 68 J (50 ft · lb). The quantitative interpretation can be developed using sampling theory as follows. If there is a probability p that the impact energy will be less than 68 J (50 ft · lb), and three samples are taken, the probability P that none will have less than 68 J (50 ft · lb energy) is given by the first term of the binomial distribution [*10*]

$$P = 3p \tag{1}$$

where P is the probability of having three specimens with more than 68 J (50 ft · lb energy).

If an even chance of success is assumed ($P = 0.5$), then $\ell n\ p = \ell n\ (0.5)/3$, and $p = 0.794$. That is, the RT_{NDT} value is based, on the average, on the single-side 80% lower bound of the CVN energy data plus 33°C (60°F), as shown in Fig. 6.

Since CVN energy can be used to predict fracture toughness [*6*], and since, as shown here, NDTT can be modeled on a fracture toughness basis, it is possible to predict circumstances in which NDTT or CVN data will set the

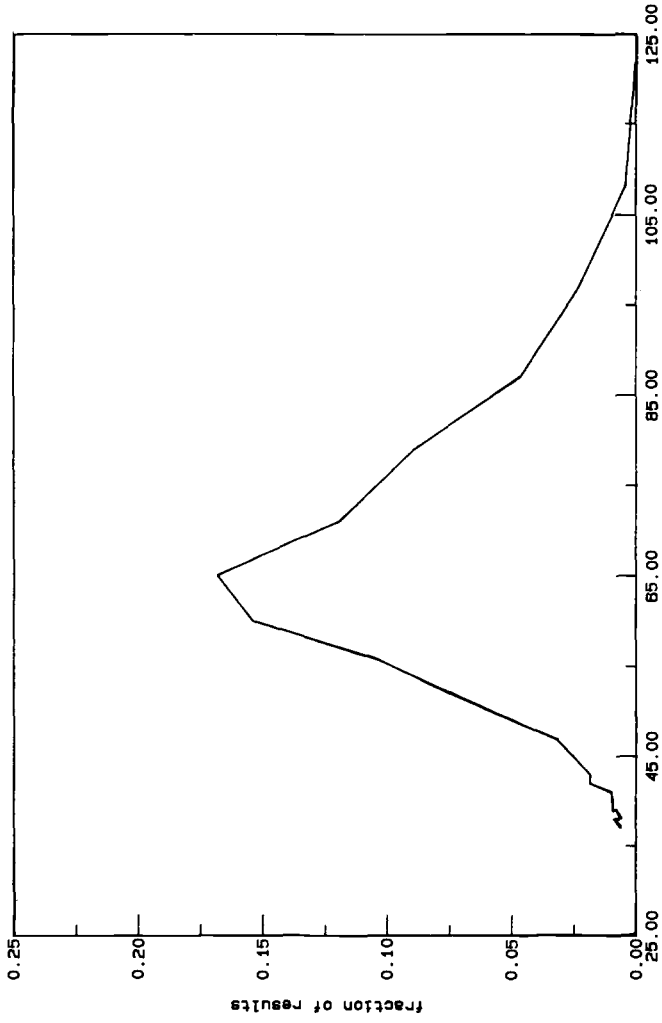

FIG. 3—*Predicted* K_{Id} *values for SA508-2 steel.*

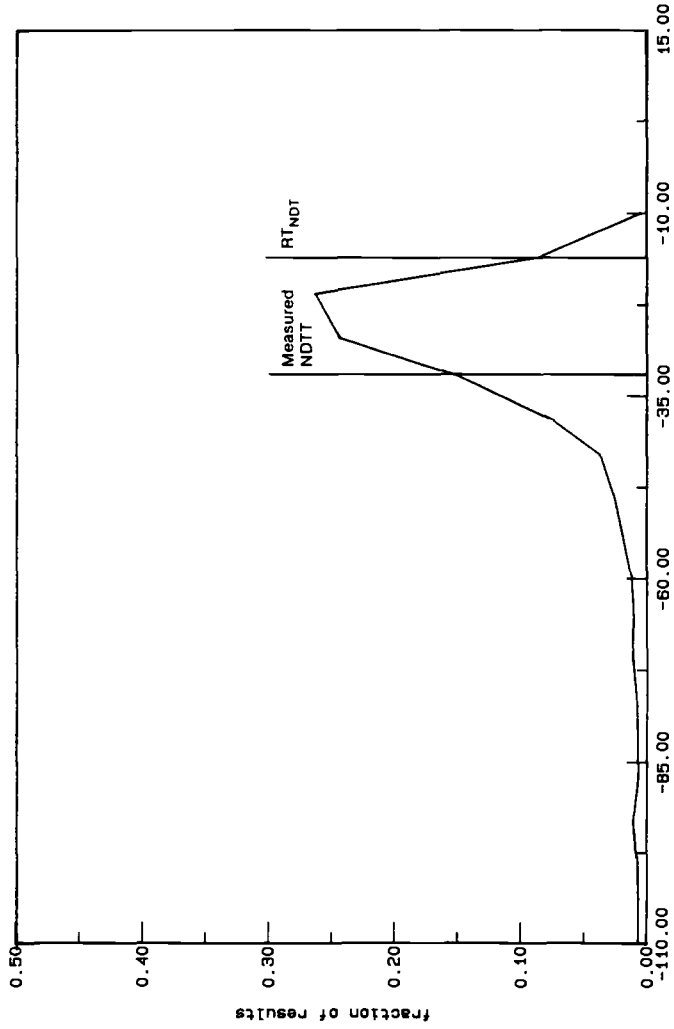

FIG. 4—*Predicted NDTT for SA533B-1 steel.*

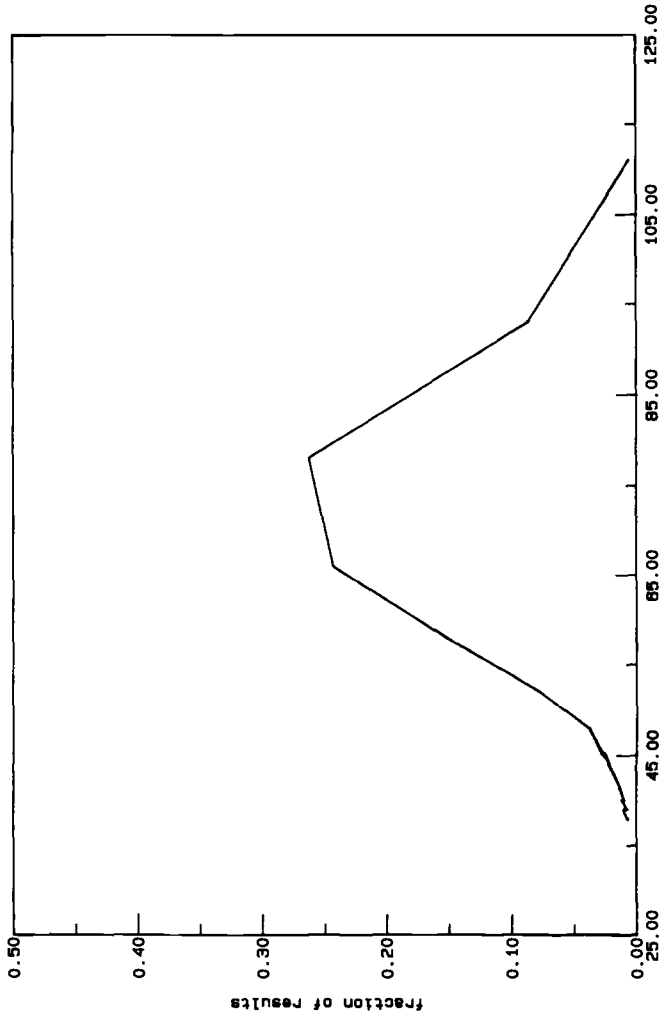

FIG. 5—*Predicted* K_{Id} *values for SA533B-1 steel.*

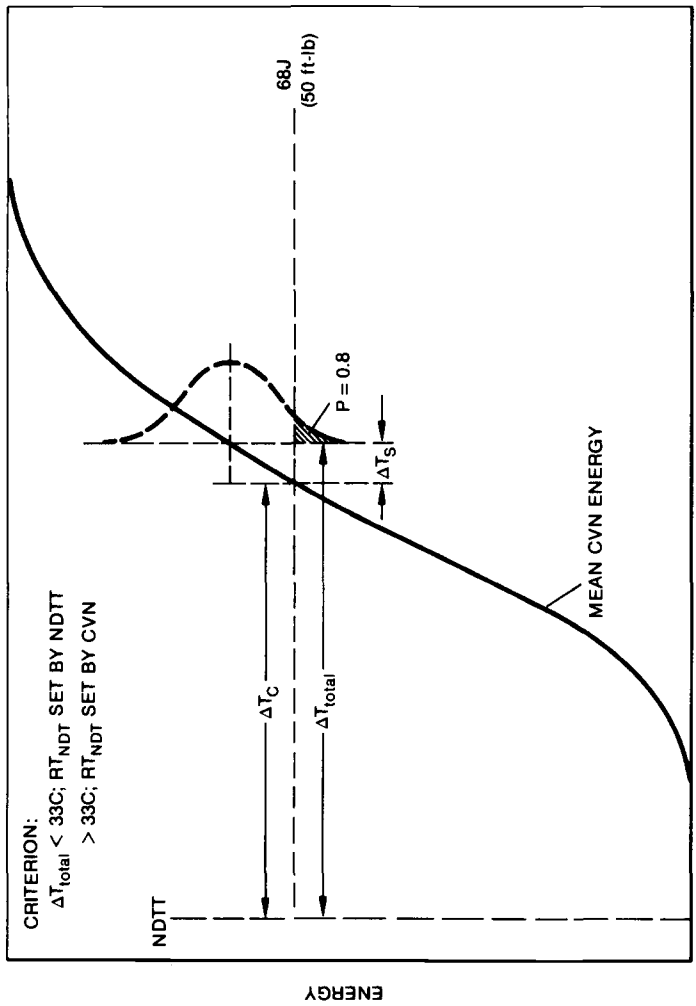

FIG. 6—*Statistical interpretation of* RT_{NDT}.

RT_{NDT} value. While this can be analyzed in detail, the mathematics is rather cumbersome, and it is better to discuss the issue in qualitative terms. As a first step, the midpoint of the Charpy transition [*6*], defined by the relationship

$$\text{CVN} = A + B \tanh\left(\frac{T - T_0}{C}\right) \tag{2}$$

(where A, B, T_0, and C are constants determined by nonlinear regression to yield the best fit between the function and test data), was evaluated. Referring to Fig. 6, the quantity ΔT is made up of a temperature difference between the CVN curve and the NDTT, which we will term ΔT_c, plus a statistical component related to the variance of the CVN data, termed ΔT_s. Extensive studies [*6*] have revealed the relationship between the CVN data and fracture toughness data. Simplifying the results, and assuming that NDTT on the average depicts the temperature at which the material has a K_{Id} of 60 MPa $\sqrt{m}$ (55 ksi $\sqrt{in.}$), ΔT_c is related to the height of the upper shelf. (This is equal to $A + B$ in Eq 2.) Hence, the test that sets NDTT should depend on either the variance of CVN data or the upper shelf height determined from the CVN data. To check this point, the property data base was examined. The values of the variance and upper shelf height were summed and averaged for all cases where NDTT set RT_{NDT} and all cases where it was set by CVN. The results showed no significant difference between the two average variance estimates. On the other hand, the upper shelf estimates showed that those cases where RT_{NDT} was set by NDTT had an average upper shelf level of 190 J, while those set by the CVN data had an average upper shelf level of only 154 J. This difference in upper shelf level appears to be the cause of differences in the behavior in setting RT_{NDT} for the different materials. This observation is not surprising, since the original intent of the RT_{NDT} was to ensure an adequate degree of toughness above the ductile-brittle transition temperature, as determined by the NDTT.

Conclusions

The key feature shown in this work is the relationship between the NDTT test and dynamic fracture toughness. The existence of considerable skewness and scatter in the relationship should be a cause for concern, since this scatter can lead to high values of NDTT. While a more direct relationship between CVN data and fracture toughness measurements has been shown elsewhere, the tenuous relationship between NDTT and various measures taken from the CVN curve should not be surprising in view of these high degrees of variability. The setting of the RT_{NDT} appears to be related to the level of the upper shelf energy; for lower upper shelf energies, the RT_{NDT} is set by the CVN data, while the higher upper shelf energy materials have the RT_{NDT} set by the

NDTT. Materials in-between can be set by either approach, depending upon the data scatter.

Acknowledgments

The authors wish to acknowledge the financial support given to the work on which this paper is based by the Electric Power Research Institute, with D. M. Norris as project manager, through Research Project RP2180-9.

References

[1] Pressure Vessel Research Committee (PVRC) Ad Hoc Group on Toughness Requirements, "PVRG Recommendations on Toughness Requirements for Ferritic Materials," *WRC Bulletin*, No. 175, Welding Research Council, New York, August 1972.

[2] Griffith, A. A. "Theory of Rupture," *Proceedings of the International Congress on Applied Mechanics*, Vol. 55, 1924, pp. 55-63.

[3] Irwin, G. R. in *Fracture I, Encyclopedia of Physics*, Vol. VI, Springer, Heidelberg, Germany, 1958, pp. 558-590.

[4] Server, W. L. and Oldfield, W., "Nuclear Pressure Vessel Steel Database," EPRI NP-933, Electric Power Research Institute, Palo Alto, CA, December 1978.

[5] McConnell, P., Server, W. L., Oldfield, W., and Oldfield, F. M., "Irradiated Nuclear Pressure Vessel Steel Database," EPRI NP-2428, Electric Power Research Institute, Palo Alto, CA, June 1982.

[6] Marston, T. U., Oldfield, W., and Server, W. L., "Reference Toughness Curves for Reactor Vessel Steels," *Reference Fracture Toughness Procedures Applied to Pressure Vessel Materials*, MPC-24, American Society of Mechanical Engineers, New York, December 1984.

[7] Oldfield, W., Wullaert, R. A., Server, W. L., and Wilshaw, T. R., "Fracture Toughness Data for Ferritic Nuclear Pressure Vessel Materials: Task A—Program Office, Control Material Round Robin Program," ETI Technical Report 75-34R, Effects Technolog, Inc., Santa Barbara, CA, July 1975.

[8] Oldfield, W., Server, W. L., Wullaert, R. A., and Stahlkopf, K. E., "Statistically Defined Reference Toughness (KIR) Curves," *Proceedings*, Third International Conference on Pressure Vessel Technology, Part II, Tokyo, Japan, April 1977.

[9] Richardson, A. K., Server, W. L., and Reuter, W. G., "Adequacy of Estimates and Variability of Fracture-Related Properties for Reactor Pressure Vessel Materials," *International Journal of Pressure Vessels and Piping*, Vol. 19, 1985, pp. 299-315.

[10] Davies, O. L. and Goldsmith, P. L., *Statistical Methods in Research and Production*, Fourth Revised Edition, Hafner, New York, 1972.

John D. G. Sumpter[1]

Fracture Mechanics Interpretation of the Drop-Weight NDT Temperature

REFERENCE: Sumpter, J. D. G., **"Fracture Mechanics Interpretation of the Drop-Weight NDT Temperature,"** *Drop-Weight Test for Determination of Nil-Ductility Transition Temperature: User's Experience with ASTM Method E 208. ASTM STP 919*, J. M. Holt and P. P. Puzak, Eds., American Society for Testing and Materials, Philadelphia, 1986, pp. 142-160.

ABSTRACT: Difficulties associated with a fracture mechanics interpretation of the drop-weight nil-ductility transition temperature (DW NDTT) test are reviewed. Analytical correlations between the plane-strain fracture toughness for unstable fracture under dynamic loading K_{Id} and DW NDTT presented in the literature usually assume that stress intensity can be calculated by postulating a small thumbnail-shaped crack subjected to dynamic yield stress loading. In practice, cracking continues to be extensive well above DW NDTT, while the region near the Hardex bead is subjected to high plastic strain. The paper presents analyses that attempt to take these factors into account, but none are felt to be entirely convincing. A more appealing explanation of why DW NDTT occurs at the temperature at which it does can be made by comparing the energy available from the specimen and tup with that required to propagate the crack. The author postulates that shear lip development may be the common factor which explains the empirically observed correlation between K_{Id} and DW NDTT.

KEY WORDS: crack propagation, fracture mechanics, nil-ductility transition temperature, drop-weight test, ASTM standard E 208

Nomenclature

a	Crack depth
B	Specimen thickness
B_{SL}	Shear lip width
DW NDTT	Drop-weight nil-ductility transition temperature
E	Young's modulus
e	Strain
e_p	Plastic strain

[1]Principal scientific officer, Admiralty Research Establishment, Dunfermline, Fife, Scotland KY11 5PW.

e_y Yield strain
HAZ Heat-affected zone
J Elastic-plastic crack-tip characterizing parameter
J_c Value of J at unstable fracture
K_{Ia} Plane-strain fracture toughness at crack arrest calculated from the final crack size and static load
K_{Id} Plane-strain fracture toughness for unstable fracture under dynamic loading
K_{cd} Dynamic fracture toughness for a subsize specimen
K_{J_c} J_c expressed in units of stress intensity
ℓ Crack surface length
ΔP Load drop during fracture
P_Y, P_L Analytically predicted loads for the yield of outer fibers and the plastic limit load failure in bending
P_M Experimentally observed maximum load
Q Semielliptical crack flaw shape parameter
RT_{NDT} Reference nil-ductility temperature from ASME III[2]
r_y Crack-tip plastic zone radius
S Loading span
W Specimen width
Y Geometry factor used in the stress-intensity expression $K = Y\sigma\sqrt{\pi a}$
α Percentage of cracked area in the DW NDTT specimen after testing
β A constant, linking shear lip width to crack-tip plastic zone size
γ Absorbed energy per unit area in shear fracture
λ_f Total strain at failure
σ_y Yield stress
σ_{Yd} Dynamic yield stress
σ_u Ultimate tensile stress

There are a number of features of the drop-weight nil-ductility transition temperature (DW NDTT) test that make a clear-cut fracture mechanics interpretation of its significance difficult to achieve.

1. The reference crack size is ill-defined. Figure 1 shows four possible interpretations of crack depth, depending on whether the initial height of the Hardex bead, and the HAZ, are considered to be part of the crack:

(*a*) crack depth equals the bead height plus the fusion zone depth (very shallow);

(*b*) crack depth equals the bead height plus the HAZ depth;

(*c*) crack depth equals the HAZ depth, ignoring the effect of the starter bead; and

[2]American Society of Mechanical Engineers Boiler and Pressure Vessel Code, Section III.

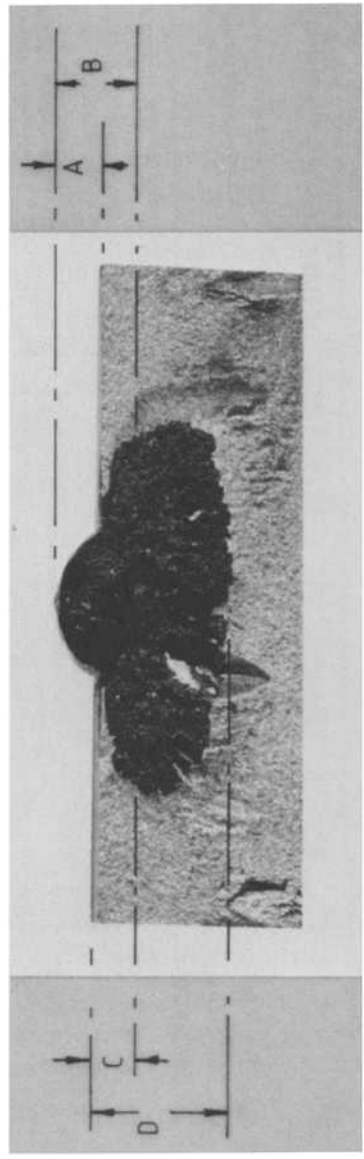

FIG. 1—*Alternative crack depth interpretations.*

(*d*) crack depth equals that of a fairly large arrested crack in the parent material (for correlation with crack arrest toughness).

If the Hardex bead is considered to be part of the crack, there remains the problem of determining a stress intensity for the complex three-dimensional geometry involved. If the effect of the Hardex bead is ignored, stress intensities for a semielliptical crack in a plate of finite width under bending can be used, but these are only approximate in the case of Interpretation *d*, where the crack shape is very irregular.

2. Although the standard suggests that crack initiation should occur while the specimen is still elastic, there is no guarantee that this will happen in practice. The author's experience is that significant plastic strain can occur on the tension surface of the specimen before cracking initiates. This places a question mark against any fracture mechanics analysis based purely on linear elastic stress intensity. Even if an elastic-plastic fracture characterization in terms of J and plastic strain is achieved, it is very doubtful that J_c for the very shallow crack emerging from the Hardex bead will bear any relationship to J_c at failure in a deeply notched, near-elastic, bend or compact tension specimen, since local plastic flow fields will be very different for the two configurations.

3. The crack dynamics of the test are very uncertain. Other standard dynamic fracture toughness tests involve rapid loading of a specimen containing an initially stationary crack. Although dynamic loading is used in the drop-weight test to initiate the crack from the notch in the Hardex bead, the actual toughness characterization must refer to the arrest or continued extension of the propagating crack when it reaches the material under test. In some circumstances the test may involve reinitiation of an arrested crack.

Literature Review

The first fracture mechanics interpretation of DW NDTT was provided by Irwin et al [*1*], who suggested that the test involved the application of dynamic yield stress loading σ_{Yd} to a thumbnail crack with a depth a of 5 mm and length ℓ of 20 mm. The apparent dynamic fracture toughness K_{Id} at DW NDTT was then derived from the linear elastic fracture mechanics (LEFM) formula for a small semielliptical crack in a semiinfinite plate under uniform tension

$$\frac{K_{Id}}{\sigma_{Yd}} = 1.1\sqrt{\frac{\pi a}{Q}} \tag{1}$$

where Q, the flaw shape factor including plasticity, is 1.25 for a defect with $a/\ell = 0.25$. This gave

$$\frac{K_{Id}}{\sigma_{Yd}} = 0.78\sqrt{\text{in.}} = 3.93\sqrt{\text{mm}} \text{ at DW NDTT} \tag{2}$$

Shoemaker and Rolfe [*2*] also used Eq 1, but with a slightly different crack size, and arrived at

$$\frac{K_{Id}}{\sigma_{Yd}} = 0.70\sqrt{\text{in.}} = 3.53\sqrt{\text{mm}} \text{ at DW NDTT} \tag{3}$$

Loss and Pellini [*3*] improved on Eq 1 by using a stress-intensity solution more appropriate to a plate in bending and deduced that K_{Id} lay in the range of 0.4 to 0.6 $\sigma_{Yd}\sqrt{\text{in.}}$, depending on the exact aspect ratio of the crack and the thickness of the DW NDTT specimen. They suggested

$$\frac{K_{Id}}{\sigma_{Yd}} = 0.5\sqrt{\text{in.}} = 2.52\sqrt{\text{mm}} \text{ at DW NDTT} \tag{4}$$

as an average value. This particular relationship has been widely quoted in papers describing the Pellini fracture analysis diagram.

Holzmann et al [*4*] remedied one of the questionable assumptions in these analyses by making use of the actually observed load at crack arrest from instrumented drop-weight tests. On the average they found that the maximum load reached during the test was, in fact, 1.8 times the load required to cause outer fiber yield, and that the arrest load was 0.83 times the maximum load. Their experimental observations led them to suggest an arrested crack size of 6 mm deep by 19 mm long. They then calculated an arrest toughness K_{Ia} equated to K_{Id}, using a stress intensity geometry factor Y of 0.54. In spite of changes in many of the assumptions, the net result arrived at by Holzmann et al is very similar to that of Shoemaker and Rolfe [*2*], namely

$$\frac{K_{Ia}}{\sigma_{Yd}} = \frac{K_{Id}}{\sigma_{Yd}} = 0.72\sqrt{\text{in.}} = 3.61\sqrt{\text{mm}} \text{ at DW NDTT} \tag{5}$$

The only author to attempt an elastic-plastic analysis of the DW NDTT test has been Loechel [*5*]. Noting that the predicted failure strain at DW NDTT from Eq 1 is only 0.3%, whereas the experimentally observed failure strain is many times this value, he produced an empirical relationship to describe the apparent toughness of the specimen as a function of total failure strain λ_f and plastic strain e_p

$$\lambda_f = \frac{K_{Id}(1 + 270e_p)}{1.3E\sqrt{a}} \tag{6}$$

As $e_p \rightarrow 0$, Eq 6 reverts to Eq 1 for the value of Q appropriate to the $a/\ell = 0.45$ arrested cracks which Loechel observed in his drop-weight specimens. Equation 6 essentially predicts that, in the DW NDTT geometry, toughness increases with increasing plastic flow.

Experimental Data

The analyses presented in the present paper are based on instrument DW NDTT tests performed in the author's laboratory on a submerged arc weld, with a chemical composition, in weight percents, of 0.09 carbon, 1.2 manganese, 0.4 silicon, 0.01 phosphorus, 0.01 sulfur, 2.0 nickel, 0.4 chromium, 0.4 molybdenum, and 0.14 copper and with a yield stress of around 500 MPa. The weld was deposited in 50-mm-thick HY80 plate at a heat input of 4.5 kJ/mm and subjected to a postweld heat treatment comprising 12 h at 600°C and 6 h at 650°C. The DW NDTT (determined according to the ASTM Method for Conducting Drop-Weight Test to Determine Nil-Ductility Transition Temperature of Ferritic Steels (E 208-81) and the Charpy V-notch 40-J energy absorption temperature both fell at −35°C. Instrumented DW NDTT tests, performed on a high-rate servohydraulic machine at a displacement rate of 1 m/s, gave a slightly reduced DW NDTT of −45°C. Some prefatigued and statically loaded DW NDTT tests were also carried out. In both cases a further reduction in apparent DW NDTT occurred, to −55°C for the prefatigued tests and to −75°C for the static tests. All the Hardex beads were deposited in a single pass. Fatigue-cracked Charpy ($a/W = 0.2$) and static and dynamic 35-mm compact tension tests were also performed. Results of these tests are given in Fig. 2.

Fracture Mechanics Analysis

The load versus displacement and load versus strain relationships recorded on a slowly loaded, plain (no Hardex bead) P-3 size specimen are shown in Fig. 3. The theoretical load for the first yield of the outer fibers, P_Y, and the plastic limit load P_L are also marked on the diagram; these loads have the following values.

$$P_Y = \frac{2}{3}\sigma_y \frac{BW^2}{S} = 42.7\text{kN} \tag{7}$$

$$P_L = \sigma_u \frac{BW^2}{S} = 75.3\text{kN} \tag{8}$$

where B, the breadth of the specimen, W, its depth, and S, its span, are 50, 16, and 102 mm, respectively, for the P-3 specimen drop weight. The average

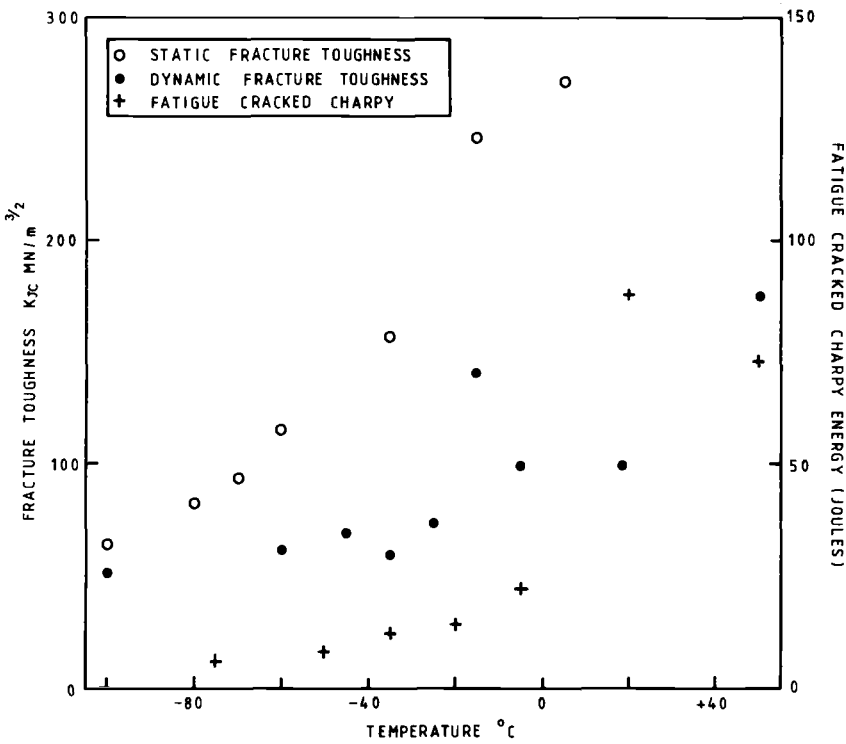

FIG. 2—K_{Jc} *and fatigue-cracked Charpy* (a/W = *0.2) data.*

yield stress for the weld at room temperature is 510 MPa. The ultimate stress is 600 MPa. Figure 4 shows static load traces for actual DW NDTT tests (with test temperatures of −35 and −45°C). The addition of the Hardex bead allows higher maximum loads to be achieved in comparison with those for the plain specimen. Rearranging Eq 7 and using the peak load for the static test at −45°C gives a nominal outer fiber elastic stress of 1133 MPa, approximately twice the static yield stress at this temperature. A similar conclusion can be reached for the dynamic tests illustrated in Fig. 5 (with test temperatures of −30 and −45°C).

Heat-tinted fracture surfaces of a typical drop-weight series are shown in Fig. 6. It is evident that extensive crack propagation continues to occur well above DW NDTT. It is thus impossible to associate the fracture toughness at DW NDTT with the conditions for arrest or continued propagation of a small thumbnail crack only a few millimetres deep. Eventually, at some temperature well above DW NDTT, a small crack is arrested as it emerges from the vicinity of the Hardex bead, but the appropriate toughness with which to correlate this event is that at the temperature of the particular DW NDTT test

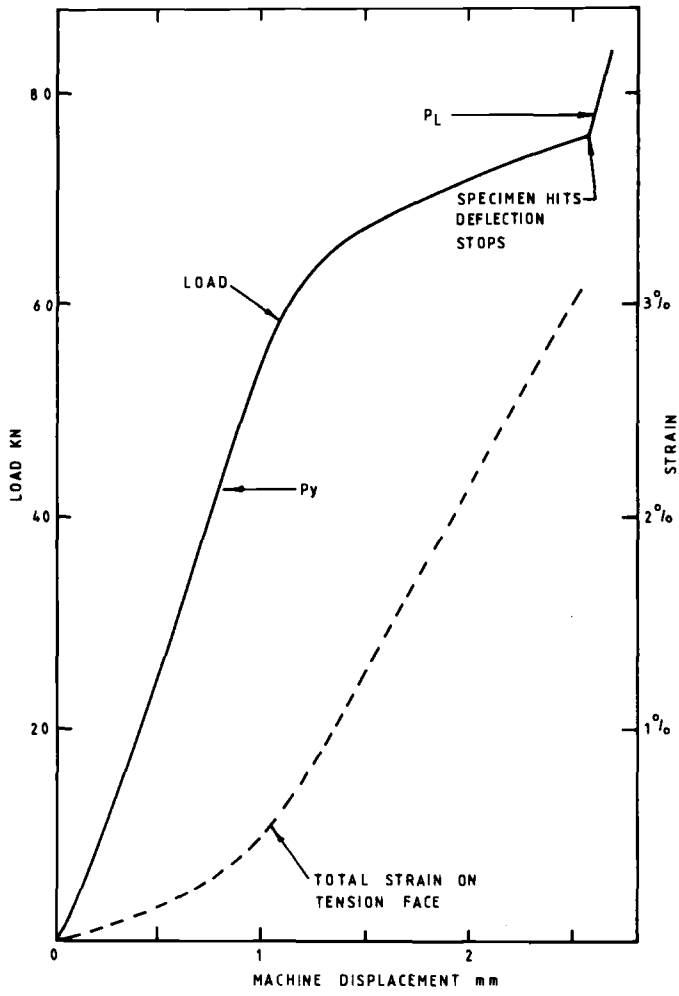

FIG. 3—*Static trace for a DW NDTT specimen with no Hardex bead.*

involved, typically a DW NDTT of +30 to +60°C. Just above DW NDTT, arrested cracks are large, typically 10 mm deep by 40 mm in maximum length. They are "ear shaped," with relatively little crack extension occurring along the tension surface of the specimen.

Table 1 lists final crack dimensions and loads for instrumented DW NDTT tests at temperatures just above DW NDTT. Stress intensity has been calculated on the surface of the specimen and on the deepest part of the crack using solutions for a semielliptical crack in bending developed by Newman and Raju [6]. These solutions are superior to those used by any of the authors cited in the literature survey in that they take into account the breadth as well

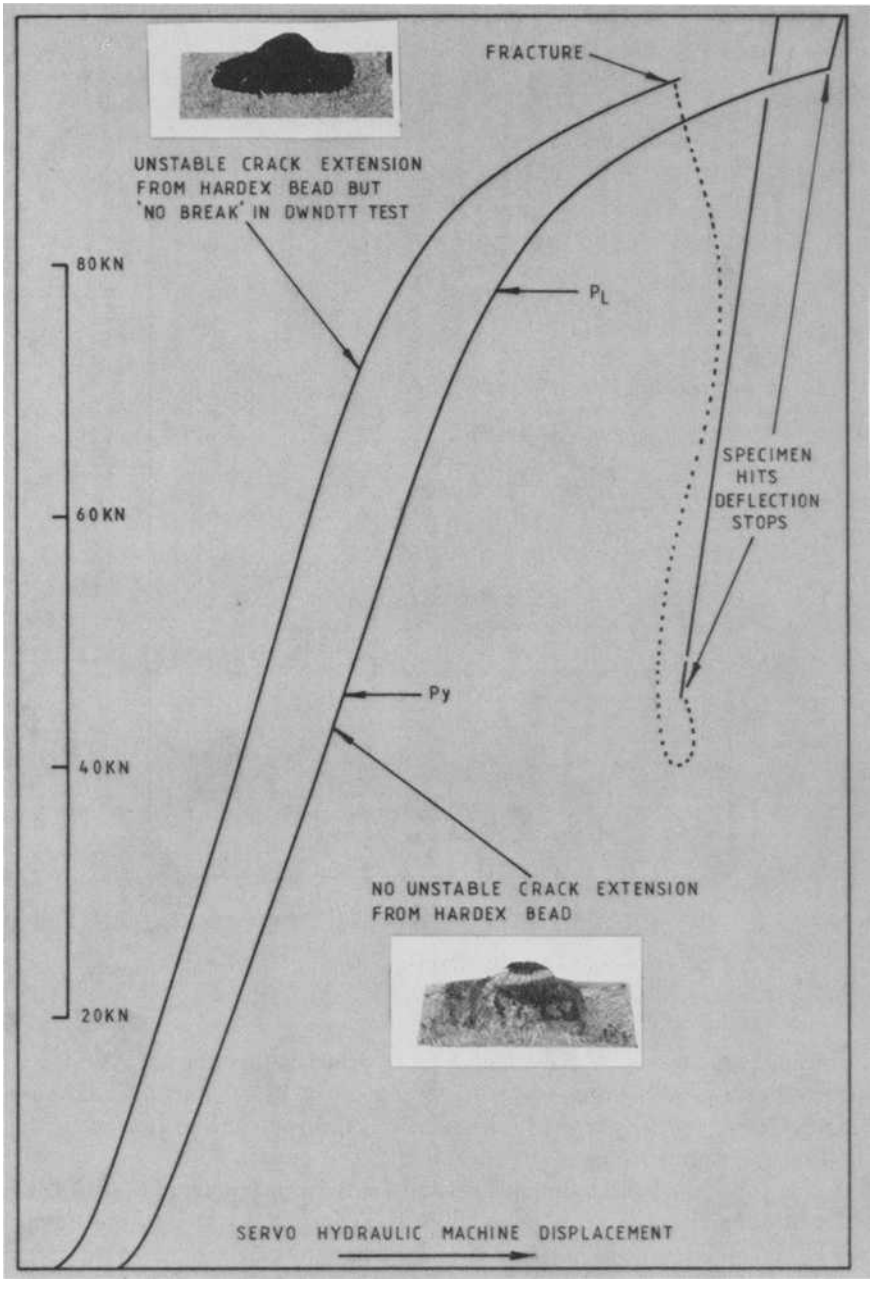

FIG. 4—*Static traces for standard DW NDTT specimens.*

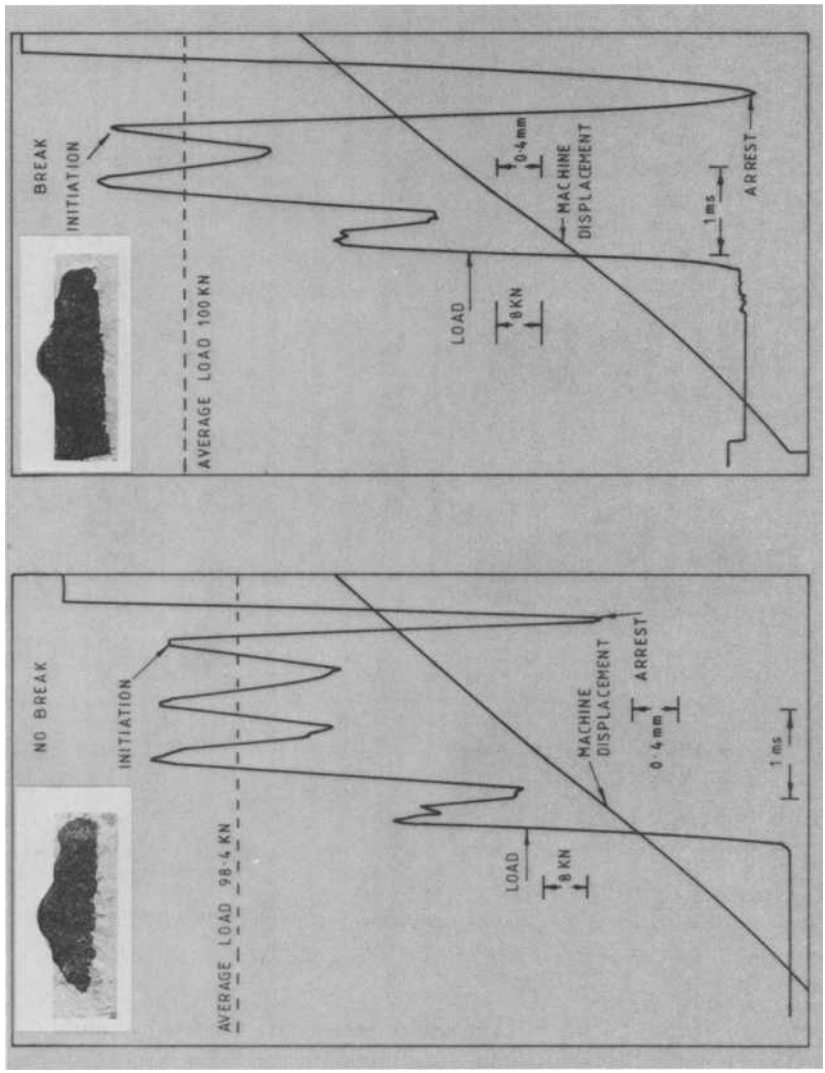

FIG. 5—*Dynamic traces for standard DW NDTT specimens.*

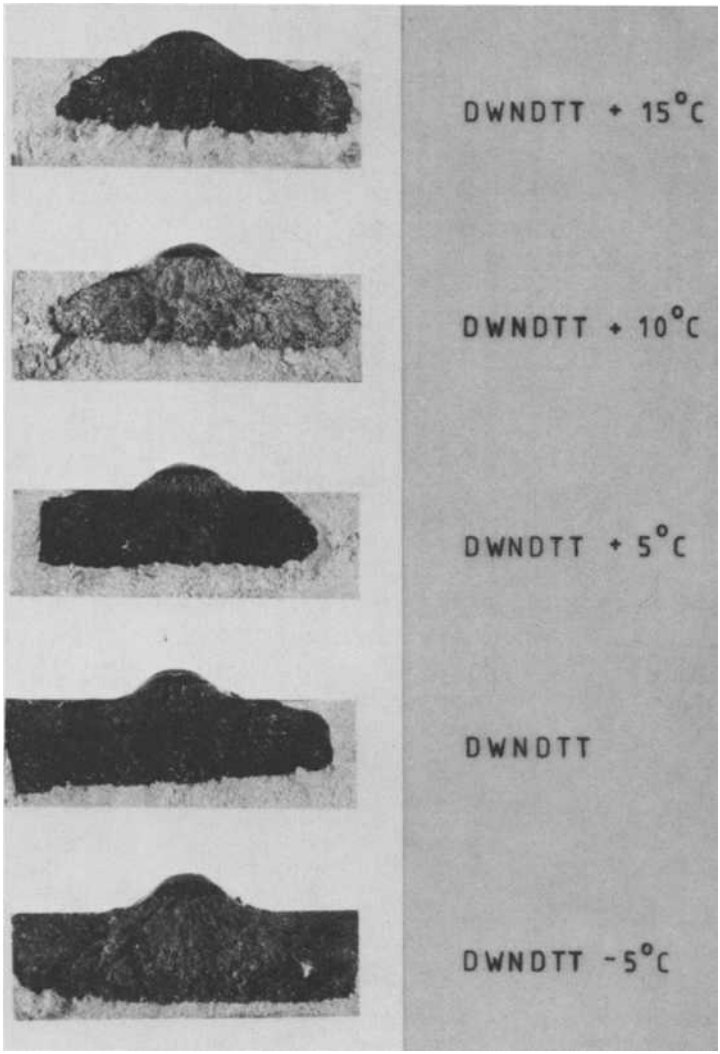

FIG. 6—*Heat-tinted fracture surfaces in instrumented dynamic DW NDTT tests.*

as the depth of the specimen. (The use of elastic stress intensity solutions, although still not entirely justifiable, is more appropriate for large cracks at relatively low arrest loads than for small thumbnail cracks in the high plastic strain region near the Hardex bead.) Table 1 shows that the average stress intensity at the surface is 69 MPa $\sqrt{m}$ in comparison with 25 MPa $\sqrt{m}$ at the deepest point. The surface value is close to that of the average dynamic toughness of the weld (see Fig. 2) just above DW NDTT. Since the fail/no fail crite-

TABLE 1—*Final loads and crack dimensions for instrumented DW NDTT specimens.*

Type of Test	Temperature, °C	Final Crack Dimensions			Load			Final Nominal Stress, MPa	K, MPa$\sqrt{m}$	
		Area, %	Depth, mm	Length, mm	Maximum, kN	Final, kN	Drop, %		Bottom	Surface
Low rate, DW NDTT = −75°C	DW NDTT + 30	38	9	33	94.8	45.5	52	546	33	76
	DW NDTT + 15	41	10	38	94.8	32.2	66	386	22	64
High rate, DW NDTT = −45°C	DW NDTT + 15	44	9	40	98.4	30.5	69	366	28	56
	DW NDTT + 10	47	10	42	103.2	45.4	56	545	36	98
	DW NDTT + 5	50	10	39	100.0	22.0	78	264	16	44
High rate fatigue crack, DW NDTT = −55°C	DW NDTT + 15	34	10	29	88.8	52.4	41	629	23	88
	DW NDTT + 5	63	11	46	92.8	21.3	77	256	15	57
Average stress intensity factor at crack arrest									25	69

rion in the DW NDTT test depends on lengthwise propagation of the crack, it seems logical that any correlation with fracture toughness should be with stress intensity at the surface rather than with stress intensity at the deepest point. In practice, a true three-dimensional stress analysis of the acute angle at which the ear-shaped crack meets the free surface would show the stress intensity to be many times the value calculated here based on a semielliptical idealization. It is consequently considered unwise to attach undue emphasis to this apparently successful correlation.

A general stress intensity history for a crack in a drop-weight test specimen can be attempted by making use of the empirical observation (Fig. 7) that the drop in load ΔP as the crack extends is linked approximately to the percentage of the cracked area α by a relationship of the form

$$\frac{\Delta P}{P_M} = \frac{\alpha}{70} \tag{9}$$

where P_M is the maximum load reached before fracture. The area of a semielliptical crack is $\pi a \ell/4$, and the nominal outer fiber stress has been observed to

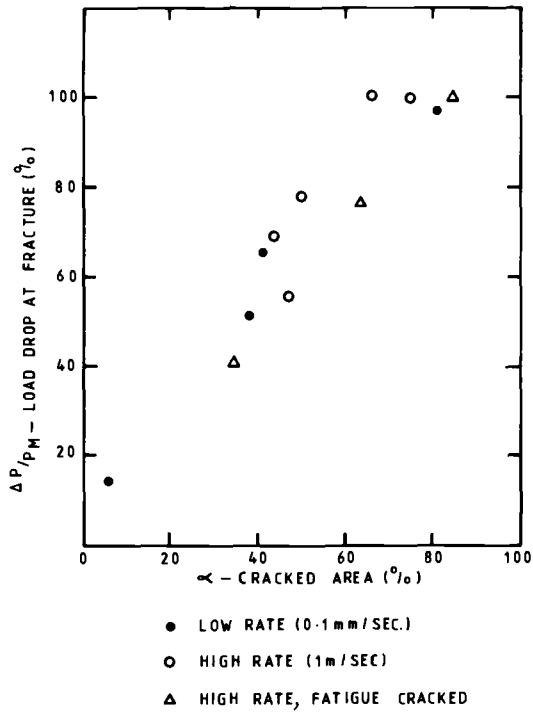

FIG. 7—*Relationship between the cracked area and the load drop at fracture in the DW NDTT test.*

be approximately twice the yield stress at fracture. The stress intensity for a crack at any depth a and surface length ℓ can thus be written

$$K = 2\sigma_y\left(1 - \frac{\pi a \ell}{2240}\right) Y\sqrt{\pi a} \tag{10}$$

where Y is the geometry factor of Newman and Raju and the total cross-sectional area of the drop-weight test specimen is 800 mm^2. Results are illustrated in Fig. 8 for $\sigma_y = 550$ MPa. This figure shows that the stress intensity that can be developed by a semielliptical crack in the DW NDTT specimen has a limiting upper bound value irrespective of crack extension. This obser-

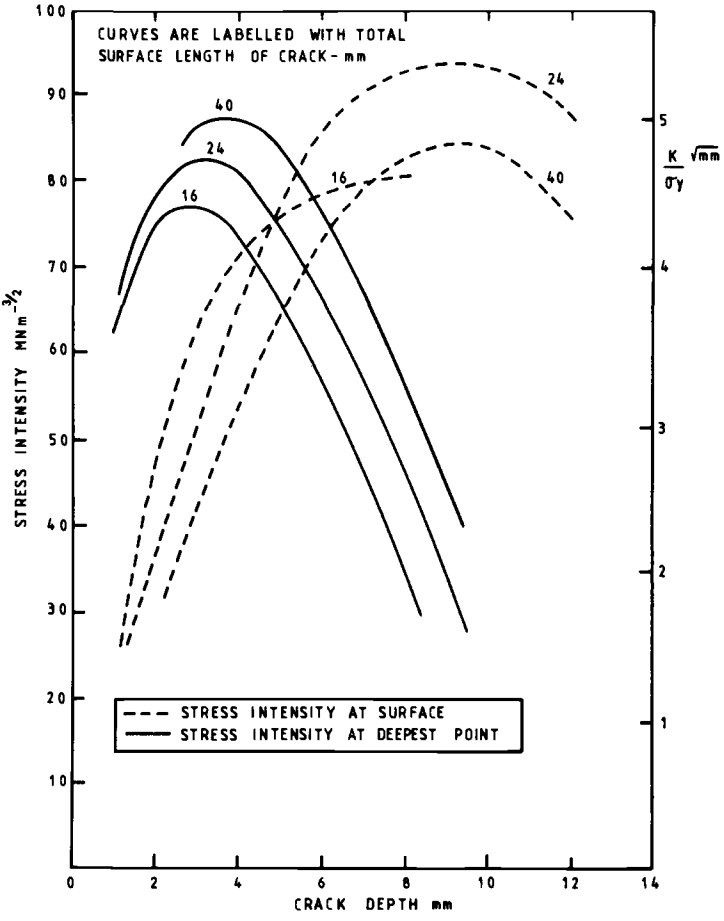

FIG. 8—*Change of stress intensity in the DW NDTT test allowing for falloff in load and change of crack shape.*

vation could be translated into a statement that cracks will not extend very far in the DW NDTT specimen once

$$\frac{K_{Id}}{\sigma_{Yd}} \approx 5\sqrt{mm} \approx 1.0\sqrt{in.} \tag{11}$$

This statement is not linked to the toughness of DW NDTT, since the specimen actually fails at that temperature, but to some temperature around a DW NDTT of +30°C, where the crack arrests after propagating a few millimetres into the base material.

An estimate of the toughness at which the crack would be expected to arrest immediately on leaving the Hardex bead can be attempted using a J solution for a crack in a highly plastic field. The engineering J curve developed by Turner [7] uses a relationship

$$\frac{K_{Jc}^2}{Y^2\sigma_y^2\pi a} = 2.5\left(\frac{e}{e_y} - 0.2\right) \tag{12}$$

For $e/e_y = 10$, the condition existing in a typical DW NDTT specimen at Hardex bead failure, the crack depth $a = 4$ mm (the height of the Hardex bead plus the fusion zone depth), and $Y = 1.12$ (edge cracked plate)

$$\frac{K_{Jc}}{\sigma_y} = 19.7\sqrt{mm} = 3.9\sqrt{in.} \tag{13}$$

For $\sigma_y = 550$ MPa this implies a dynamic K_{Jc} of 342 MPa $\sqrt{m}$ to ensure crack arrest, which is essentially upper shelf toughness for a deeply notched J specimen. The prediction is, however, complicated by the known effect of notch depth on toughness in the brittle-to-ductile transition [8].

Energy Balance Analysis

In an early paper on transition temperature phenomena, Pellini [9] noted that complete fractures were obtained in explosion bulge crack starter tests on mild steel when the shear lip width was less than 0.5 mm and that no shear lips were visible on the surface of DW NDTT specimens at DW NDTT. Quenched and tempered low-alloy steels were observed to have small, but visible, shear lips at DW NDTT. This was ascribed to these steels' high yield-to-ultimate strength ratio allowing shear lip formation with less energy absorption. The weld tested in the present study also showed very small shear lips at DW NDTT, the largest shear lips being less than 1 mm in thickness. These observations, together with the definition of DW NDTT, which focuses attention on crack propagation along the *surface* of the specimen, suggests that DW NDTT is closely associated with shear lip formation. This, in turn, sug-

gests that the mechanics of the test might be best explained in terms of energy balances.

At the point of fracture the total available stored elastic energy in the specimen is only about 35 J. All of this energy is released only if the specimen fractures completely and the load drops to zero. If the point of fracture occurs very near the stopping distance, no further energy is available from the tup. On average, in the present tests, fracture initiation from the Hardex bead occurred about 0.3 mm short of the stopping distance. Hence, even if the load did not fall at all from its 100 kN maximum value, the tup would only be able to supply an additional 30 J of energy to aid the fracture process. In practice, if the crack propagates, the load must fall off, and the amount of energy supplied by the tup might conservatively be estimated as only half this amount. This gives a total of only about 50 J to fracture a specimen with a cross-sectional area of 800 mm^2, ten times that of the Charpy V-notch test, and greater than that of the 16-mm dynamic tear test.

These arguments may be developed to make an approximate prediction of the energy required to fracture a fatigue-cracked Charpy specimen at DW NDTT. (Direct correlation between DW NDTT and Charpy V-notch energy is impossible because of the effect of the V-notch on crack initiation energy). It has been noted that, at DW NDTT, the average percentage of the cracked area of a DW NDTT specimen is about 70%. The crack usually breaks preferentially to one side leaving some of the other shoulder of the specimen unbroken. If the width of the shear lip at fracture is put at 1 mm, the areas of shear and flat fracture in a DW NDTT specimen at DW NDTT may be estimated to be

shear: $1 \times 30 = 30$ mm^2 (The total width of specimen outside the Hardex bead is 37.5 mm.)
flat: $(0.7 \times 800) - 30 = 530$ mm^2

The equivalent areas in a fatigue-cracked Charpy specimen with $a/W = 0.2$ are

shear: $1 \times 16 = 16$ mm^2
flat: $(8 \times 10) - 16 = 64$ mm^2

If the energy required to fracture a DW NDTT specimen at DW NDTT is 50 J, as suggested earlier, and if it is further assumed that the energy absorbed per unit area γ in shear fracture is ten times that absorbed in flat fracture (the approximate factor between upper and lower shelf energy absorption), it is possible to deduce the value of γ for the DW NDTT specimen as

$$30\gamma + 530(\gamma/10) = 50$$

where γ is 0.6 J/mm^2. The energy absorbed by a fatigue-cracked $a/W = 0.2$ Charpy-sized specimen at DW NDTT may then be predicted as $(16 + 6.4)\gamma = 13$ J, which is close to the value observed in tests near DW NDTT (see Fig. 2).

Discussion

In spite of the difficulties involved in providing a direct fracture mechanics interpretation of DW NDTT, a number of published studies have shown that K_{Id} at DW NDTT does assume a reasonably consistent value for a range of different materials. A comprehensive survey of the literature has not been attempted, and would in any case be difficult because of the authors' habit of quoting the reference nil-ductility transition temperature (RT_{NDT}), used by the American Society of Mechanical Engineers (ASME), rather than DW NDTT, but Table 2 lists four references that have specifically quoted dynamic toughness/DW NDTT data for several materials [*2,4,10,11*]. Holzmann et al [*4*], in support of their analytically derived relationship in Eq 5, observed that K_{Id} at DW NDTT lay in the range

$$\frac{K_{Id}}{\sigma_{Yd}} = (3.4 \pm 0.3)\sqrt{\text{mm}} \tag{14}$$

TABLE 2—*Published data on dynamic fracture toughness at DW NDTT.*

Reference	Steels	K_{Id} at DW NDTT, MPa$\sqrt{\text{m}}$
Shoemaker and Rolfe [*2*]	ABS-C	55
	A302-B	60
	HY80	87
	A517-F	100
	HY130	96
Holzmann, Vlach and Man [*4*]	seven steels with σ_{YD} between 515 and 625 MPa	56
		61
		53
		54
		71
		55
		68
Tenge and Karlsen [*10*]	eleven heats of fine-grained carbon-manganese steel with σ_{YS} of 321 to 530 MPa	K_{cd} transition (based on $K_{cd} = 95$ MPa$\sqrt{\text{m}}$) took place between DW NDTT − 10°C and DW NDTT + 10°C for all eleven steels
Hahn et al [*11*]		Individual crack arrest K_{Ia} toughnesses:
	A533B Heat 1	87, 81, 55, 85, 76, 52, 49, 47
	A533B Heat 2	102, 84, 69
	A508	96, 71, 64, 72, 60
	A533B Weld	85, 77, 87

A possible way of linking the energy balance interpretation of DW NDTT to K_{Id} is via shear lip size. The link between K_{Id} and the shear lip width B_{SL} is through the plastic zone radius r_y at fracture. This is customarily expressed in the form

$$B_{SL} = r_y = \beta\left[\frac{K_{Id}}{\sigma_{Yd}}\right]^2 \tag{15}$$

where β is a constant, commonly ascribed a value of $1/2\pi$ for plane stress conditions. If Eq 15 is correct, the empirical observation that K_{Id}/σ_{Yd} assumes a constant value at DW NDTT is obviously consistent with a criterion that B_{SL} should attain a minimum critical value to assure no break conditions. For instance, if K_{Id}/σ_{Yd} is set at the value of 3.4 $\sqrt{\text{mm}}$ observed by Holzmann et al

$$B_{SL} = \frac{1}{2\pi}(3.4)^2 = 1.8\text{mm} \tag{16}$$

which constitutes a size of shear lip in excess of that commonly seen on the surface of DW NDTT specimens.

Conclusions

Previously published analytical correlations between K_{Id} and DW NDTT have failed to take into account the full complexity of the test specimen configuration and loading conditions. More refined analysis, incorporating realistic crack size and strain assumptions have been attempted in this paper, but none are felt to be totally satisfactory. Shear lip development appears to play a crucial role in determining DW NDTT. It seems probable that once shear lip formation, rather than cleavage, becomes the favored mechanism of failure at the specimen free surface, there is simply insufficient energy available in the DW NDTT test to achieve a break condition. K_{Id} is also linked to shear lip width through the crack-tip plastic zone size, and this may provide the most plausible explanation for the loose empirical link between K_{Id} and DW NDTT observed by many authors.

References

[1] Irwin, G. R., Kraftt, J. M., Paris, P. C., and Wells, A. A., "Basic Aspects of Crack Growth and Fracture," NRL Report 6598, Naval Research Laboratory, Washington, DC, 1967.

[2] Shoemaker, A. K. and Rolfe, S. T., "The Static and Dynamic Low-Temperature Crack Toughness of Seven Structural Steels," *Engineering Fracture Mechanics*, Vol. 2, No. 4, June 1971, pp. 319-340.

[3] Loss, F. J. and Pellini, W. S., "Coupling of Fracture Mechanics and Transition Temperature Approaches to Fracture Safe Design," *Practical Fracture Mechanics for Structural Steel*, United Kingdom Atomic Energy Authority Conference, Risley, England, 1969.

[4] Holzmann, M., Vlach, B., and Man, J., "The Relation Between Temperature T_{NDT} and the Dynamic Fracture Toughness K_{Id}," *Kovove Materialy*, Vol. 18, No. 5, 1980, pp. 635–640, Defence Research Information Centre Translation 6492.

[5] Loechel, L. W., "The Effect of Testing Variables on the Transition Temperature in Steel," Report HSSTP-TR-2, Martin Marietta Corp., Bethesda, MD, 1969.

[6] Newman, J. and Raju, I. S., "Analyses of Surface Cracks in Finite Plates under Tension or Bending Loads," NASA Technical Paper 1578, National Aeronautics and Space Administration, Washington, DC, 1979.

[7] Turner, C. E., "The *J*-Estimation Curve, R Curve, and Tearing Resistance Leading to a Proposal for a *J*-Based Design Curve Against Fracture," *Proceedings*, Conference on Fitness for Purpose Validation of Welded Constructions, The Welding Institute, London, UK, November 1981.

[8] Sumpter, J. D. G., "The Effect of Notch Depth and Orientation on the Fracture Toughness of Multipass Weldments," *International Journal of Pressure Vessels and Piping*, Vol. 10, 1982, pp. 169–180.

[9] Pellini, W. S., "Evaluation of the Significance of Charpy Tests," *Symposium on Effect of Temperature on the Brittle Behavior of Metals with Particular Reference to Low Temperatures, ASTM STP 158*, American Society for Testing and Materials, Philadelphia, 1953, p. 216.

[10] Tenge, P. and Karlsen, A., "Dynamic Fracture Toughness of C-Mn Weldments and Some Practical Consequences," *Proceedings*, Conference on Dynamic Fracture Toughness, The Welding Institute, London, UK, July 1976.

[11] Hahn, G. T., Hoagland, R. G., Lereim, J., Markworth, A. J., and Rosenfield, A. R., "Fast Fracture Toughness and Crack Arrest Toughness of Reactor Pressure Vessel Steel," *Crack Arrest Methodology and Applications, ASTM STP 711*, G. T. Hahn and M. F. Kanninen, Eds., American Society for Testing and Materials, Philadelphia, 1980, pp. 289–320.

Appendix:
ASTM Method E 208-85

APPENDIX

Designation: E 208 - 85

Standard Method for
CONDUCTING DROP-WEIGHT TEST TO DETERMINE NIL-DUCTILITY TRANSITION TEMPERATURE OF FERRITIC STEELS[1]

This standard is issued under the fixed designation E 208; the number immediately following the designation indicates the year of original adoption or, in the case of revision, the year of last revision. A number in parentheses indicates the year of last reapproval. A superscript epsilon (ε) indicates an editorial change since the last revision or reapproval.

INTRODUCTION

This drop-weight test was developed at the Naval Research Laboratory in 1952 and has been used extensively to investigate the conditions required for initiation of brittle fractures in structural steels. Drop-weight test facilities have been established at several Naval activities, research institutions, and industrial organizations in this country and abroad. The method is used for specification purposes by industrial organizations and is referenced in several ASTM specifications and the ASME Boiler and Pressure Vessel Code. This procedure was prepared to ensure that tests conducted at all locations would have a common meaning.

1. Scope

1.1 This method covers the determination of the nil-ductility transition (NDT) temperature of ferritic steels, 5/8 in. (15.9 mm) and thicker.

1.2 This method may be used whenever the inquiry, contract, order, or specification states that the steels are subject to fracture toughness requirements as determined by the drop-weight test.

1.3 The values stated in inch-pound units are to be regarded as the standard.

1.4 *This standard may involve hazardous materials, operations, and equipment. This standard does not purport to address all of the safety problems associated with its use. It is the responsibility of whoever uses this standard to consult and establish appropriate safety and health practices and determine the applicability of regulatory limitations prior to use.*

2. Definitions

2.1 *nil-ductility transition (NDT) temperature*—the maximum temperature where a standard drop-weight specimen breaks when tested according to the provisions of this method.

2.2 *ferritic*—the word ferritic as used hereafter refers to all α-Fe steels. This includes martensitic, pearlitic, and all other nonaustenitic steels.

3. Summary of Method

3.1 The drop-weight test employs simple beam specimens specially prepared to create a material crack in their tensile surfaces at an early time interval of the test. The test is conducted by subjecting each of a series (generally four to eight) of specimens of a given material to a single impact load at a sequence of selected temperatures to determine the maximum temperature at which a specimen breaks. The impact load is provided by a guided, free-falling weight with an energy of 250 to 1200 ft-lbf (340 to 1630 J) depending on the yield strength of the steel to be tested. The specimens are prevented by a stop from deflecting more than a few tenths of an inch.

3.2 The usual test sequence is as follows: After the preparation and temperature conditioning of the specimen, the initial drop-weight test is con-

[1] This method is under the jurisdiction of the ASTM Committee E-28 on Mechanical Testing and is the direct responsibility of Subcommittee E28.07 on Impact Testing.

Current edition approved Nov. 29, 1985. Published January 1986. Originally published as E 208 - 63 T. Last previous edition E 208 - 84a.

ducted at a test temperature estimated to be near the NDT temperature. Depending upon the results of the first test, tests of the other specimens are conducted at suitable temperature intervals to establish the limits within 10°F (5°C) for break and no-break performance. A duplicate test at the lowest no-break temperature of the series is conducted to confirm no-break performance at this temperature.

4. Significance and Use

4.1 The fracture-strength transitions of ferritic steels used in the notched condition are markedly affected by temperature. For a given "low" temperature, the size and acuity of the flaw (notch) determines the stress level required for initiation of brittle fracture. The significance of this test method is related to establishing that temperature, defined herein as the NDT temperature, at which the "small flaw" initiation curve, Fig. 1, falls to nominal yield strength stress levels with decreasing temperature, that is, the point marked NDT in Fig. 1.

4.2 Interpretations to other conditions required for fracture initiation may be made by the use of the generalized flaw-size, stress-temperature diagram shown in Fig. 1. The diagram was derived from a wide variety of tests, both fracture-initiation and fracture-arrest tests, as correlated with the NDT temperature established by the drop-weight test. Validation of the NDT concept has been documented by correlations with numerous service failures encountered in ship, pressure vessel, machinery component, forged, and cast steel applications.

5. Precautions

5.1 The drop-weight test was devised for measuring fracture initiation characteristics of ⅝-in. (15.9-mm) and thicker structural materials. This test is not recommended for steels less than ⅝-in. thick.

5.2 This method establishes standard specimens and conditions to determine the NDT temperature of a given steel. The use of standard specimens with nonstandard test conditions or the use of nonstandard specimens shall not be allowed for specification purposes.

5.3 This method employs a small weld bead deposited on the specimen surface, whose sole purpose is to provide a brittle material for the initiation of a small, cleavage crack-flaw in the specimen base material during the test. Anomalous behavior may be expected for materials where the heat-affected zone created by deposition of the crack-starter weld is made more fracture resistant than the unaffected plate. This condition is developed for quenched and tempered steels of high hardness obtained by tempering at low temperatures. The problem may be avoided by placing the crack-starter weld on these steels before conducting the quenching and tempering heat treatment. Except for other cases which may be readily rationalized in metallurgical terms (for example, it is possible to recrystallize heavily cold-worked steels in the heat-affected zone and to develop a region of improved ductility), the heat-affected zone problem is not encountered with conventional structural grade steels of a pearlitic microstructure or quenched and tempered steels tempered at high temperatures to develop maximum fracture toughness.

6. Apparatus

6.1 The drop-weight machine is of simple design based on the use of readily available structural steel products.[2] The principal components of a drop-weight machine are a vertically guided, free-falling weight, and a rigidly supported anvil which provides for the loading of a rectangular plate specimen as a simple beam under the falling weight. Figure 2(*a*) illustrates a typical drop-weight machine built of standard structural shapes.

6.2 A rail, or rails, rigidly held in a vertical position and in a fixed relationship to the base shall be provided to guide the weight. The weight shall be provided with suitable devices which engage the rail, or rails, and ensure that it will drop freely in a single, vertical plane. The weight may be raised by any convenient means. A weight-release mechanism, functioning similarly to that shown in Fig. 2(*b*), shall be provided to release the weight quickly without affecting its free fall. The weight shall be made in one piece, or if made of several pieces, its construction shall be rigid to ensure that it acts as a unit when it strikes the specimen. The striking tup of the weight shall be a steel cylindrical surface with a radius of 1 in. (25.4 mm) and a minimum hardness of HRC 50 throughout the section. The weight shall be between 50 and 300 lb (22.7 and

[2] Detail drawings for the construction of this machine are available from ASTM Headquarters. Order PCN 12-502080-00.

136 kg). The rails and hoisting device shall permit raising the weight various fixed distances to obtain potential energies of 250 to 1200 ft-lbf (340 to 1630 J).

6.3 A horizontal base, located under the guide rails, shall be provided to hold and position precisely the several styles of anvils required for the standard specimens. The anvil guides shall position the anvil with the centerline of the deflection stops under the centerline of the striking tup of the weight. In general, the base will also support the guide rails, but this is not a requirement. The base shall rest on the rigid foundation. The base-foundation system shall be sufficiently rigid to allow the normal drop-weight energy (Table 1) to deflect a standard specimen to the stop at temperatures above the NDT. The base shall not jump or shift during the test, and shall be secured to the foundation if necessary to prevent motion.

6.4 A guard screen, similar to that shown in Fig. 2*(c)*, is recommended to stop broken specimen halves of the very brittle steels which break into two pieces with both halves being ejected forcefully from the machine.

6.5 The general characteristics of two of the anvils required are illustrated in Fig. 3. The anvils shall be made in accordance with the dimensions shown in Fig. 4. The anvil supports and deflection stops shall be steel-hardened to a minimum hardness of HRC 50 throughout their cross section. The space between the two stops is provided as clearance for the crack-starter weld on the specimen. The deflection stops may be made in two separate pieces, if desired. The anvil-base system shall be sufficiently rigid to allow the normal drop-weight energy (Table 1) to deflect the specimen to the stop at temperatures well above the NDT.

6.6 A measuring system shall be provided to assure that the weight is released from the desired height for each test, within the limits of +10, −0 %.

6.7 Modifications of the equipment or assembly details of the drop-weight machine shown in Fig. 2 are permitted provided that the modified machine is functionally equivalent. Figure 5 illustrates a portable machine design used by an industrial concern for drop-weight tests of materials used for pressure vessel components at different fabrication sites.

7. Test Specimens

7.1 *Identification of Material*—All sample material and specimens removed from a given plate, shape, forging, or casting product shall be marked to identify their particular source (heat number, slab number, etc.). A simple identification system shall be used which can be employed in conjunction with an itemized table to obtain all the pertinent information.

7.2 *Orientation*—The drop-weight test is insensitive to specimen orientation with respect to rolling or forging direction. However, unless otherwise agreed to, all specimens specified by the purchaser shall be of the same orientation and it shall be noted in the test report.

7.3 *Relation to Other Specimens*—Unless otherwise specified by the purchaser, the specimens shall be removed from the material at positions adjacent to the location of other type test specimens (for example, mechanical test specimens) required for evaluation of other material properties.

7.4 *Special Conditions for Forgings and Castings*—Where drop-weight testing of cast or forged material is specified, the size and location of integrally attached pad projections or prolongations to be used for specimen fabrication shall be agreed to in advance by the purchaser. If the design of the casting or forging does not allow an attached test-material coupon, the following requirements shall apply:

7.4.1 Drop-weight specimens cast or forged separately to the dimensions required for testing shall be allowed only where the product dimensions are equivalent and the purchaser agrees.

7.4.2 Specimens may be taken from a separately produced test-material coupon if the supplier can demonstrate that it is equivalent to the product with respect to chemical composition, soundness, and metallurgical conditions. The material shall be from the same heat and shall have been fabricated under identical conditions as the product. The specimens shall be machine-cut from locations agreed to in advance by the purchaser.

7.4.3 Specifically, in the case of casting requiring X-ray quality standard, the separate test-material coupon shall be cast separately but simultaneously with the product. Chills shall not be used. The test-material coupon shall be in proportion to the thickness, T, in the cast product, where T is diameter of the largest circle that can be inscribed in any cross section of the casting, or where T is defined in advance by the purchaser as the nominal design thick-

ness, as follows:

Thickness, T, in. (mm)	Separately Cast, Nonchilled, Test-Coupon Size
½ (12.7) and less	None required
⅝ to 2 (15.9 to 50.8)	When several small castings are poured from one heat, one casting shall be used to provide test specimens, if adaptable
⅝ to 1 (15.9 to 25.4)	T by 2 by 5 in. (127 mm) for irregularly shaped castings
>1 to 3 (25.4 to 76.2)	T by 4.5T by 4.5T
>3 to 5 (76.2 to 127)	T by 3T by 3T
Over 5 (127)	T by 3T by 3T for castings that are representative of cast plates
Over 5 (127)	T by T by 6 $\sqrt{T}$ for castings that are representative of cast bars

7.4.4 Specimens showing casting or metallurgical faults on broken fracture surfaces shall be "No-Test."

7.5 *Size of Blank*—Dimensions of the blank size required for standard test specimens are shown in Fig. 6. Equally significant NDT temperatures, within ±10°F (±5°C), are determined for a given steel with tests using any of the standard specimens. As may be convenient for the particular thickness of material, any of the standard specimens shown in Fig. 6 and prepared as described in Section 7 may be chosen for this method. The results obtained with standard test conditions shall comply with the requirements of this method for determining the NDT temperature.

7.6 *Specimen Cutting*—The specimen sample material and the specimen ends may be flame-cut. The specimen sides shall be saw-cut or machined, using adequate coolant to prevent specimen overheating, and shall be a minimum of 1 in. from any flame-cut surface. Products thicker than the standard specimen thickness shall be machine-cut to standard thickness from one side, preserving an as-fabricated surface unless otherwise specified, or agreed to, in advance by the purchaser. The as-fabricated surface so preserved shall be the welded (tension) surface of the specimen during testing.

7.7 *Crack-Starter Weld*—The crack-starter weld, which is a centrally located weld bead, approximately 2½ in. (63.5 mm) long and ½ in. (12.7 mm) wide, shall be deposited on the as-fabricated tension surface of the drop-weight specimen in a single pass.[3] To assist the welding operator in centering the weld deposit properly on the test piece, two punch marks as shown in Fig. 7*(a)* or a copper template containing a 1 by 3-in. (25 by 76-mm) centrally positioned slot, Fig. 7*(b)*, shall be used.[4] The weld shall start from either Point *A* or *D* and shall proceed without interrruption as a stringer bead (no weaving) to the other point. The bead appearance is determined by the amperage, arc voltage, and speed of travel used. A current of 180 to 200 A, a medium arc length, and a travel speed that will result in a moderately high-crowned bead have been found to be suitable conditions. An enlarged view of an as-deposited crack-starter weld is shown in Fig. 7*(c)*.

7.7.1 *Microstructure of Base Metal*—Data presented show that the method of depositing the weld bead can influence the microstructure of the heat-affected zone under the weld notch which in turn can influence the NDT determined especially in heat-treated steels.[5]

7.8 *Weld Notch*—The final preparation of the specimen consists of notching the deposited weld at the center of the bead length. Care shall be taken to ensure that only the weld deposit is notched and that the cutting tools do not contact the specimen surface. The notch may be cut with thin abrasive disks, as shown in Fig. 8, or other convenient cutting tools such as mechanical saws, hack saws, etc. The weld-notch details and a representative example of a notched weld is given in Fig. 9.

7.9 *Measuring Weld-Notch Depth*—The depth of the notch from the crown of the weld will vary with expected variations in weld-crown dimensions. The depth of the notch is not measured, since it is the thickness of the weld remaining above the specimen and under the bottom of the notch that has been standardized, as

[3] Murex-Hardex-N electrodes (available as Stock No. 1316-5376 from Murex Welding Products, 575 Mountain Avenue, P.O. Box 922, New Providence, NJ 07974) and NRL-S welding electrodes (available from Kobe Steel, Ltd., Los Angeles, CA) have been shown, by data on file at ASTM Headquarters, to be satisfactory for the crack-starter weld. However, each new lot of these electrodes shall be checked for suitability in accordance with requirements of 7.10.

[4] The copper template is especially recommended for the Type P-2 and P-3 specimens since it eliminates weld spatter which may interfere with proper seating of the specimen during test.

[5] Tsukada, H., Suzuki, I. I., and Tanaka, Y., "A Study on Drop-Weight Test Using A508 Class 2 Steel," *Japan Steel Works, Ltd.*, December 1, 1981.

shown in Fig. 9. This weld thickness above the specimen shall be maintained across as much of the weld width as permitted by the bead contour. Figure 10 illustrates a device for measuring the thickness of weld metal at the bottom of the notch. The adjustable dial indicator with bridge-support is set at zero while in position on the specimen with the indicator tip contacting the specimen surface immediately adjacent to the notch. The bridge is then placed over the weld with the indicator tip resting on the bottom of the notch to measure the weld metal thickness directly. After the operator has gained experience in the preparation of a few specimens, the instrument need be used only in the final checking of the finished notch.

7.10 *Other Crack-Starter Welds*—The satisfactory completion of drop-weight tests is dependent upon the "crack-starting" conditions developed by the notched weld. As shown schematically in Fig. 11, the specimen deflection, D_C, that cracks the weld, is significantly less than the allowable anvil stop deflection, D_A, for all standard thickness, T, specimens tested on the proper span, S. The carefully prepared and specially handled electrode (described in 7.7[3]) has been proved successful for crack-starting purposes for all temperatures up to approximately 400°F (200°C). Other weld materials shall be considered to perform satisfactorily as crack-starters if they also develop cleavage cracks at suitably high test temperatures at or near the instant that yielding occurs in the surface fibers of the test specimen. Weld materials, other than those described in 7.7, may be used for the crack-starter bead provided the following requirements are met:

7.10.1 Using standard conditions as specified in Table 1, three standard Type P-2 specimens (¾ by 2 by 5 in.) (19 by 51 by 127 mm) shall be drop-weight tested at a temperature 100°F (55°C) or more above the NDT temperatures of the plate material.

7.10.2 If the three tests demonstrate that the weld notch is always cracked upon deflection of the specimen tension surface to the maximum amount permitted by the proper anvil stop, the other crack-starter weld shall be authorized and considered to conform to the requirements of this method.

7.10.3 Welding procedures or crack-starter weld dimensions other than those described in 7.7 shall be considered to perform satisfactorily as crack-starters if they are demonstrated to develop cleavage cracks at suitably high test temperatures at or near the instant that yielding occurs in the surface fibers of the test specimens. For example, a ¾ to 1-in. long crack-starter weld deposited in one direction only with the welding conditions and the electrodes described in 7.7 has been used successfully as a crack-starter weld for the Type P-3 specimen. The shorter weld reduces to total heat input into the specimen and is considered less likely to cause metallurgical changes in the specimen base materials of the low-alloy, high-tensile strength pressure vessel steels. For the Type P-1 specimen, the shorter weld does not provide the reproducibility or consistency for crack-starting purposes obtained with the standard crack-starter weld described in 7.7. Other welding procedures or crack-starter weld dimensions than those described in 7.7 may be used as the crack-starter bead for a given standard type (P-1, P-2, or P-3) specimen provided that three specimens are tested in accordance with 7.10.1 and results obtained in accordance with 7.10.2.

8. Procedure—General

8.1 Some care and thought are necessary to make a successful drop-weight determination of the NDT temperature. Adequate auxiliary equipment and a definite procedure will aid in making the test. The following sections will define in detail and in orderly fashion the equipment and procedure requirements:

8.2 Conduct the test by placing a specimen in a heating or cooling device until it is at the desired temperature. Then place it with minimum loss of time (see 12.4) on the anvil and align where it will be struck squarely by the weight. Allow the weight to drop from a known preselected height on the specimen. Examine the specimen after the strike to determine its condition as defined by the requirements of this method. Repeat this process until the NDT temperature has been determined.

8.3 The number of specimens required to determine the NDT temperature is a function of the experience of the operator with the material and of the use of an adequate procedure. A skilled operator working with known material can determine the NDT temperature with

as few as three specimens. Generally, six to eight specimens are required.

9. Specimen—Anvil Alignment

9.1 *Anvil Requirements*—Test each type of drop-weight specimen only on the anvil designated for that type specimen in accordance with Table 1.

9.2 *Specimen-Anvil Alignment*—In order to obtain a valid test properly align the specimen on the anvil. Align the specimen, anvil, and weigh so the specimen is struck under the following conditions:

9.2.1 The specimen shall be horizontal and the ends shall rest on the anvil supports.

9.2.2 The striking tup of the weight shall strike within ±0.1 in. (±2.5 mm) of a line on the compression side of the specimen, normal to a long edge and directly opposite the notch in the crack-starter weld.

9.2.3 No part of the crack-starter weld will touch the deflection stops at any time during the test.

9.2.4 The specimen sides and ends shall be free from any interference during the test.

9.3 *Alignment Tool*—The technique shown in Fig. 12 has been used successfully to achieve longitudinal and angular specimen alignment of the specimen. Draw a wax-pencil line on the compression surface of the specimen normal to a long edge and directly opposite the notch. Place the specimen on the anvil so this line coincides with the edge of a removable guide bar. Place the bar against the machine rails so that its edge defines the striking line of the tup on the weight.

10. Selection of Test Energy

10.1 Strike the specimen by a free-falling weight having adequate energy to deflect the specimen sufficiently to crack the weld deposit and to make the tension surface contact the anvil stop. The design of the machine permits the use of various impact energies to accommodate the different strength levels of the various materials tested. The standard test conditions shown in Table 1 have been developed by experience and shall be used for the test series of a given steel unless "No-Test" performance is experienced. The indicated energies can be obtained by lifting the weight the required distance from the compression surface of the specimen.

10.2 Proper contact of the tension surface of the specimen with the deflection stop shall be defined as follows: Scribe a wax-pencil line on the tension surface of a standard specimen parallel to and in line with the mechanical notch cut in the crack-starter weld deposit, Fig. 13 (*a*). Apply clean masking tape, or a similar material, to the top surface of the anvil deflection stop blocks, Fig. 13(*b*). Align the test specimen on the anvil and strike once by the weight with the standard conditions, Table 1, for the steel involved. Transfer of the wax-pencil line from specimen to the tape shall indicate that the specimen was bent sufficiently (Fig. 13(*c*)). The above procedure, to ensure proper contact of the tension surface of the specimen with the deflection stop blocks, is considered a "built-in" standardization feature of the test method, and it shall be employed for each drop-weight test to preclude "No-Test" performance as described in 13.2.3 and 13.3.

10.3 If the weld crack and anvil stop contact criteria are not met by the Table 1 energies, increase the drop-weight energy in 100-ft-lb increments for the Type P-1 specimens or 50-ft-lb (68-J) increments for the Type P-2 and P-3 specimens until they are met. Do not use drop-weight energies above those posted on the table unless the above procedure has been followed to determine the excess energy requirements.

11. Selection of Test Temperatures

11.1 The selection of test temperatures is based on finding, with as few specimens as possible, a lower temperature where the specimen breaks and an upper temperature where it does not break, and then testing at intervals between these temperatures until the temperature limits for break and no-break performance are determined within 10°F (5°C). The NDT temperature is the highest temperature where a specimen breaks when the test is conducted by this procedure. Test at least two specimens that show no-break performance at a temperature 10°F (5°C) above the temperature judged to be the NDT point.

11.2 Conduct the initial test at a temperature estimated to be near the NDT. This temperature and all subsequent test temperatures shall be integral multiples of 10°F or 5°C. Additional tests can be conducted at temperatures

based on the experience of the operator or on those suggested in Table 2.

12. Measurement of Specimen Temperatures

12.1 The entire test specimen shall be at a known and uniform temperature during the test. It shall be assumed that if it is fully immersed in a stirred-liquid, constant temperature bath of known temperature and separated from an adjacent specimen by a minimum of 1 in. (25.4 mm) all around for a period of at least 45 min prior to the test, the specimen temperature shall be the same as the bath temperature. If a gas heat-transfer medium is used, increase the required minimum holding time to 60 min. If it can be shown by appropriate test techniques, such as using a thermocouple buried in the center of a dummy test specimen, that specimen equilibrium temperatures can be developed in a shorter period, the tester can reduce the specimen-holding period provided that he has prior approval of the purchaser. The constant-temperature baths or ovens may be of any type that will beat or cool the specimens to a known and uniform temperature.

12.2 Measure the bath temperature by a device with calibration known to ±2°F or ±1°C.

12.3 Any convenient means may be used to remove the specimen from the temperature bath and transfer it to the test machine provided it shall not affect the specimen temperature control. Tongs, if used, shall be kept in the temperature bath to maintain a temperature equivalent to the specimen temperature. Rubber-gloved hands, in general, are the most convenient handling tool. The specimen shall be handled away from the fracture area.

12.4 If more than 20 s elapse in the period of removing the specimen from the bath prior to release of the weight, temperature control shall presume to have been lost and the specimen shall be returned to the bath.

12.5 Considerable experience has been accumulated with baths of the following type, and it is described here for the convenience of the tester. A deep, insulated metal container holding from ½ to 10 gal (1.9 to 38 L) of a suitable heat-transfer liquid, such as alcohol, will maintain a given temperature for the required specimen-holding period with minor manual adjustments. By immersing an open basket of cracked dry ice or a high-wattage electrical heat in the bath, its temperature can be adjusted slightly or can be lowered or raised to a new constant level in a short period. For low-density heat-transfer liquids, a walnut-sized piece of dry ice added to the bath will sink and bubble vigorously and help stir it. If this type of bath is used, it should be deep enough to cover the specimens fully. It has been found by experience that standing the specimens on one end in the bath with their upper ends leaning on the vessel wall is most satisfactory. Specimens placed horizontally in the bath should be laid on a screen held at least ¼ in. (6.4 mm) from the bottom. If multiple specimens are placed in one bath, they should be spaced a minimum of 1 in. apart to ensure adequate heat-transfer liquid flow around each. The most convenient method of bath temperature measurement is to use a bare thermocouple connected to an automatic recorder.

13. Interpretation of Test Results

13.1 The success of the drop-weight test depends upon the development of a small cleavage crack in the crack-starter weld after a minute bending of the test specimen. The test evaluates the ability of the steel to withstand yield point loading in the presence of a small flaw. The steel either accepts initiation of fracture readily under these test conditions and the test specimen is broken, or initiation of fracture is resisted and the specimen bends the small, additional amount permitted by the anvil stop without complete fracturing.

13.2 After completion of each drop-weight test, the specimen shall be examined and the result of the test shall be recorded in accordance with the following criteria:

13.2.1 *Break*—A specimen is considered broken if fractured to one or both edges of the tension surface. Complete separation at the compression side of the specimen is not required for break performance. Typical examples of break performance are illustrated in Fig. 4.

NOTE—Should any crack, whether initiated at the crack-starter or not, propagate to the specimen edge on the tension face, consider the test a break-performance.

13.2.2 *No-Break*—The specimen develops a visible crack in the crack-starter weld bead that is not propagated to either edge of the tension

surface. Typical examples of no-break performance are illustrated in Fig. 15.

13.2.3 *No-Test*—The test shall be considered not valid if either weld-deposit notch is not visibly cracked after completion of a test, or if the drop-weight specimen is not deflected fully to contact the anvil stop as evidenced by transfer of the wax-pencil lines to the masking tape on the anvil deflection stop.

13.3 A No-Test performance (13.2.3) may result from the use of insufficient impact energy, the use of a too-ductile weld metal for crack-starter purposes, or misalignment of the specimen so that the weld-crown obstructs full deflection to the anvil stop. The No-Test sample shall be discarded and a retest, using another sample, shall be required. Retests, or tests of additional specimens, of a given steel found to develop insufficient deflections with the standard test condition, Table 1, shall be conducted with higher impact energies (see 10.3).

14. Report

14.1 The report shall include the following:

14.1.1 Type of steel and heat treatment,

14.1.2 Identification of product tested—heat number, plate number, etc.,

14.1.3 Identification, orientation, and location of test specimens,

14.1.4 Specimen type, test conditions and test temperatures employed,

14.1.5 Result of test (break, no-break, or no-test) for each specimen, and

14.1.6 Deviations, if any, from this test method.

15. Use of Test for Material-Qualification Testing

15.1 Specification tests conducted at a given test temperature, on a go, no-go basis, shall require that a minimum of two drop-weight specimens be tested. All specimens thus tested shall exhibit no-break performance to ensure that the NDT temperature of the steel under test is below the specification test temperature. The breaking of one (or more) specimens at the test temperature shall indicate the NDT temperature of the material to be at or above the specification test temperature.

16. Precision and Bias

16.1 *Precision*—The precision of this method is being established.

16.2 *Bias*—There is no basis for determining the bias of this method.

TABLE 1 Standard Drop-Weight Test Conditions

Type of Specimen	Specimen Size, in. (mm)	Span, in. (mm)	Deflection Stop, in. (mm)	Yield Strength Level, ksi (MPa)	Drop-Weight Energy for Given Yield Strength Level[A]	
					ft-lbf	J
P-1	1 by 3½ by 14	12.0	0.3	30 to 50 (210 to 340)	600	800
	(25.4 by 89 by 356)	(305)	(7.6)	50 to 70 (340 to 480)	800	1100
				70 to 90 (480 to 620)	1000	1350
				90 to 110 (620 to 760)	1200	1650
P-2	¾ by 2 by 5	4.0	0.06	30 to 60 (210 to 410)	250	350
	(19 by 51 by 127)	(102)	(1.5)	60 to 90 (410 to 620)	300	400
				90 to 120 (620 to 830)	350	450
				120 to 150 (830 to 1030)	400	550
P-3	⅝ by 2 by 5	4.0	0.075	30 to 60 (210 to 410)	250	350
	(15.9 by 51 by 127)	(102)	(1.9)	60 to 90 (410 to 620)	300	400
				90 to 120 (620 to 830)	350	450
				120 to 150 (830 to 1030)	400	550

[A] Initial tests of a given strength level steel shall be conducted with the drop-weight energy stated in this column. In the event that insufficient deflection is developed (no-test performance) an increased drop-weight energy shall be employed for other specimens of the given steel.

TABLE 2 Suggested Sequence of Drop-Weight Test Temperatures

Specimen Condition After Test at Temperature T_n	Suggested Test Temperature for Succeeding Test
No crack in weld notch	No-Test performance (see 13.2.3 and 13.3)
Weld crack extending less than 1/16 in. (1.6 mm) into specimen surface	$T_n - 60°F$ $T_n - 30°C$
Weld crack extending 1/8 to 1/4 in. (3.2 to 6.4 mm) into specimen surface	$T_n - 40°F$ $T_n - 20°C$
Weld crack extending approximately 1/2 the distance between specimen edge and toe of crack-starter weld bead	$T_n - 20°F$ $T_n - 10°C$
Weld crack extending to within 1/4 in. (6.4 mm) of specimen edge	$T_n - 10°F$ $T_n - 5°C$
Specimen "Breaks" (see 13.2.1)	$T_n + 40°F$ $T_n + 20°C$
	Continue testing as described in 11.1 and 11.2

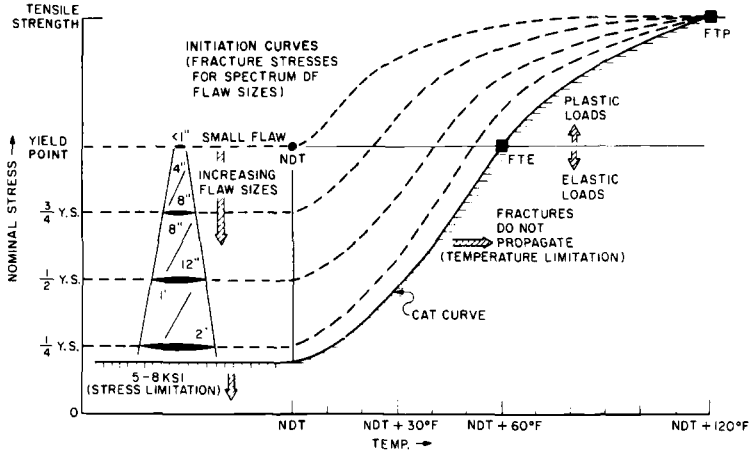

FIG. 1 Generalized Fracture Analysis Diagram Indicating the Approximate Range of Flaw Sizes Required for Fracture Initiation at Various Levels of Nominal Stress, as Referenced by the NDT Temperature[6,7]

[6] Pellini, W. S., and Puzak, P. P., "Fracture Analysis Diagram Procedures for the Fracture-Safe Engineering Design of Steel Structures," *NRL Report 5920*, March 15, 1963; also *Welding Research Council Bulletin*, Series No. 88, May, 1963.

[7] Pellini, W. S., and Puzak, P. P., "Practical Considerations in Applying Laboratory Fracture Test Criteria to the Fracture-Safe Design of Pressure Vessels," *NRL Report 6030*, November 5, 1963; also *Transactions*, Am. Soc. Mechanical Engrs., Series A., *Journal of Engineering for Power*, October 1964, pp. 429–443.

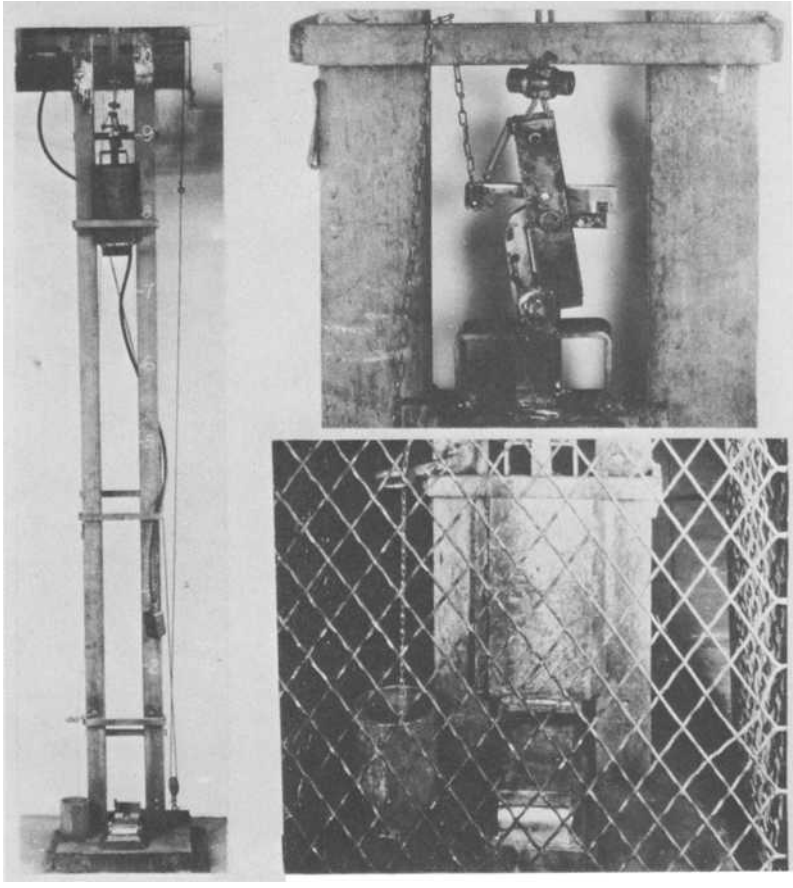

(a) *Left*—Complete Assembly
(b) *Upper Right*—Quick-Release Mechanism
(c) *Lower Right*—Guard Screen

FIG. 2 Drop-Weight Test Apparatus

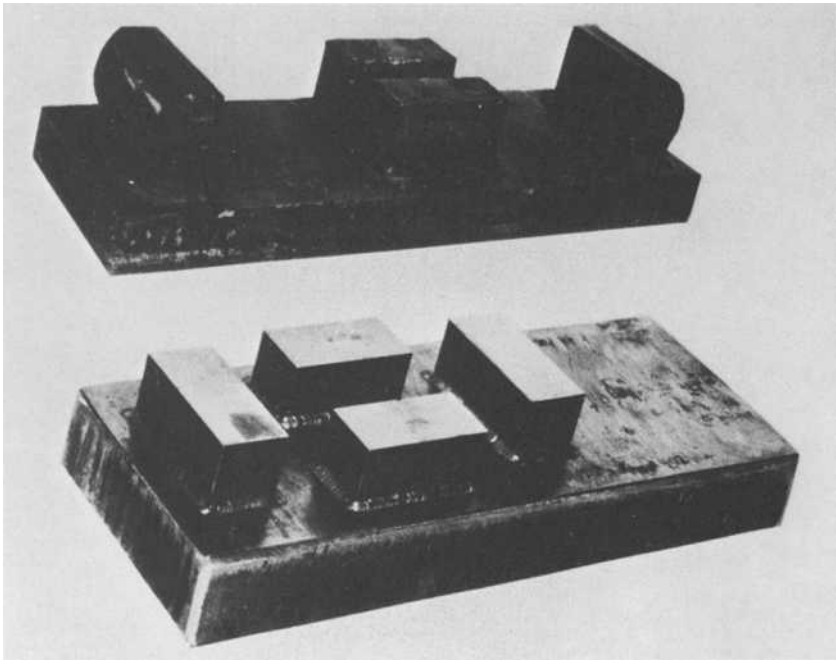

FIG. 3 General Appearance of the Anvils Required for Drop-Weight NDT Tests

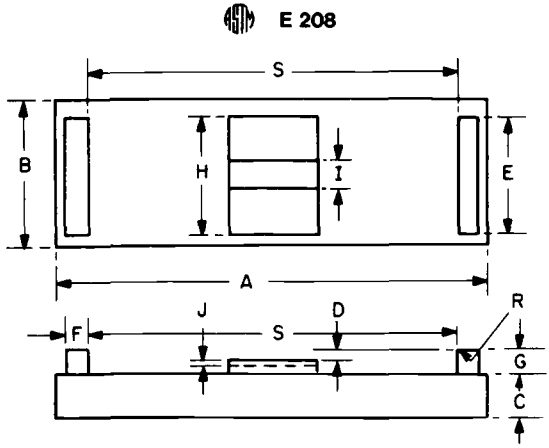

Anvil Dimension	Units	Specimen Type			Tolerance
		P-1	P-2	P-3	
S, Span	in.	12.0	4.0	4.0	±0.05
	mm	305	100	100	±1.5
D, Deflection stop	in.	0.30	0.060	0.075	±0.002
	mm	7.60	1.50	1.90	±0.05
A, Anvil length	←		not critical		→
B, Anvil width	←		not critical		→
C, Anvil thickness	in.	1.5 min	1.5 min	1.5 min	
	mm	38 min	38 min	38 min	
E, Support length	in.	3.5 min	2.0 min	2.0 min	
	mm	90 min	50 min	50 min	
F, Support width	←		not less than *G*		→
G, Support height	in.	2.0	2.0	2.0	±1
	mm	50	50	50	±25
R, Support radius	in.	0.075	0.075	0.075	±0.025
	mm	1.0	1.0	1.0	±0.1
H, Stop width	in.	3.5 min	2.0 min	2.0 min	±2
	mm	90 min	50 min	50 min	±50
I, Weld clearance	in.	0.9	0.9	0.9	±0.1
	mm	22	22	22	±3
J, Weld clearance depth	in.	0.4 min	0.4 min	0.4 min	
	mm	10 min	10 min	10 min	

FIG. 4 Anvil Dimensions

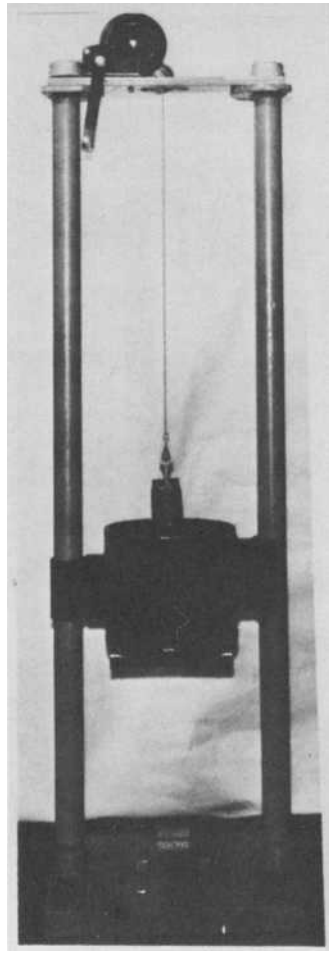

FIG. 5 Portable Drop-Weight Test Machine Used for Tests at Different Fabrication Sites

E 208

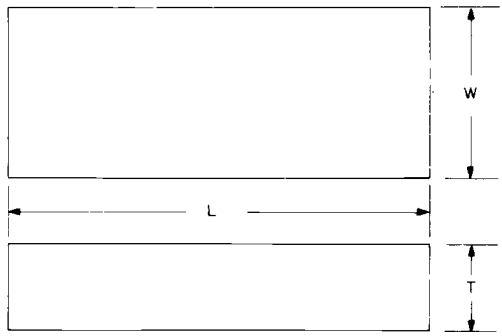

Dimension	Units	Specimen Type					
		P-1		P-2		P-3	
		Dimension	Tolerance	Dimension	Tolerance	Dimension	Tolerance
T, Thickness	in.	1.0	±0.12	0.75	±0.04	0.62	±0.02
	mm	25	±2.5	19	±1.0	16	±0.5
L, Length	in.	14.0	±0.5	5.0	±0.5	5.0	±0.5
	mm	360	±10	130	±10	130	±10
W, Width	in.	3.5	±0.1	2.0	±0.04	2.0	±0.04
	mm	90	±2.0	50	±1.0	50	±1.0
WL, Weld length	in.	2.5	±0.5	1.75	±0.75	1.75	±0.75
	mm	63.5	±12.7	44.5	±19	44.5	±19

NOTE—The length of the weld bead is not critical, provided that the crack-starter notch is at the center of specimen and that the weld bead does not contact the support fixture when the specimen is fully deflected.

FIG. 6 Standard Drop-Weight Specimen Dimensions

(a) Punch Marks

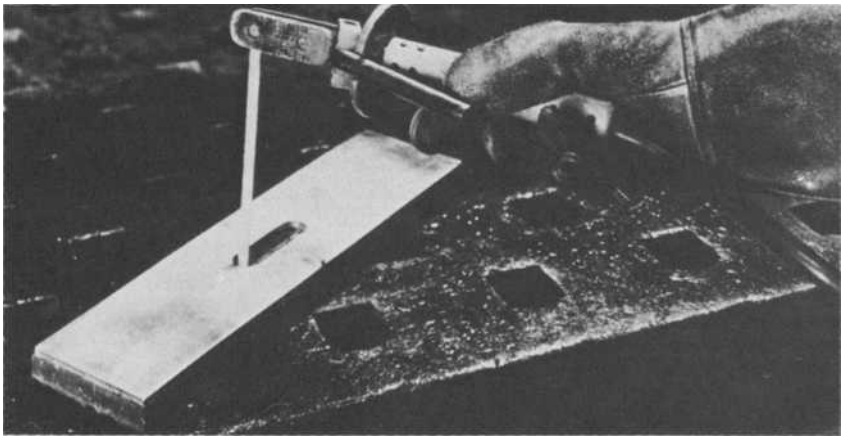

(b) Copper Template

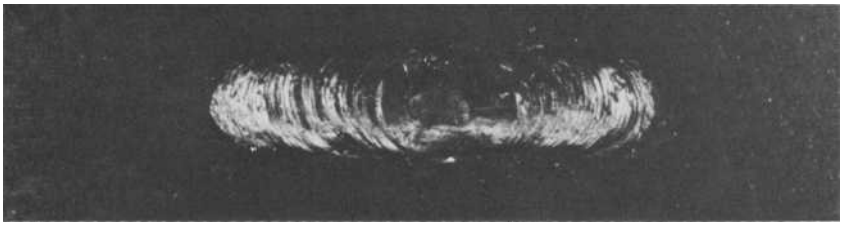

(c) Crack-Starter Weld

FIG. 7 Methods of Locating the Weld Deposit Properly on the Test Specimen

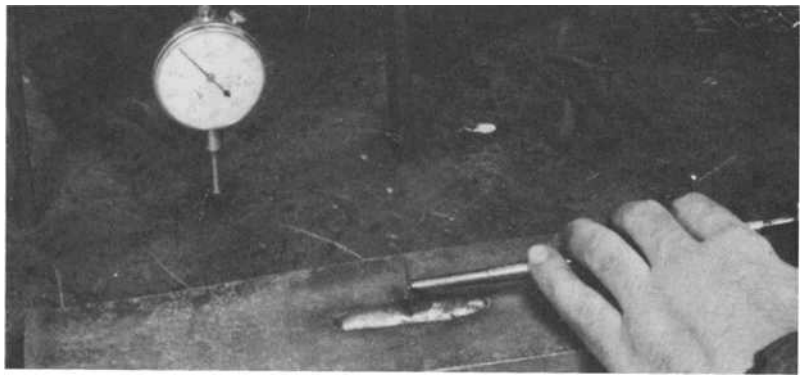

FIG. 8 Notching of Crack-Starter Weld Deposit

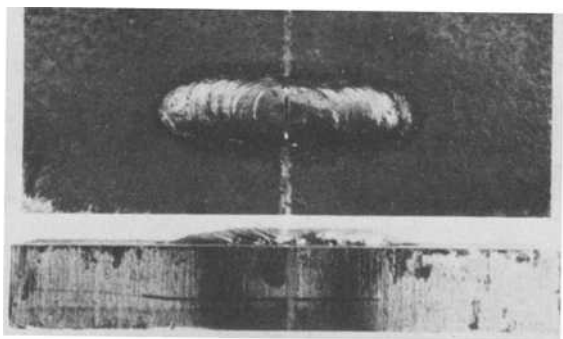

FIG. 9 Weld-Notch Details and Example of a Notched Weld

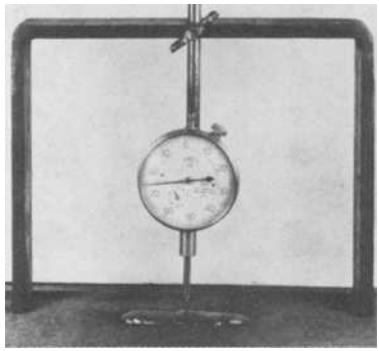

FIG. 10 Method for Measuring Weld Metal Thickness at the Bottom of the Notch

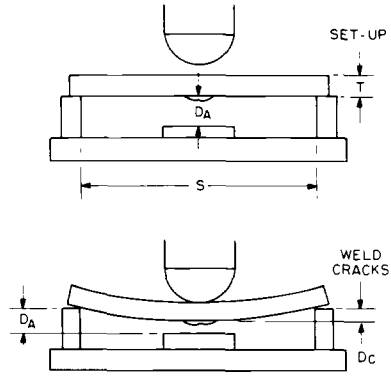

YIELD POINT LOADING IN PRESENCE OF SMALL CRACK IS TERMINATED BY CONTACT WITH STOP

FIG. 11 Drop-Weight Test Method

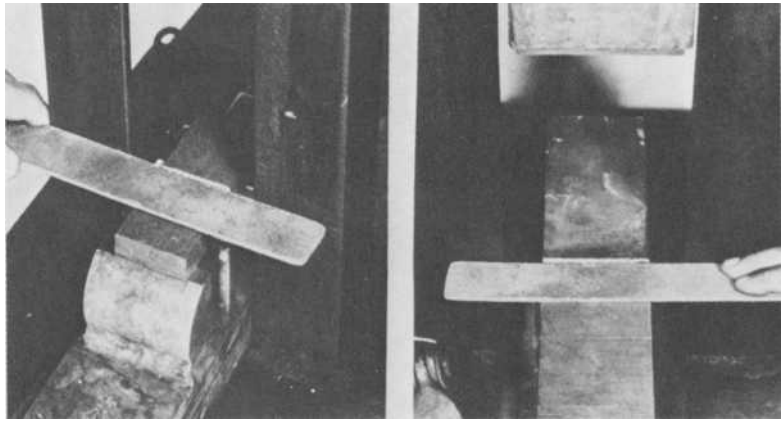

FIG. 12 Method for Alignment of Specimen

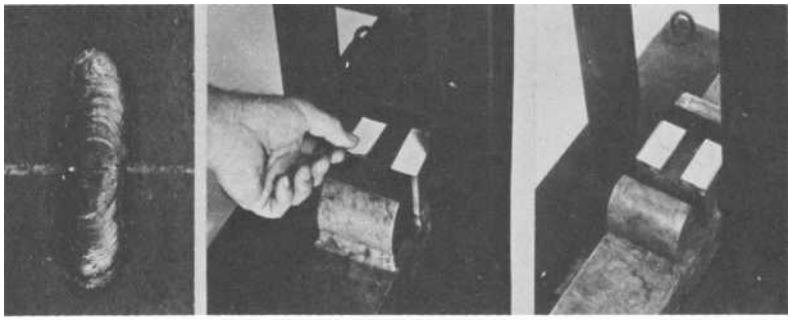

(a) (b) (c)

(*a*) Wax Pencil Line Scribed on Tension Side of a Specimen
(*b*) Application of Masking Tape to Anvil Stop Surfaces
(*c*) Transfer of Wax Lines to the Tape When the Specimen Hits the Stop

FIG. 13 Method Employed to Indicate Contact of the Specimen with the Anvil Stop

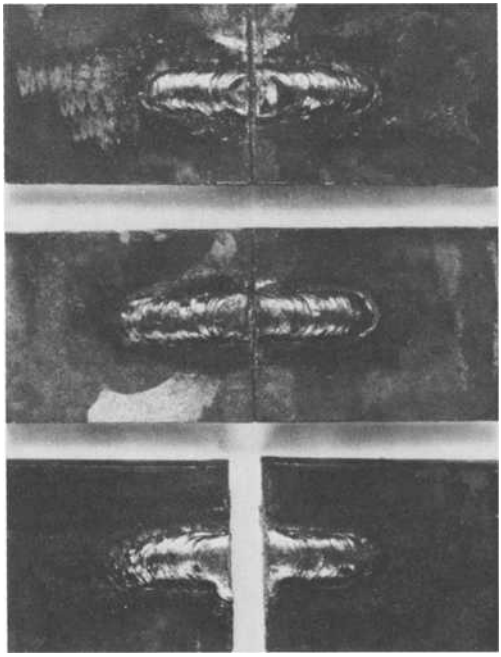

FIG. 14 Typical Examples of Broken Drop-Weight Specimens. Fracture Reaches to at Least One Edge

E 208

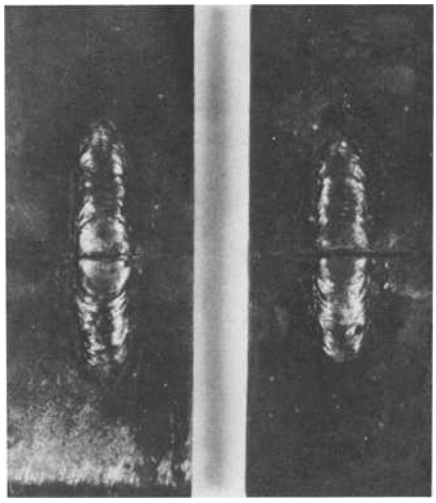

FIG. 15 Typical Examples of No-Break Performance in Drop-Weight Specimens. Fracture Does Not Reach Edge

ADDITIONAL REFERENCES

Selected References Relating to Development of Drop-Weight Test:

Pellini, W. S., "Notch Ductility of Weld Metal," *Welding Journal*, Am. Welding Soc., Vol 35, May, 1956, p. 217-s.

Pellini, W. S., Brandt, F. A., and Layne, E. E., "Performance to Cast and Rolled Steels in Relation to the Problem of Brittle Fracture," *Transactions*, Am. Foundryman's Soc., Vol 61, 1953, p. 243.

Pellini, W. S., and Srawley, J. E., "I. Evaluating Fracture Toughness in Pressure Vessels for Space, Aerospace, and Hydrospace—A Symposium," *Journal of Metals*, March, 1961, pp. 195–198.

Puzak, P. P., and Babecki, A. J., "Normalization Procedures for NRL Drop-Weight Test," *Welding Journal*, Am. Welding Soc., Vol 38, May, 1959, p. 209-s.

Puzak, P. P., and Pellini, W. S., "Evaluation of the Significance of Charpy Tests for Quenched and Tempered Steels," *Welding Journal*, Am. Welding Soc., Vol 35, No. 6, 1956, p. 275-s.

Puzak, P. P., Schuster, M. E., and Pellini, W. S., "Applicability of Charpy Test Data," *Welding Journal*, Am. Welding Soc., Vol 33, September, 1954, p. 443-s.

Puzak, P. P., Schuster, M. E., and Pellini, W. S., "Crack Starter Tests of Ship Fracture and Project Steels," Appendix entitled, "Procedures for NRL Drop Weight Test," *Welding Journal*, Am. Welding Soc., Vol 33, No. 10, October, 1954, p. 481-s.

Selected References Relating to Correlation of NDT to Service Failures:

Babecki, A. J., Puzak, P. P., and Pellini, W. S., "Report of Anomalous 'Brittle' Failures of Heavy Steel Forgings at Elevated Temperatures," *Paper No. 59-MET-6*, Am. Soc. Mechanical Engrs., May, 1959.

Lange, E. A., and Klier, E. P., "A Study of Fracture Development and Materials Properties in PVRC Vessels 1 and 2," *Welding Journal*, Am. Welding Soc., Vol 41, February, 1962, p. 53-s.

Pellini, W. S., Steele, L. E., and Hawthorne, J. R., "Analysis of Engineering and Basic Research Aspects of Neutron Embrittlement of Steels," *NRL Report 5780*, April 17, 1962; also *Welding Journal*, Am. Welding Soc., October, 1962.

Puzak, P. P., Babecki, A. J., and Pellini, W. S., "Correlations of Brittle Fracture Service Failures with Laboratory Notch-Ductility Tests," *Welding Journal*, Am. Welding Soc., Vol 37, No. 9, September, 1958, p. 391-s.

Selected References Relating to Neutron Irradiation Embrittlement:

Hawthorne, J. R., and Steele, L. E., "Effect of Neutron Irradiation on Charpy-V Drop Weight Test Transition Temperatures of Various Steels and Weld Metals," *ASTM STP 286*, Am. Soc. Testing Mats., 1960, pp. 33–56.

Hawthorne, J. R., Steele, L. E., and Pellini, W. S., "Effects of Properties of Reactor Structural Materials," *Paper No. 61-WA-332*, Am. Soc. Mechanical Engrs., October 1961.

Steele, L. E., and Hawthorne, J. R., "Effect of Irradiation Temperature on Neutron-Induced Changes in Notch Ductility of Pressure-Vessel Steels," *NRL Report 5629*, June 28, 1961.

Indexes

Author Index

Subject Index

ISBN 0-8031-0487-1